

Investigation of the Quorum-Sensing Regulon in the Corn Pathogen *Pantoea stewartii*

Revathy Ramachandran

Dissertation submitted to the faculty of Virginia Tech in partial fulfillment of the requirements
for the degree of

Doctor of Philosophy

In

Biological Sciences

Ann M. Stevens, Committee Chair

Roderick V. Jensen

Timothy J. Larson

David L. Popham

Birgit E. Scharf

March 21st, 2014

Blacksburg, VA, USA

Keywords: quorum sensing, *Pantoea stewartii*, Stewart's wilt, EsaR, regulon, transcription regulation, RNA-Seq, phytopathogen

Investigation of the Quorum-Sensing Regulon in the Corn Pathogen

Pantoea stewartii

Revathy Ramachandran

ABSTRACT

Pantoea stewartii subsp. *stewartii* is a bacterium that causes Stewart's wilt disease in corn plants. The bacteria are transmitted to the plants via an insect vector, the corn flea beetle *Chaetocnema pulicaria*. Once in the plant, the bacteria migrate to the xylem and grow to high cell densities, forming a biofilm by secreting excess capsular exopolysaccharide, which blocks water transport and causes wilting. The timing of virulence factor synthesis is regulated by the cell-density dependent quorum sensing (QS) system. Such temporal regulation is crucial in establishing infection and is orchestrated by the QS-dependent transcriptional regulator EsaR. EsaR represses expression of capsular exopolysaccharide at low cell densities. At high cell densities, an acylated homoserine lactone (AHL) molecule produced during growth by the cognate AHL-synthase EsaI accumulates. The AHL binds to and inactivates EsaR, causing derepression of capsule production.

EsaR is a member of the LuxR family of QS-dependent transcriptional factors. Most LuxR homologs are unstable and/or insoluble in the absence of AHL which has hindered structural studies. Chapter Two describes the changes in the structure of EsaR due to binding of AHL ligand as determined through biochemical methods. EsaR was found to be stable and retain its multimeric state in the absence or presence of AHL, but intra- and inter-domain changes occurred that affect its DNA-binding capacity.

Apart from repressing expression of capsule at low cell-densities, EsaR represses its own expression and activates production of a small RNA, EsaS, with unknown function. In Chapter Three a proteomic approach was used to identify an additional 30 QS-controlled proteins. Genes encoding three of these proteins are directly regulated by EsaR and the EsaR binding sites in the respective promoters were defined. In Chapter Four, a high-throughput RNA-Seq method identified even more genes in the QS regulon that the proteomic approach overlooked. RNA-Seq analysis of rRNA-depleted RNA from two strains of *P. stewartii* was used as a screen to help identify 11 promoters, subsequently shown to be directly regulated by EsaR *in vitro*. Most of the genes controlled by QS grouped into three major physiological responses, capsule & cell wall production, surface motility & adhesion and stress response. In Chapter Five, the role of two QS regulated genes, *dkgA* (encoding 2, 5-diketo-D-gluconate) and *lrhA* (encoding a repressor of chemotaxis, adhesion and motility), in plant virulence were examined.

These studies have better characterized the QS regulator EsaR and its interaction with the AHL ligand, and shown that QS has a more global response in *P. stewartii* than previously recognized. Further characterization of the genes identified in this study could facilitate identification of factors crucial in plant pathogenesis or insect-vector symbiosis and aid in the development of molecular-based approaches for possible disease intervention.

ACKNOWLEDGEMENTS

I would like to thank Ann Stevens for selecting me to join her lab 6 years ago. Her decision has changed my life in a wonderful way, and for that I will be always thankful. Ann, you were my first academic mentor and I have learnt a lot from you. Thank you for always looking out for me, and thank you for your patience. From being Professor Stevens, you have become Ann to me and I hope that we will remain colleagues all our life.

Next I would like to thank my committee members, Dr. Popham, Dr. Scharf, Dr. Larson and Dr. Jensen for their constant encouragement and consistent feedback. I was lucky to have four open doors that always gave me advice, scientific and otherwise.

I would also like to make a special mention to Daniel Schu for being my graduate student mentor during the first year of my research. My attitude towards research was shaped by your views and for that I'm always thankful. Later, your insights on post-docs helped me greatly during my job search.

Next, I would like to thank the Micro group, for being so inclusive that I felt more at home in Life Sciences 1 than my real home the first few years of grad school. I will miss the camaraderie and I hope I am lucky enough to find a group that is as friendly and supportive in my next place of work. To the current members of the Stevens lab, Alison and An, I would like to wish them luck in experiments. Alison, I would be lucky if my next lab mate has half your sense of humor. You guys are in a great lab that will forever be part of our professional identity.

Gratitude is not enough, but I would still like to thank my parents, KV Ramachandran and Nalini Ramachandran for taking the scary decision of allowing their daughter to go to a new country far away. Their trust has been the foundation of my PhD. I would like to thank my sister, Chitra Ramachandran, my cousins and extended family for making the distance feel smaller.

And lastly, I would like to thank Raj Kishore for being the driving force to help me finish my PhD. He has also been the balancing force that never allowed me to become too upset or bogged down with the ups and downs of research. Thank you for making grad school fun and making my life awesome.

TABLE OF CONTENTS

	Page number
Chapter One: Literature Review	1
Introduction	2
Historical perspective on quorum sensing	2
Diverse autoinducer structures	4
The LuxR-LuxI quorum-sensing model	4
The LuxR protein family	5
The EsaR-EsaI system of <i>Pantoea stewartii</i>	7
The plant pathogen <i>Pantoea stewartii</i>	9
QS strategies in plant pathogenic bacteria	10
Research Plan	11
References	13
Chapter Two: Probing the Impact of Ligand Binding on the Acyl-Homoserine Lactone-Hindered Transcription Factor EsaR of <i>Pantoea stewartii</i> subsp. <i>stewartii</i>	22
Abstract	23
Introduction	24
Materials and Methods	
Measurement of EsaR stability in <i>P. stewartii</i>	26
Measurements of EsaR stability in recombinant <i>E. coli</i>	27
Generation and purification of HMGE fusion protein	28
Generation and purification of EsaR NTD178	29
EMSA analysis of HMGE activity	30
Partial <i>in vitro</i> proteolysis	31
Gel filtration of HMGE	32
BS ³ cross-linking of the EsaR NTD178	33
Results	
EsaR is stable <i>in vivo</i> in the absence and presence of AHL	33
A His-Maltose Binding Protein (MBP)-glycine linker-tagged EsaR construct (HMGE) is biologically active	34
Partial <i>in vitro</i> proteolysis reveals AHL-dependent protection and conformational changes in EsaR	35
EsaR dimerizes in the absence and presence of AHL	37
The NTD of EsaR binds AHL and is capable of dimerizing in the absence and presence of AHL	38
Discussion	39
Acknowledgements	43
References	44

Chapter Three: Proteomic Analysis of the Quorum-Sensing Regulon in <i>Pantoea stewartii</i> and Identification of Direct Targets of EsaR	53
Abstract	54
Introduction	55
Materials and Methods	
Bacterial strains, plasmids, and growth conditions	57
Two-dimensional SDS-PAGE	57
Mass spectrometry and protein identification	58
Purification of EsaR fusion protein	58
EMSA analysis	59
qRT-PCR	60
DNase I footprinting analysis	61
Results	
Identification of QS-regulated proteins	62
Identification of direct targets of EsaR	63
Verification of transcriptional control of <i>dkgA</i> , <i>glpF</i> and <i>lrhA</i>	64
Determination of the EsaR binding site at the <i>dkgA</i> , <i>glpF</i> and <i>lrhA</i> promoters	65
Analysis of EsaR binding sites	66
Discussion	67
Acknowledgements	72
References	73
Chapter Four: Transcriptome-based Analysis of the Quorum-Sensing Regulon in <i>Pantoea stewartii</i>	84
Abstract	85
Introduction	86
Materials and Methods	
RNA purification and rRNA depletion for RNA-Seq	88
Processing of Illumina sequencing data	88
EMSA analysis	89
Quantitative Real-Time PCR (qRT-PCR)	90
Results	
RNA-Seq analysis of the QS regulon of <i>P. stewartii</i> :	91
Bioinformatic approach to identify direct targets of EsaR	92
Validating transcriptional control and identifying putative direct targets	93
EMSA analysis on putative targets	94
Discussion	95
Acknowledgements	101
References	102

Chapter Five: Role of Two Quorum-Sensing Controlled Genes, <i>dkgA</i> and <i>lrhA</i>, in the Virulence of the Phytopathogen <i>Pantoea stewartii</i> subsp. <i>stewartii</i>	112
Abstract	113
Introduction	114
Materials and Methods	
Bacterial strains, plasmids and growth conditions	116
Construction of unmarked DC283 $\Delta dkgA$ and DC283 $\Delta lrhA$	116
Generation of complementation strains	117
Capsule production assays	117
Surface motility assays	117
Plant infection assays	118
Results	
Phenotypic analysis of <i>P. stewartii</i> DC283 $\Delta dkgA$ and DC283 $\Delta lrhA$	119
Role of <i>dkgA</i> in <i>P. stewartii</i> virulence	119
Discussion	120
Acknowledgements	123
References	124
Chapter Six: Overall Conclusions	131
References	136
Appendix A- Chapter Three Supplementary Materials	137
Appendix B- Chapter Four Supplementary Materials	144
References	155
Appendix C- Analysis of EsaR Binding Sites Within the Promoter of <i>uspA</i> Using DNase I Footprinting Assays	156

LIST OF FIGURES

	Page numbers
Chapter One	
Figure 1.1: Model of the QS circuit of <i>Vibrio fischeri</i> .	18
Figure 1.2: The different classes of LuxR homologues.	19
Figure 1.3: Model of QS in <i>Pantoea stewartii</i> .	20
Figure 1.4: Mechanism of <i>P. stewartii</i> infection in <i>Zea mays</i> .	21
Chapter Two	
Figure 2.1: EsaR accumulation and stability <i>in vivo</i> .	48
Figure 2.2: HMGE activity assays.	49
Figure 2.3: Limited <i>in vitro</i> digestion of EsaR by thermolysin and trypsin.	50
Figure 2.4: Multimeric state of HMGE fusion protein in presence and absence of AHL.	51
Figure 2.5: Ability of EsaR NTD178 to resist proteolytic digestion and to form dimers.	52
Chapter Three	
Figure 3.1: Electrophoretic mobility shift assays of putative QS regulon promoters with the His-MBP-glycine linker-EsaR fusion protein, HMGE.	79
Figure 3.2: Relative change in mRNA expression in <i>P. stewartii</i> ESΔIR (pSVB60) versus ESΔIR (pBBR1MCS-3).	80
Figure 3.3: DNase I footprinting assay of EsaR binding sites in the noncoding strand of P _{dkgA} , coding strand of P _{glpF} , and noncoding strand of P _{lrhA} .	81
Figure 3.4: Nested deletion EMSA analysis of EsaR direct targets.	82
Figure 3.5: Alignment of <i>esa</i> boxes recognized by EsaR in <i>P. stewartii</i> .	83
Chapter Four	
Figure 4.1: Comparison of mRNA expression.	107
Figure 4.2: EMSA analysis to confirm direct binding by EsaR.	108
Figure 4.3: Validating transcriptional control of putative EsaR direct targets.	109
Figure 4.4: EMSA analysis to test direct binding of 12 promoters by EsaR.	110
Figure 4.5: Genetic organization of the gene loci of <i>P. stewartii</i> directly regulated by EsaR.	111
Chapter Five	
Figure 5.1: Phenotypic characterization of DC283 Δ <i>dkgA</i> and DC283 Δ <i>lrhA</i> .	129

Figure 5.2: Plant virulence assays in sweet corn seedlings.	130
Appendix A	
Figure A.1: Two-dimensional SDS PAGE experiments of <i>P. stewartii</i> DC283 strains.	141
Figure A.2: Electrophoretic mobility shift assays on the promoters of genes in the QS regulon.	142
Figure A.3: Relative positions of <i>esa</i> box on the promoters of the direct targets of EsaR.	143
Appendix C	
Figure C.1: The promoter region of <i>uspA</i> .	157
Figure C.2: DNase I footprinting assay of EsaR binding sites in the non-coding strand of P _{<i>uspA</i>} .	158

LIST OF TABLES

	Page number
Chapter Three	
Table 3.1: Plasmids and strains used in this study.	77
Table 3.2: The QS regulon of <i>Pantoea stewartii</i> regulated by EsaR.	78
Chapter Four	
Table 4.1: Genes in the RNA-Seq dataset that possess high-scoring predicted <i>esa</i> boxes in their upstream promoter regions and are differentially expressed two-fold or higher.	105
Table 4.2: Genes in the RNA-Seq dataset differentially expressed four-fold or higher that possess a clear +1 and a possible <i>esa</i> box nearby.	106
Chapter Five	
Table 5.1: Strains and plasmids utilized in this study.	127
Table 5.2: Primers utilized in this study.	128
Appendix A	
Table A.1: Primers utilized in this study.	138
Appendix B	
Table B.1: Primers utilized for amplifying EMSA probes and for qRT-PCR.	145
Table B.2: List of genes differentially expressed 2-fold or higher in the RNA-Seq data.	148

Chapter One

Literature Review

INTRODUCTION

Quorum sensing (QS) is a process that allows a population of single-celled bacteria to behave in a coordinated manner as a multi-cellular unit. Bacteria that possess components of QS can coordinate expression of select genes, leading to the simultaneous production of the respective protein products. During QS, microorganisms recognize and respond to others in a population by measuring the concentration of self-produced intercellular signaling molecules, commonly known as autoinducers. The concentration of autoinducer in the surrounding medium is directly proportional to the population of cells in the batch culture. Receptors within the cell sense and respond to a threshold concentration of the autoinducer to subsequently alter gene expression patterns. This cell-density dependent response forms the basis of a simple communication network that defines the concept of prokaryotic multicellularity (1). QS is a widely known phenomenon in many bacteria, with more species being added to the list of QS proficient organisms as research in the field progresses. Important bacterial processes are regulated in this manner, including antibiotic production, release of exoenzymes, biofilm formation, bioluminescence, production of virulence factors, induction of genetic competence and conjugative plasmid transfer (2, 3). Such cooperation is expensive for an individual cell, mostly due to the cost of signal production, but is beneficial to the population as a whole (4).

Historical perspective on quorum sensing

The term QS was first coined in 1994 by Fuqua et al. (5), although studies on QS-controlled luminescence in *Vibrio fischeri* had been initiated as early as the 1960s. The presence of a 'dialyzable substance' was shown by Kempner and Hanson (6), but it was initially argued to be an inhibitor of luminescence that was metabolically degraded by the bacteria during growth,

resulting in light production. It is now known that these Gram-negative proteobacteria were producing a diffusible compound which accumulates in the growth medium and above a critical concentration stimulated expression of the luminescence genes. The diffusible compound was termed 'autoinducer', as it was first discovered while studying autoinduction of luminescence in *V. fischeri* and *Vibrio harveyi* (7, 8).

The first autoinducer molecule identified was an acylated homoserine lactone, which can diffuse across the plasma membrane (9). AHL molecules are produced by AHL synthase enzymes. At a threshold concentration, autoinducer is sensed by a receptor protein within the cell that also functions as a DNA-binding transcriptional regulator. These receptor proteins respond to autoinducer binding by regulating gene expression when they associate with the DNA at or near target promoter regions. Thus, gene expression is controlled in a cell-density dependent manner.

QS in Gram-positive bacteria has evolved to use short oligopeptides and two-component regulatory systems including a surface-associated sensor that can recognize the oligopeptide (10). Binding of the oligopeptide to the sensor histidine kinase triggers a phosphorylation cascade that feeds to a transcriptional response regulator which then influences downstream gene expression (11). A second QS system was discovered in Gram-negative proteobacteria that resembles the Gram-positive phosphorelay system (12) and utilizes autoinducers, called AI-2, that are sensed by receptors on the cell-surface. Binding of the autoinducer in this case leads to a cascade of phosphorylation which feeds to a transcriptional regulator, affecting downstream gene expression.

Diverse autoinducer structures

Many bacterial species use different compounds as autoinducers, such as the furanosyl borate diester AI-2 signal of *V. harveyi* (13), γ -butyrolactone in *Streptomyces* (14), cyclic dipeptides in some Gram-negative species (14), and bradyoxetin in *Bradyrhizobium japonicum* (16). However, acylated homoserine lactones (AHLs) are the most common autoinducer signal used by proteobacteria. AHLs have a homoserine lactone ring carrying acyl side chains 4-18 carbons in length (3). Variations are usually in the length of the acyl side chain and the substituents on it, like keto or hydroxyl groups and double bonds. AHL is produced by AHL synthases, which are grouped into three families: the LuxI family, the AinS family, and the HdtS family (17). *V. fischeri* LuxI synthesizes N-3-oxo-hexanoyl-L-homoserine lactone (3-oxo-C6-HSL) from S-adenosyl methionine and 3-oxo-hexanoyl-acyl carrier protein (18). *V. fischeri* also produces two other autoinducers, N-octanoyl-L-homoserine lactone and N-hexanoyl-L-homoserine (19). *V. harveyi*, another bioluminescent marine bacterium, synthesizes three autoinducers and has three systems in place to respond to each (20). Variation in AHL structures allows a particular LuxR homologue to recognize its cognate AHL in an environment with mixed populations (17).

The LuxR-LuxI quorum-sensing model

The LuxR-LuxI system that controls QS in *V. fischeri* has served as a model for defining most other QS systems in proteobacteria (5). LuxI produces the autoinducer 3-oxo-C6-HSL and is encoded by *luxI*, the first gene in the *lux* operon that consists of 6 other genes. Together, the *luxICDABEG* genes are responsible for bioluminescence in *V. fischeri*. The *luxR* gene codes for the cognate transcriptional regulator and is divergently transcribed from the *lux* operon (FIGURE 1.1). LuxR complexed with AHL positively interacts with RNA polymerase to activate

transcription of the *lux* operon, allowing for the cell-density dependent expression of genes required for bioluminescence. LuxR belongs to a family of transcriptional activators defined by sequence similarities in a C-terminal helix-turn-helix (H-T-H)-containing region (21). LuxR was the first protein defined in the LuxR-type protein family of AHL-responsive QS transcription factors. It is a 250 amino acid polypeptide consisting of two domains. The C-terminal domain (CTD) functions in DNA binding while the N-terminal domain (NTD) functions in AHL binding (22). Once the NTD is bound by AHL, LuxR forms a homodimer, and the CTD interacts with the *lux* box on target promoters to activate transcription. The *lux* box upstream of the *lux* operon is a 20-bp palindromic sequence centered around -42.5 of the promoter, at which a dimerized LuxR binds (23). Studies have shown that RNA polymerase cannot bind to the Class II type *lux* promoter on its own; it requires interactions with the LuxR CTD (24). Apart from activating the *lux* operon, LuxR positively autoregulates itself and regulates around 10 other promoters, which comprise of the LuxR regulon (25–27).

The LuxR protein family

LuxR requires AHL to attain a proper fold during translation of the mRNA. However, the formation of the LuxR-AHL complex is reversible (28). Once functionally folded and dimerized, it can assume stable conformations both in the absence and presence of AHL, thus allowing *V. fischeri* to adapt to sudden changes in population density rapidly. For this reason it has been classified as a Class-2 QS regulator (FIGURE 1.2) (29). In contrast, Class-1 LuxR family proteins, such as TraR from *Agrobacterium tumefaciens*, require AHL co-translationally and are incapable of binding it reversibly (30). TraR is rapidly degraded by proteases when synthesized in the absence of AHL (30). Class-3 receptors fold into an inactive form that is incapable of

binding DNA in the absence of AHL, but can bind DNA once associated with AHL. Class-5 receptors are the only class that remain monomeric when bound to AHL, (e.g; SdiA from *E. coli* (31)). These four classes of receptors are similar in their necessity to be bound by the AHL ligand in order to bind to DNA. However, Class-4 receptors function in an opposite manner. They maintain functional conformation in the absence of AHL and are incapable of binding to DNA when bound by AHL. EsaR, the master QS regulator in the corn pathogen *Pantoea stewartii* is a Class-4 type LuxR receptor. EsaR controls exopolysaccharide production in *P. stewartii*, which is a virulence factor responsible for causing Stewart's wilt in corn. Other Class-4 AHL-hindered LuxR homologues include ExpR of *Erwinia chrysanthemi* (32), YenR of *Yersinia enterocolitica* (33) and EanR from *Pantoea ananatis* (34).

Structural information for the LuxR family is limited, in part due to the solubility issues during purification and the instability of the structures in the absence of their ligands. Two LuxR homologues, TraR from *A. tumefaciens* and the NTD of LasR from *Pseudomonas aeruginosa*, have been crystallized with their cognate AHL molecules (35, 36). TraR is an asymmetric dimer with the two monomers at 90° to each other. LasR is also a dimer, but possesses a symmetric axis between the two monomers. Crystal structure is also available for another LuxR homologue from *P. aeruginosa*, QscR (37). AHL-bound QscR forms a dimer with a distinct cross-subunit arrangement. NMR data exists for the NTD of the monomeric Class-5 LuxR homologue, SdiA with a candidate AHL. *Escherichia coli* does not possess a cognate AHL and thus SdiA is thought to serve as a sensor of AHLs produced by other bacterial species (31). Each receptor, though sharing similarities in their monomeric subunits, possess variations in their quaternary structures (29). The crystal structure of CviR bound to an antagonist ligand suggests a model for the

inactive state of LuxR proteins (38), but there is no structural information for any LuxR homologue in the absence of the ligand. Class-4 QS receptors such as EsaR provide a unique opportunity to study the structural changes associated with AHL binding in the AHL-hindered subfamily of QS regulators.

The EsaR-EsaI system of *Pantoea stewartii*

Similar to all members of the LuxR family, EsaR is a two-domain protein with an AHL-binding NTD and a DNA-binding CTD (39). EsaR, as well as other members of the AHL-hindered subfamily, also contain two unique regions in comparison to the rest of the larger LuxR family, an extended linker region between the AHL binding NTD and DNA binding CTD (residues 171 to 178) and extra residues at the C-terminus of the polypeptide (residues 237 to 249) (29). Deletion of either of these regions renders the protein nonfunctional (40). The promoter region of *esaR* features a well conserved *lux* box-like element, the *esa* box, centered on the -10 site. Presence of dimeric EsaR on the palindromic *esa* box prevents transcription by RNA polymerase. Biochemical confirmation for EsaR as a DNA binding protein came from electrophoretic mobility shift assays (EMSAs) and surface plasmon resonance (SPR) studies. These studies showed that purified, AHL-free EsaR specifically binds DNA fragments containing the *esaR* box palindrome as a dimer. However in the EMSA assays, even excess levels of synthetic 3-oxo-C6-HSL failed to induce EsaR/DNA complex dissociation (39, 41). Genetic studies in an *E. coli* background showed that a *PesaR::lacZ* reporter was fully active in the absence of EsaR, but was repressed by EsaR in a dose-dependent manner. Moreover, the EsaR repressor activity was rapidly neutralized by addition of exogenous AHL (39). EsaR is also capable of binding to *esa* boxes further upstream of transcriptional start sites and activating

transcription by positively interacting with RNA polymerase (40). Initially, EsaR was demonstrated to bind to the *lux* box in recombinant *E. coli* and activate transcription from the *lux* operon, although the recognition efficiency was about four-fold less than the native *esa* box (42). The ability of EsaR to function as an activator was first demonstrated in its native host by identification of an EsaR-activated native promoter of *P. stewartii* that controls the expression of a small non-coding RNA, EsaS (40) (FIGURE 1.3).

Critical to plant virulence, EsaR regulates exopolysaccharide production by repressing transcription of *rcaA*, which encodes a transcriptional activator involved in a two-component environmental sensory pathway (43). At low cell density, EsaR represses itself by binding to the *esa* box within its own promoter and also blocks transcription within the promoter of *rcaA*. The *esaR* gene is convergently transcribed with the constitutively expressed *esaI* gene, which encodes for the cognate AHL synthase, EsaI. At high cell density, an EsaR-AHL complex forms, which leads to dissociation of EsaR from DNA and expression of both *esaR* and *rcaA* (FIGURE 1.3). RcsA in turn activates expression of the *cps* operons, leading to production of the exopolysaccharide, stewartan (44, 45). A deletion in *esaR* results in an increase in exopolysaccharide production, independent of AHL concentrations. Strains with inactivated *esaR* are capable of synthesizing exopolysaccharide at low cell density and produce excess amounts of capsule. Hypermucoid strains are less virulent than the wild-type parent and form indeterminate 'floating' biofilms (46). Interestingly, strains without *esaI* that possess EsaR at high cell densities, are deficient in capsule production and are avirulent in plant infection assays. This suggests that *P. stewartii* uses QS to delay the expression of stewartan during the early stages of infection so that it does not interfere with other mechanisms of pathogenesis (47). Thus

in *P. stewartii*, AHL production is instrumental to pathogenesis by controlling the timing of the QS response.

The plant pathogen *Pantoea stewartii*

P. stewartii, a Gram-negative proteobacterium is the causative agent of Stewart's wilt disease of corn. *P. stewartii* is an agriculturally relevant pathogen that has caused severe reductions in crop yields during the 1930s. Seedlings can contract the disease from soil, manure or seed, but the most common mode of transmission is via the insect vector *Chaetocnema pulicaria*, the corn flea beetle. Incidence of wilt is directly proportional to winter temperatures and the survival of the beetle (48). Currently, control of Stewart's wilt in corn is achieved by using resistant cultivars, disease-free seeds or eliminating vector populations (48). The *Pantoea* genus is similar to the plant pathogenic *Erwinia* and *Pectobacterium* genera. *Erwinia amylovora* causes fire blight in apples and pears and *Pectobacterium carotovora* causes bacterial soft rot in a wide variety of plants. Other plant pathogenic *Pantoea* species include *P. ananatis*, known to cause soft-rot in onions and *Tautumella citrea* (previously *Pantoea citrea*) that causes pink rot of pineapples (49, 50).

P. stewartii is carried in the mid-gut of the corn flea beetle and can be transmitted to plants throughout the beetle's life. Springtime feeding by beetles deposits the bacterium directly into wounds on leaf tissue (51). Once within the plants, the bacteria express a Hrp-Hrc1(hypersensitive response and pathogenicity)- Type 3 secretion system (T3SS) that secretes effector proteins and induces electrolyte leakage and tissue watersoaking (52). This symptom is characteristic of the early phase of infection when the bacteria reside in the host apoplast. The

bacteria subsequently migrate to the xylem where they grow to high cell densities and form a biofilm. One of the characteristic symptoms of Stewart's wilt is the extrusion of yellow bacterial slime from the stems of infected plants. In the xylem, the bacteria overproduce the exopolysaccharide stewartan that acts as a barrier against plant host defenses and obstructs the free flow of xylem fluid, leading to seedling wilt. Blockage of water flow also causes the chlorotic and necrotic parallel streaks on leaves (48) (FIGURE 1.4). Production of stewartan is regulated by the EsaR/EsaI Q-S circuit of *P. stewartii* as described above. *P. stewartii* possesses another Type 3 secretion system, a PSI-2 (*Pantoea* secretion island 2) T3SS that is required for persistence in the corn flea beetle (53). Interestingly, the Hrp-Hrc1 T3SS is not under control by QS, and it is not currently known whether the PSI-2 T3SS is regulated by QS. The function of EsaR as a repressor and activator at low cell-densities allows for the temporal regulation of two different sets of genes over growth. Identifying additional genes regulated by QS would elucidate factors important in the pathogenesis of *P. stewartii*, aiding in the development of QS intervention strategies.

QS strategies in plant pathogenic bacteria

Many plant-associated pathogens have been studied that utilize QS to regulate colonization and disease progression in plant hosts, for example *P. carotovora*, *E. chrysanthemi*, *Ralstonia solanacearum*, *Pseudomonas syringae*, *Xanthomonas campestris* and *Xanthomonas oryzae* (54). A major goal of studying QS is to develop methods by which plants can be made resistant to diseases caused by bacterial pathogens. One strategy of interest is the inactivation of AHL signals by enzymes, which could be a convenient approach for engineering disease-resistant plants (54). One such enzyme, AiiA, a lactonase from *Bacillus cereus*, has been well-studied for

degrading the lactone ring of many AHLs, thus reducing their potency by 1000-fold (55). Expression of AiiA *in trans* in *P. carotovora* was shown to disrupt QS and reduce virulence (56). Transgenic *Amorphophallus konjac*, an economically important crop affected by bacterial soft rot, was highly resistant to infection by *E. carotovora* during expression of *aiiA* in the genome (57). The potential to create transgenic plants that express AiiA is attractive, but can also lead to drastic consequences in the environment if the QS system is not studied thoroughly. AiiA production in the economically important *Sinorhizobium meliloti* reduced formation of nodule and interrupted QS signaling in the bacterium (58). More detailed studies on the effect of such intervention strategies on pathogens, as well as beneficial symbionts, needs to be performed in order to implement effective measures involving manipulation of the QS response.

Research Plan

P. stewartii provides an excellent model to study QS in plant pathogenic bacteria and to study the AHL responsiveness of the QS regulator EsaR, a Class-4 LuxR homologue. There is an evident gap in current literature about the structure of LuxR homologues in the presence and absence of the AHL ligand, and how AHL binding in the NTD translates to changes in the DNA-binding capacity of the CTD. Chapter Two describes attempts to better understand the structural and functional changes in EsaR due to binding of AHL. Such information provides valuable insights into the mechanism of action of LuxR homologues, which are difficult to study *in vitro*. A lack of information exists about the extent of QS regulation in agriculturally-relevant plant pathogenic bacteria. Chapter Three and Four describe efforts to identify the genes involved in the QS regulon of *P. stewartii* and the genes whose expression is directly regulated by EsaR.

Chapter Five analyzes the function of two EsaR directly regulated genes in plant pathogenesis in an attempt to understand their role in Stewart's wilt disease. These studies will help in broadening our understanding of QS and may aid in understanding the process of plant pathogenesis. Ultimately this can lead to the development of specific therapies in combating *P. stewartii* and could translate to other agriculturally relevant plant pathogens, especially those causing wilt.

REFERENCES:

1. **von Bodman SB, Willey JM, Diggle SP.** 2008. Cell-cell communication in bacteria: united we stand. *J. Bacteriol.* **190**:4377–4391.
2. **Fuqua C, Parsek MR, Greenberg EP.** 2001. Regulation of gene expression by cell-to-cell communication: acyl-homoserine lactone quorum sensing. *Annu. Rev. Genet.* **35**:439–468.
3. **Ng WL, Bassler BL.** 2009. Bacterial quorum-sensing network architectures. *Annu. Rev. Genet.* **43**:197–222.
4. **West SA, Griffin AS, Gardner A.** 2007. Evolutionary explanations for cooperation. *Curr. Biol.* **17**:R661–R672.
5. **Fuqua WC, Winans SC, Greenberg EP.** 1994. Quorum sensing in bacteria: the LuxR-LuxI family of cell density-responsive transcriptional regulators. *J. Bacteriol.* **176**:269–275.
6. **Kempner ES, Hanson FE.** 1968. Aspects of light production by *Photobacterium fischeri*. *J. Bacteriol.* **95**:975–9.
7. **Fuqua C, Winans SC, Greenberg EP.** 1996. Census and consensus in bacterial ecosystems: the LuxR-LuxI family of quorum-sensing transcriptional regulators. *Annu. Rev. Microbiol.* **50**:727–751.
8. **Visick KL, Ruby EG.** 2006. *Vibrio fischeri* and its host: it takes two to tango. *Curr. Opin. Microbiol.* **9**:632–638.
9. **Kaplan HB, Greenberg EP.** 1985. Diffusion of autoinducer is involved in regulation of the *Vibrio fischeri* luminescence system. *J. Bacteriol.* **163**:1210–1214.
10. **Kleerebezem M, Quadri LE, Kuipers OP, de Vos WM.** 1997. Quorum sensing by peptide pheromones and two-component signal-transduction systems in Gram-positive bacteria. *Mol. Microbiol.* **24**:895–904.
11. **Håvarstein LS, Coomaraswamy G, Morrison DA.** 1995. An unmodified heptadecapeptide pheromone induces competence for genetic transformation in *Streptococcus pneumoniae*. *Proc. Natl. Acad. Sci. U. S. A.* **92**:11140–11144.
12. **Waters CM, Bassler BL.** 2005. Quorum sensing: cell-to-cell communication in bacteria. *Annu. Rev. Cell Dev. Biol.* **21**:319–346.

13. **McKenzie KM, Meijler MM, Lowery CA, Boldt GE, Janda KD.** 2005. A furanosyl-carbonate autoinducer in cell-to-cell communication of *V. harveyi*. *Chem. Commun. (Camb)*. 4863–4865.
14. **Liu G, Chater KF, Chandra G, Niu G, Tan H.** 2013. Molecular regulation of antibiotic biosynthesis in streptomyces. *Microbiol. Mol. Biol. Rev.* **77**:112–43.
15. **Holden MT, Ram Chhabra S, de Nys R, Stead P, Bainton NJ, Hill PJ, Manefield M, Kumar N, Labatte M, England D, Rice S, Givskov M, Salmond GP, Stewart GS, Bycroft BW, Kjelleberg S, Williams P.** 1999. Quorum-sensing cross talk: isolation and chemical characterization of cyclic dipeptides from *Pseudomonas aeruginosa* and other gram-negative bacteria. *Mol. Microbiol.* **33**:1254–1266.
16. **Loh J, Pierson EA, Pierson LS, Stacey G, Chatterjee A.** 2002. Quorum sensing in plant-associated bacteria. *Curr. Opin. Plant Biol.* **5**:285–290.
17. **Nasser W, Reverchon S.** 2007. New insights into the regulatory mechanisms of the LuxR family of quorum sensing regulators. *Anal. Bioanal. Chem.* **387**:381–390.
18. **Moré MI, Finger LD, Stryker JL, Fuqua C, Eberhard A, Winans SC.** 1996. Enzymatic synthesis of a quorum-sensing autoinducer through use of defined substrates. *Science* **272**:1655–1658.
19. **Kuo A, Blough N V, Dunlap P V.** 1994. Multiple N-acyl-L-homoserine lactone autoinducers of luminescence in the marine symbiotic bacterium *Vibrio fischeri*. *J. Bacteriol.* **176**:7558–7565.
20. **Waters CM, Bassler BL.** 2006. The *Vibrio harveyi* quorum-sensing system uses shared regulatory components to discriminate between multiple autoinducers. *Genes Dev.* **20**:2754–2767.
21. **Henikoff S, Wallace JC, Brown JP.** 1990. Finding protein similarities with nucleotide sequence databases. *Methods Enzymol.* **183**:111–132.
22. **Choi SH, Greenberg EP.** 1992. Genetic dissection of DNA binding and luminescence gene activation by the *Vibrio fischeri* LuxR protein. *J. Bacteriol.* **174**:4064–9.
23. **Antunes LCM, Ferreira RBR, Lostroh CP, Greenberg EP.** 2008. A mutational analysis defines *Vibrio fischeri* LuxR binding sites. *J. Bacteriol.* **190**:4392–7.
24. **Stevens a M, Dolan KM, Greenberg EP.** 1994. Synergistic binding of the *Vibrio fischeri* LuxR transcriptional activator domain and RNA polymerase to the lux promoter region. *Proc. Natl. Acad. Sci. U. S. A.* **91**:12619–23.
25. **Williams JW, Cui X, Levchenko A, Stevens AM.** 2008. Robust and sensitive control of a quorum-sensing circuit by two interlocked feedback loops. *Mol. Syst. Biol.* **4**:234.

26. **Qin N, Callahan SM, Dunlap P V, Stevens AM.** 2007. Analysis of LuxR regulon gene expression during quorum sensing in *Vibrio fischeri*. *J. Bacteriol.* **189**:4127–4134.
27. **Antunes LCM, Schaefer AL, Ferreira RBR, Qin N, Stevens AM, Ruby EG, Greenberg EP.** 2007. Transcriptome analysis of the *Vibrio fischeri* LuxR-LuxI regulon. *J. Bacteriol.* **189**:8387–8391.
28. **Urbanowski ML, Lostroh CP, Greenberg EP.** 2004. Reversible acyl-homoserine lactone binding to purified *Vibrio fischeri* LuxR protein. *J. Bacteriol.* **186**:631–637.
29. **Stevens AM, Queneau Y, Soulère L, von Bodman S, Doutheau A.** 2011. Mechanisms and synthetic modulators of AHL-dependent gene regulation. *Chem. Rev.* **111**:4–27.
30. **Zhu J, Winans SC.** 2001. The quorum-sensing transcriptional regulator TraR requires its cognate signaling ligand for protein folding, protease resistance, and dimerization. *Proc. Natl. Acad. Sci. U. S. A.* **98**:1507–1512.
31. **Yao Y, Martinez-Yamout MA, Dickerson TJ, Brogan AP, Wright PE, Dyson HJ.** 2006. Structure of the *Escherichia coli* quorum sensing protein SdiA: Activation of the folding switch by acyl homoserine lactones. *J. Mol. Biol.* **355**:262–273.
32. **Castang S, Reverchon S, Gouet P, Nasser W.** 2006. Direct evidence for the modulation of the activity of the *Erwinia chrysanthemi* quorum-sensing regulator ExpR by acylhomoserine lactone pheromone. *J. Biol. Chem.* **281**:29972–87.
33. **Atkinson S, Chang C-Y, Sockett RE, Cámara M, Williams P.** 2006. Quorum sensing in *Yersinia enterocolitica* controls swimming and swarming motility. *J. Bacteriol.* **188**:1451–1461.
34. **Morohoshi T, Nakamura Y, Yamazaki G, Ishida A, Kato N, Ikeda T.** 2007. The plant pathogen *Pantoea ananatis* produces N-acylhomoserine lactone and causes center rot disease of onion by quorum sensing. *J. Bacteriol.* **189**:8333–8338.
35. **Zhang R, Pappas KM, Pappas T, Brace JL, Miller PC, Oulmassov T, Molyneux JM, Anderson JC, Bashkin JK, Winans SC, Joachimiak A.** 2002. Structure of a bacterial quorum-sensing transcription factor complexed with pheromone and DNA. *Nature* **417**:971–4.
36. **Bottomley MJ, Muraglia E, Bazzo R, Carfi A.** 2007. Molecular insights into quorum sensing in the human pathogen *Pseudomonas aeruginosa* from the structure of the virulence regulator LasR bound to its autoinducer. *J. Biol. Chem.* **282**:13592–600.
37. **Lintz MJ, Oinuma K-I, Wysoczynski CL, Greenberg EP, Churchill ME a.** 2011. Crystal structure of QscR, a *Pseudomonas aeruginosa* quorum sensing signal receptor. *Proc. Natl. Acad. Sci. U. S. A.* **108**:15763–8.

38. **Chen G, Swem LR, Swem DL, Stauff DL, O’Loughlin CT, Jeffrey PD, Bassler BL, Hughson FM.** 2011. A strategy for antagonizing quorum sensing. *Mol. Cell* **42**:199–209.
39. **Minogue TD, Wehland-von Trebra M, Bernhard F, von Bodman SB.** 2002. The autoregulatory role of EsaR, a quorum-sensing regulator in *Pantoea stewartii* ssp. *stewartii*: evidence for a repressor function. *Mol. Microbiol.* **44**:1625–35.
40. **Schu DJ, Carlier AL, Jamison KP, von Bodman S, Stevens AM.** 2009. Structure/function analysis of the *Pantoea stewartii* quorum-sensing regulator EsaR as an activator of transcription. *J. Bacteriol.* **191**:7402–7409.
41. **Minogue TD, Carlier AL, Koutsoudis MD, Bodman SB von.** 2005. The cell density-dependent expression of stewartan exopolysaccharide in *Pantoea stewartii* ssp. *stewartii* is a function of EsaR-mediated repression of the *rcsA* gene. *Mol. Microbiol.* **56**:189–203.
42. **Bodman SB von, Ball JK, Faini MA, Herrera CM, Minogue TD, Urbanowski ML, Stevens AM.** 2003. The quorum sensing negative regulators EsaR and ExpR Ecc , homologues within the LuxR family, retain the ability to function as activators of transcription. *Society* **185**:7001–7007.
43. **Carlier AL, von Bodman SB.** 2006. The *rcsA* promoter of *Pantoea stewartii* subsp. *stewartii* features a low-level constitutive promoter and an EsaR quorum-sensing-regulated promoter. *J. Bacteriol.* **188**:4581–4.
44. **Herrera CM, Koutsoudis MD, Wang X, Bodman SB von.** 2008. *Pantoea stewartii* subsp. *stewartii* exhibits surface motility, which is a critical aspect of Stewart ’s wilt disease development on maize. *Mol. Plant-Microbe Interact.* **21**:1359–1370.
45. **Torres-Cabassa AS, Gottesman S.** 1987. Capsule synthesis in *Escherichia coli* K-12 is regulated by proteolysis. *J. Bacteriol.* **169**:981–989.
46. **Koutsoudis MD, Tsaltas D, Minogue TD, von Bodman SB.** 2006. Quorum-sensing regulation governs bacterial adhesion, biofilm development, and host colonization in *Pantoea stewartii* subspecies *stewartii*. *Proc. Natl. Acad. Sci. U. S. A.* **103**:5983–5988.
47. **von Bodman SB, Majerczak DR, Coplin DL.** 1998. A negative regulator mediates quorum-sensing control of exopolysaccharide production in *Pantoea stewartii* subsp. *stewartii*. *Proc. Natl. Acad. Sci. U. S. A.* **95**:7687–7692.
48. **Pataky J.** 2003. Stewart’s wilt of corn. doi:10.1094/APSnetFeature-2003-0703.
49. **Coutinho TA, Venter SN.** 2009. *Pantoea ananatis*: an unconventional plant pathogen. *Mol. Plant Pathol.* **10**:325–335.

50. **Brady CL, Venter SN, Cleenwerck I, Vandemeulebroecke K, De Vos P, Coutinho T.** 2010. Transfer of *Pantoea citrea*, *Pantoea punctata* and *Pantoea terrea* to the genus *Tatumella* emend. as *Tatumella citrea* comb. nov., *Tatumella punctata* comb. nov. and *Tatumella terrea* comb. nov. and description of *Tatumella morbiroseisp.* nov. Int. J. Syst. Evol. Microbiol. **60**:484–94.
51. **Roper MC.** 2011. *Pantoea stewartii* subsp. *stewartii*: lessons learned from a xylem-dwelling pathogen of sweet corn. Mol. Plant Pathol. **12**:628–37.
52. **Merighi M, Majerczak DR, Stover EH, Coplin DL.** 2003. The HrpX/HrpY two-component system activates *hrpS* expression, the first step in the regulatory cascade controlling the Hrp regulon in *Pantoea stewartii* subsp. *stewartii*. Mol. Plant-Microbe Interact. MPMI **16**:238–248.
53. **Correa VR, Majerczak DR, Ammar E-D, Merighi M, Pratt RC, Hogenhout SA, Coplin DL, Redinbaugh MG.** 2012. The bacterium *Pantoea stewartii* uses two different type III secretion systems to colonize its plant host and insect vector. Appl. Environ. Microbiol.
54. **von Bodman SB, Bauer WD, Coplin DL.** 2003. Quorum sensing in plant-pathogenic bacteria. Annu. Rev. Phytopathol. **41**:455–82.
55. **Dong YH, Xu JL, Li XZ, Zhang LH.** 2000. AiiA, an enzyme that inactivates the acylhomoserine lactone quorum-sensing signal and attenuates the virulence of *Erwinia carotovora*. Proc. Natl. Acad. Sci. U. S. A. **97**:3526–3531.
56. **Mahmoudi E, Naderi D, Venturi V.** 2012. AiiA lactonase disrupts N-acylhomoserine lactone and attenuates quorum-sensing-related virulence in *Pectobacterium carotovorum* EMPCC. Ann. Microbiol.
57. **Ban H, Chai X, Lin Y, Zhou Y, Peng D, Zhou Y, Zou Y, Yu Z, Sun M.** 2009. Transgenic *Amorphophallus konjac* expressing synthesized acyl-homoserine lactonase (*aiiA*) gene exhibit enhanced resistance to soft rot disease. Plant Cell Rep. **28**:1847–1855.
58. **Gao M, Chen H, Eberhard A, Gronquist MR, Robinson JB, Connolly M, Teplitski M, Rolfe BG, Bauer WD.** 2007. Effects of AiiA-mediated quorum quenching in *Sinorhizobium meliloti* on quorum-sensing signals, proteome patterns, and symbiotic interactions. Mol. Plant. Microbe. Interact. **20**:843–856.

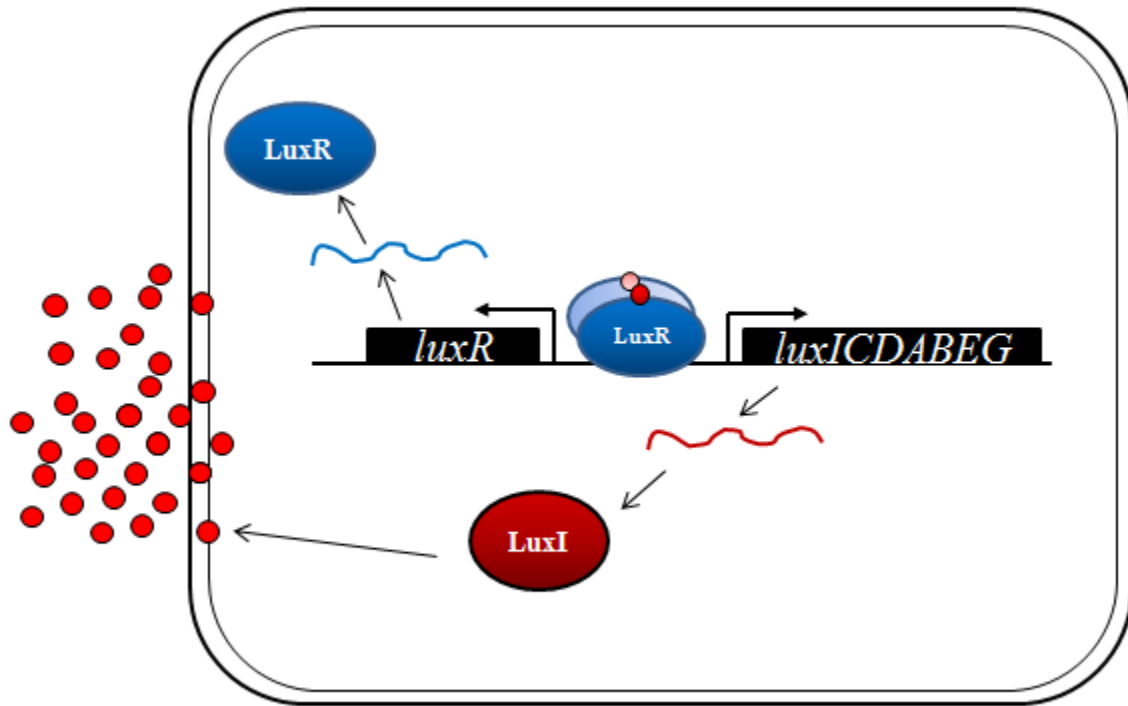


FIGURE 1.1: Model of the QS circuit of *Vibrio fischeri*. The acylated homoserine lactone signal, AHL (small red circles) are produced by the AHL-synthase LuxI. At high cell densities, the diffusible signal is bound by the transcriptional regulator LuxR which in turn binds to the *lux* box and activates transcription of the *lux* operon, causing the production of bioluminescence and creating a positive feedback loop that further amplifies AHL signal production.

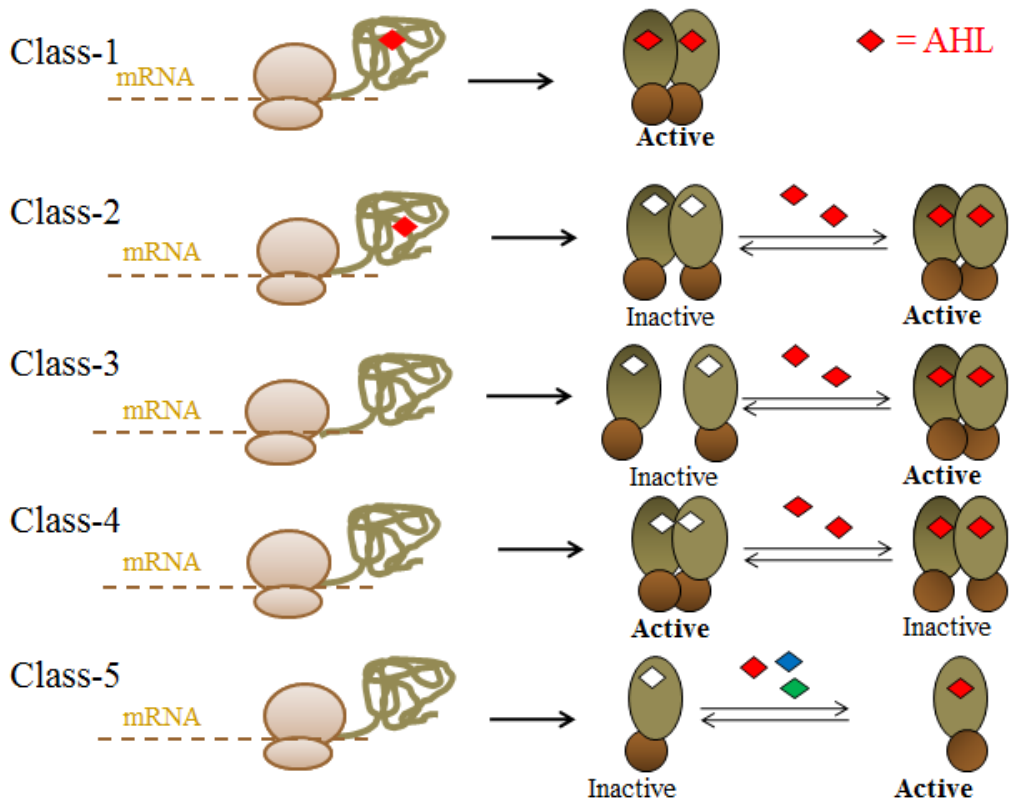


FIGURE 1.2: The different classes of LuxR homologues. ‘Active/Inactive’ refers to the ability of the protein to bind to DNA . Class-1 receptors require AHL to be folded functionally. Class-2 receptors require AHL during folding, but are capable of reversibly binding AHL. Class-3 receptors are folded into an inactive form in the absence of AHL, but are activated once bound by the ligand. Class-4 receptors are active in the absence of AHL and inactive when bound by AHL. Class-5 receptors are monomeric and can be activated by binding to a variety of AHLs. Adapted from (29).

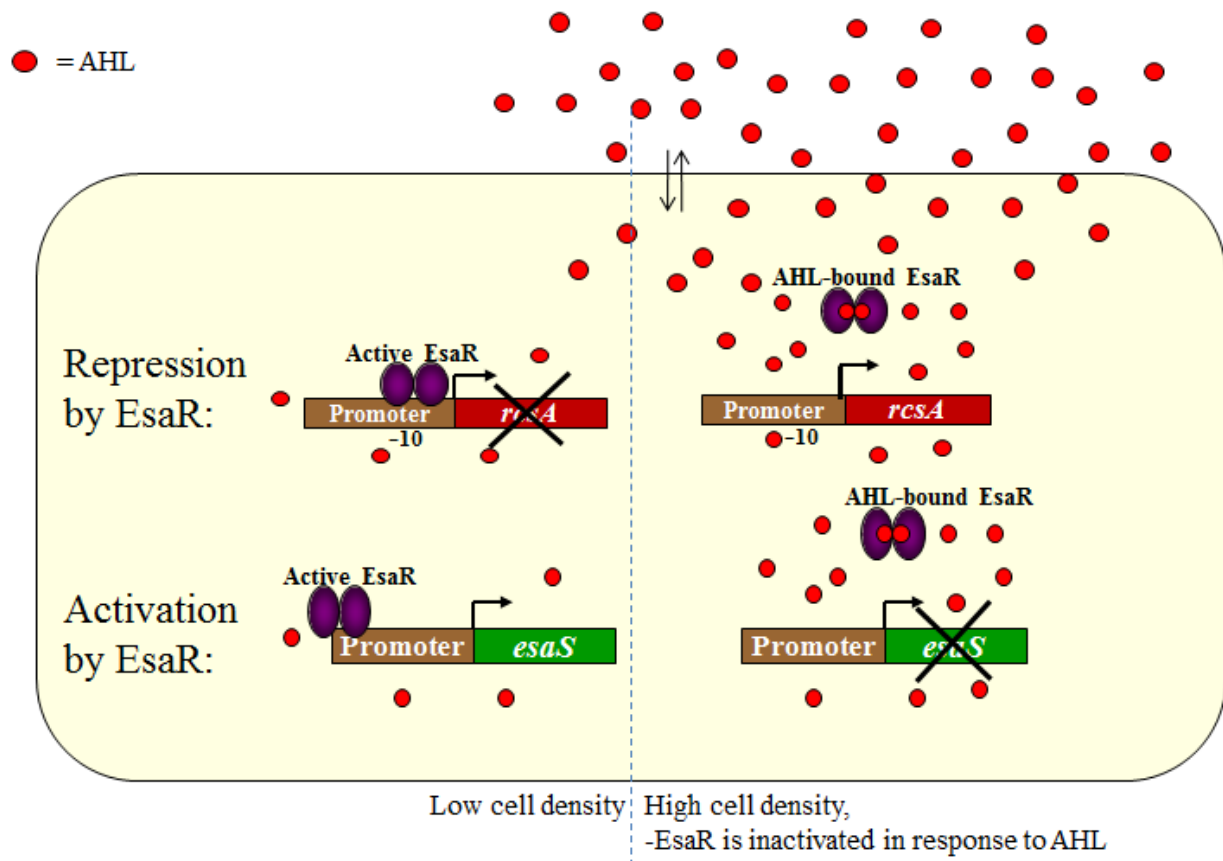


FIGURE 1.3: Model of QS in *Pantoaea stewartii*. The QS-dependent transcriptional regulator EsaR binds to 20-bp palindromic sequences in promoter regions of *rcsA* (activator of capsular synthesis operon) and *esaS* (small non-coding RNA of unknown function) and represses and activates expression at low cell-densities, respectively. At high cell-densities, EsaR is bound by AHL, 3-oxo-C6-HSL produced from the cognate AHL synthase, EsaI. This causes EsaR to release the DNA resulting in derepression of *rcsA* or deactivation of *esaS*. EsaR also autorepresses its own expression at low cell-densities.

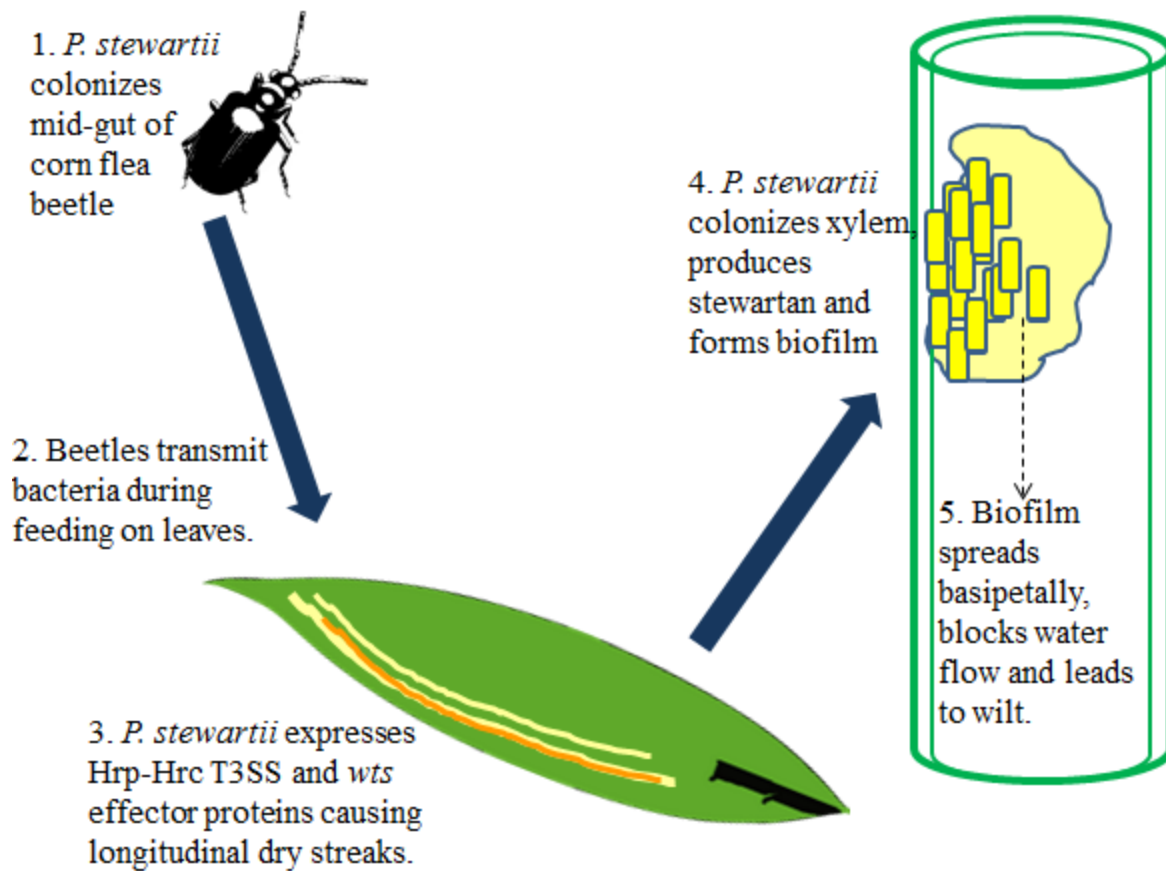


FIGURE 1.4: Mechanism of *P. stewartii* infection in *Zea mays*. 1., The bacterium overwinters in the mid-gut of the corn flea beetle, *Chaetocnema pulicaria*. 2., The beetle transmits the bacteria into wounds on the leaf during feeding. 3., *P. stewartii* expresses a Hrp-Hrc Type III secretion system (T3SS) that secretes water-soaking (*wts*) effector proteins causing electrolyte leakage and tissue water-soaking. 4., The bacterium subsequently colonizes the xylem, where it forms a biofilm and secretes excess stewartan. 5., The bacterium spreads basipetally to colonize the entire xylem lumen, leading to blockage of water transport, causing systemic wilting and in some cases, death.

Chapter Two

Probing the Impact of Ligand Binding on the Acyl-Homoserine Lactone-Hindered Transcription Factor EsaR of *Pantoea stewartii* subsp. *stewartii*

Daniel J. Schu⁺, Revathy Ramachandran⁺, Jared S. Geissinger and Ann M. Stevens*. 2011.
Probing the Impact of Ligand Binding on the Acyl-Homoserine Lactone-Hindered Transcription
Factor EsaR of *Pantoea stewartii* subsp. *stewartii*. J. Bacteriol. Vol. 193 no. 22, Page 6315-6322.

⁺authors contributed equally

*Corresponding author:

Department of Biological Sciences MC 0910
1070 Washington St. SW / Rm. 219 Life Sciences 1
Virginia Tech
Blacksburg, VA 24061
Phone (540)-231-9378
Email ams@vt.edu

Revathy Ramachandran performed the experiments illustrated in Fig 2.1 (A), Fig 2.2 and Fig. 2.4.

ABSTRACT:

The quorum-sensing regulator EsaR from *Pantoea stewartii* subsp. *stewartii* is a LuxR homologue that is inactivated by acyl-homoserine lactone (AHL). In the corn pathogen *P. stewartii*, production of exopolysaccharide (EPS) is repressed by EsaR at low cell densities. However, at high cell densities when high concentrations of its cognate AHL signal are present, EsaR is inactivated and derepression of EPS production occurs. Thus, EsaR responds to AHL in a manner opposite to that of most LuxR family members. Depending on the position of its binding site within target promoters, EsaR serves as either a repressor or activator in the absence rather than in the presence of its AHL ligand. The effect of AHL on LuxR homologues has been difficult to study *in vitro* because AHL is required for purification and stability. EsaR, however, can be purified without AHL enabling an *in vitro* analysis of the response of the protein to ligand. Western immunoblots and pulse-chase experiments demonstrated that EsaR is stable *in vivo* in the absence or presence of AHL. Limited *in vitro* proteolytic digestions of a biologically active His-MBP tagged version of EsaR highlighted intradomain and interdomain conformational changes that occur in the protein in response to AHL. Gel filtration chromatography of the full-length fusion protein and cross-linking of the N-terminal domain both suggest that this conformational change does not impact the multimeric state of the protein. These findings provide greater insight into the diverse mechanisms for AHL responsiveness found within the LuxR family.

INTRODUCTION:

The ability of a bacterium to thrive in a particular environment is dependent upon its ability to sense and respond to various environmental factors, including osmolarity, pH, temperature, nutrient availability, or even the presence of other bacteria. Cell-cell communication, or quorum sensing, has been characterized in a number of bacteria that produce and respond to signal molecules commonly termed autoinducers. The well-studied *Vibrio fischeri* quorum-sensing system has served as a model for quorum sensing in Gram-negative proteobacteria. In this system, the LuxI autoinducer synthase protein produces an acyl-homoserine lactone (AHL) autoinducer, *N*-3-oxo-hexanoyl-L-homoserine lactone (10). At a threshold concentration of AHL, the LuxR receptor protein forms complexes with this ligand. Binding of the autoinducer molecule permits LuxR to take on a functional conformation capable of binding DNA and activating genes involved in the production of bioluminescence (reviewed in references 11, 30, and 32).

Many other Gram-negative proteobacteria have been shown to carry out a similar type of signaling and recognition. For the majority of the LuxR homologues identified in different bacterial species, a model has been proposed whereby AHL binding induces multimerization of the protein, leading to stabilization and DNA binding (18, 19, 26, 36). In the case of TraR from *Agrobacterium tumefaciens*, *in vivo* experiments demonstrated that the half-life of TraR is significantly shortened in the absence of its cognate AHL. More specifically, the Clp and Lon proteases play a direct role in regulating the levels of TraR within the cell (37). Whether or not this mechanism of posttranslational regulation is conserved across the entire LuxR family is unknown.

It has been proposed that the LuxR family of proteins can be divided into at least five classes (23). The majority of the LuxR family members are activators that become functional after interacting with AHL. TraR (class I) is stable only when AHL is present during translation and AHL binding is not readily reversible (37). LuxR (class II) is stabilized by the presence of AHL, but AHL binding is reversible (26), while MrtR (class III) from *Mesorhizobium tianshanense* (33) is stable without AHL but biologically active only when it is present. Class V regulators, such as SdiA from *Escherichia coli*, have not been shown to dimerize yet are capable of recognizing multiple noncognate AHLs (34). The class IV subset of LuxR homologues, represented by EsaR from *Pantoea stewartii* subsp. *stewartii*, was initially described as repressors that function using a reverse mechanism in comparison to the other classes of LuxR homologues (29). The class IV proteins maintain a functional conformation and bind DNA in the absence of their cognate AHL; biological activity is actually hindered by the presence of the AHL *N*-3-oxo-hexanoyl-L-homoserine lactone, in the majority of cases (reviewed in reference 24). Examples of these homologues, besides EsaR from *P. stewartii*, include ExpR from *Erwinia chrysanthemi* and *Pectobacterium carotovorum* (7, 21), YenR from *Yersinia enterocolitica* (1, 25), and EanR from *Pantoea ananatis* (16). Structurally, the members of the EsaR subfamily also share the characteristics of having an extended linker region between the AHL-binding N-terminal domain (NTD) and an extended DNA-binding C-terminal domain (CTD) (23).

At low cell densities, EsaR negatively regulates its own expression and the expression of RcsA, an activator of exopolysaccharide (EPS) biosynthesis genes, which in turn positively regulates EPS production (6, 15, 29). EsaR also positively regulates expression of a small RNA (sRNA)

native to *P. stewartii* (20). In *P. stewartii* the LuxI homologue EsaI synthesizes *N*-3-oxo-hexanoyl-L-homoserine lactone (2), and at high cell densities this AHL interferes with the ability of EsaR to regulate gene expression (15, 28). Little biochemical information is available regarding the mechanism whereby AHL regulates the EsaR protein subfamily. However, in comparison to other members of the LuxR protein family, the relative stability and solubility of EsaR in the absence of its cognate AHL make it an attractive model for analyzing the impact of ligand binding.

A simple explanation for the AHL-dependent inactivation of EsaR would be a conformational shift, which causes the protein to become more susceptible to proteolytic processing. Hence, the susceptibility of EsaR to proteases in the absence and presence of its cognate AHL was examined both *in vivo* and *in vitro*. The impact of the ligand on the multimeric state of EsaR was also examined *in vitro*, as the conversion to and maintenance of a dimeric state are critical to the activity of many LuxR homologues (reviewed in reference 23). It is clear that the mode of AHL responsiveness by EsaR has distinctive features in comparison to the majority of quorum-sensing regulators.

MATERIALS AND METHODS:

Measurement of EsaR stability in *P. stewartii*. Luria-Bertani (LB) broth was inoculated with log-phase cells of *P. stewartii* DC283 (9) to an OD_{600 nm} of 0.025 and grown at 30°C. Aliquots were taken at time points during growth, cells were pelleted by centrifugation and stored at -70°C. LB supplemented with 10 μM *N*-(β-ketocaproyl)-L-homoserine lactone (AHL) (Sigma Aldrich) was similarly inoculated with *P. stewartii* DC283, grown at 30°C to an OD_{600 nm} of 1.5

and the cell pellet was harvested. After resuspension, 50 µg of each protein sample, as determined through a Bio-Rad Bradford protein assay, was analyzed via 12% SDS PAGE to confirm equal protein loads and subjected to Western immunoblotting with a 1:500 dilution of polyclonal antiserum generated against EsaR (28). Quantitation of bands of interest was performed using BioRad Quantity One 1D-Analysis software.

Measurements of EsaR stability in recombinant *E. coli*. To measure the half-life of EsaR in *E. coli* SG22163 (*malP::lacI^f*) (12), two plasmids, pT7-*esaR* and pJZ410 (37), were introduced into the strain. Plasmid pT7-*esaR* was constructed by amplifying the *esaR*-coding region from pBAD-EsaR (28) template. The reverse primer BAMESR1 (IDT) (5'GGATCCTTACTACCTGGCCGCTGACGCTG3') included a BamHI site; the upstream primer PCIES1 (IDT) (5'ACATGTTTTCTTTTTTCCTTGAAAATCAAACAATAACGG3') contained a PciI site overlapping with the *esaR* ATG start codon. The PCR product was cloned into pGEM-T (Promega) and sequenced. A 760-base pair (bp) PciI-BamHI fragment was digested from the pGEM-T construct, and ligated into NcoI-BamHI-digested pMLU115 (26). In the resulting plasmid, pT7-*esaR*, *esaR* expression is controlled by the phage T7 promoter. Plasmid pJZ410 (37) has a gene encoding T7 RNA polymerase under the control of a heat inducible promoter. Cells were cultured in LB containing 100 µg/ml ampicillin (Ap) and 20 µg/ml gentamycin at 28°C to an OD_{600nm} = 0.4. The cells were shocked at 45°C for 20 min to induce expression of T7 RNA polymerase, and treated with 200 µg/ml rifampicin to inhibit the host RNA polymerase. After 20 min at 45°C, the culture was shifted to 30°C for 30 min. At this point half of the culture volume was transferred to a tube containing 10 µM AHL, then [³⁵S] methionine was immediately added to both cultures (+/- AHL) to a final concentration of

5 μ Ci/ml. Radiolabeling was terminated after 3 min by adding excess nonlabeled methionine (5 mM). Aliquots were taken at time points up to 60 min, and cell pellets were placed at -20°C after centrifugation. Samples were analyzed using 12% SDS-PAGE and a Storm phosphorimager (GE Healthcare).

Generation and purification of HMGE fusion protein. A His6-MBP-Gly₅ linker-EsaR (HMGE) fusion protein was constructed through two rounds of PCR. Primers in the first round were used to amplify *esaR* from pKK-EsaR (EcoRI fragment encoding *esaR* from pBAD-EsaR [28] ligated into pKK223-3 [5] with the P_{tac} promoter upstream of *esaR*). Forward primer TEVESAR2 (IDT) (5'GAGAACCTGTACTTCCAGGGTGGTGGTGGTGGTATGTTTTCTTTTTTCCTTGAAAA TC3') contained a TEV cleavage site and sequences encoding part of the N-terminal end of EsaR separated by 15 nucleotides coding for 5 glycine residues. Reverse primer ATTBR (IDT) (5'GGGGACAACCTTTGTACAAGAAAGTTGCATTACTACCTGGCCGCTGACGCTC3') contained an *attB* site downstream of sequences encoding the C-terminal end of EsaR. An 800 bp PCR product was used as template in a second round of PCR. The forward primer ATTBTEV (IDT) (5'GGGGACAACCTTTGTACAAAAAAGTTGTGGAGAACCTGTACTTCCAG3'), containing the *attB* site upstream of the TEV proteolytic site, and the reverse primer from the first round of PCR were used in the second round of PCR. An 850-bp DNA fragment was recovered containing *attB*-TEV-Gly₅-*esaR*-*attB*. This DNA fragment was then used in a BP reaction following the vendor's protocol with the plasmid pDONR201 (Invitrogen). pDONR201 confers kanamycin resistance (Kn) at 50 μ g/ml, and is an entry vector in the Gateway System (Invitrogen). pDONR201 containing the fragment with *esaR* was recovered and screened by

PCR. Using the vendor's protocol, an LR reaction was performed with the vector pDEST-HISMBP (17) in which the vector contains a P_{lac} promoter controlling the expression of HMGE (pHMGE). Recovered plasmid DNA was sequenced to confirm integrity.

E. coli Top10 (13) harboring pHMGE was cultured at 30°C in LB broth containing 100 µg/ml Ap, in the presence or absence of 10 µM AHL to an $OD_{600nm} = 0.5-0.6$, at which point 0.5 mM IPTG was added, and the culture was then incubated overnight at 19°C. Cells were concentrated by centrifugation at 4°C for 10 min at 7,000 rpm in a Beckman JA-10 fixed angle rotor and resuspended in wash buffer (20 mM HEPES, 500 mM NaCl, 20 mM imidazole, 10% glycerol (pH 7.4)). The resuspension was lysed using a French pressure cell at 18,000 psi, and the lysates were cleared by ultracentrifugation at 40,000 rpm in a Beckman 70Ti ultra rotor at 4°C for 1 hr. The clarified cell lysate was filtered using a 0.2 µm syringe filter prior to loading it on to a Ni-NTA column. HMGE was purified using FPLC chromatography at 4°C (AKTAprime plus, GE Healthcare) with a 5 mL HisTrap HP column containing Ni-NTA resin (GE Healthcare). A linear gradient elution with wash buffer containing 20 to 500 mM imidazole was used to elute the HMGE from the column. All buffers utilized in purifying HMGE in the presence of AHL were supplemented with 10 µM AHL.

Generation and purification of EsaR NTD178. Using pHMGE as the DNA template, the forward primer ATTBTEV (IDT) and the reverse primer ATTBR178 (IDT) (5'GGGGACAACCTTTGTACAAGAAAGTTGCATTATCATTGTCCGCGCTCTG3') were used to amplify a PCR product that contained *attB*-TEV-Gly₅-*esaR* (amino acids 1 to 178)-*attB*. The PCR product was ligated into pGEM-T easy (Promega) and sequenced. After confirmation

of sequence integrity, the plasmid was used for the BP and LR reactions of Gateway cloning (Invitrogen) using the entry vector pDONR201 (Invitrogen) and the final destination vector pDEST-HISMBP (17), as described above. The resulting plasmid pHMGNTD178 was transformed and propagated in *E. coli* BL21 (DE3) (Stratagene).

The HMGNTD178 fusion protein (His₆-MBP-Gly₅-EsaR NTD) was purified from *E. coli* BL21 (DE3) cells in a manner very similar to that described above for HMGE, with the following changes. IPTG (1 mM) was used to induce protein expression overnight at 19°C. In addition to Ni-NTA resin, amylose resin (New England Biolabs) was used per the manufacturer's directions followed by gel filtration over a HiPrep 26/60 Sephacryl S-200 column (GE Healthcare) to further improve protein purify. After purification, fractions containing HMGNTD178, as indicated by 12% SDS-PAGE visualization, were pooled and dialyzed against an excess of wash buffer in the presence of TEV protease overnight at 4°C. The sample was then passed over a Ni-NTA column. The flowthrough (correlating to cleaved NTD178) was collected and passed over the Sephacryl S-200 column equilibrated with wash buffer without imidazole. Eluted protein was visualized on a 12% SDS-PAGE gel, and protein fractions correlating with the predicted molecular size of a monomer of NTD178 (~21 kDa) were pooled, concentrated, and stored at -70°C.

EMSA analysis of HMGE activity. The ability of purified HMGE to bind to DNA was analyzed through an electrophoretic mobility shift assay (EMSA) as previously described (15) using the ³²P-end-labeled 28-bp double-stranded oligonucleotide containing the 20-bp *esa* box sequence, *PesaR28*. HMGE (0 to 100 nM), additionally purified using a HiTrap Heparin HP

column (GE Healthcare) per the manufacturer's directions and the Sephacryl S-200 column, was incubated with 2 nM probe DNA for 20 min in EMSA binding buffer [20 mM HEPES, 1 mM EDTA, 30 mM KCl, 0.2% Tween 20, 10 mM (NH₄)₂SO₄, 50 ng/μl poly(dI-dC), 150 μg/ml acetylated bovine serum albumin (BSA), and 10% glycerol] in a total reaction volume of 20 μl. Samples were analyzed using 6% Tris-glycine-EDTA native PAGE with 1× Tris-glycine buffer at 80 V for 2 h in an apparatus packed in ice. After electrophoresis, gels were dried and visualized using a Typhoon Trio variable mode imager (GE Healthcare).

Partial *in vitro* proteolysis. Reaction mixtures of a 50-μl volume containing 13.5 μM purified HMGE were incubated with 72 nM thermolysin in the absence or presence of 67.5 μM AHL (5× concentration in relation to HMGE) for 1 h at 37°C under the following conditions: 25 μl of HMGE in wash buffer without imidazole was added to 25 μl of 2× thermolysin buffer (4 mM CaCl₂, 10% glycerol, 300 mM NaCl, 20 mM Tris-HCl [pH 8.0]). Reactions with thermolysin were stopped by the addition of 2 μl of 0.5 M EDTA (pH 8.0). Similarly, the fusion protein was also separately exposed to 54 nM trypsin for 1 h at room temperature with and without 67.5 μM AHL under the following conditions: 25 μl of HMGE in wash buffer without imidazole was added to 25 μl of 2× trypsin buffer (40 mM MgSO₄, 40 mM Tris-HCl [pH 7.5], 20 mM CaCl₂). Reactions were stopped by adding 12.5 μl of sample buffer (0.624 ml 1 M Tris [pH 6.8], 0.2 g SDS, 1.04 ml glycerol, 0.5 ml β-mercaptoethanol, trace bromophenol blue) and boiling prior to analysis via 12% SDS-PAGE.

For the limited proteolytic analysis of EsaR NTD178, 13.5 μM protein was exposed to decreasing concentrations of thermolysin (starting with 1.7 μM and serially diluted 2-fold to 110 nM). At each concentration of thermolysin, digestions were performed in the absence or

presence of AHL (67.5 μM), in a final concentration of $1\times$ thermolysin buffer and a final volume of 25 μl . After 1 h of incubation at 37°C, reactions were quenched by boiling in sample buffer prior to analysis on a 12% SDS-PAGE gel.

Similar control assays in the presence of thermolysin or trypsin were performed with 13.5 μM BSA (New England BioLabs) in the presence or absence of AHL. Matrix-assisted laser desorption ionization-tandem time of flight (MALDI-TOF/TOF) mass spectrometry analysis was performed by the Virginia Tech-Mass Spectrometry Incubator on protein fragments of interest.

Gel filtration of HMGE. *E. coli* Top 10 cells expressing HMGE were grown separately in LB medium without and with 10 μM AHL. HMGE samples (5 ml) purified as described above, in the absence or presence of 10 μM AHL throughout the purification scheme, were passed over a 320-ml HiPrep 26/60 Sephacryl 200-S (GE Healthcare) gel filtration column using the AKTAPrime system. The concentration of the HMGE sample without AHL was 5.7 μM , while the sample with AHL was 7.8 μM . Each sample was separately loaded onto the column, following equilibration with conjugation buffer (20 mM HEPES, 300 mM NaCl, 10% glycerol [pH 7.4]) at 4°C, using a flow rate of 0.7 ml/min, and 5.0-ml fractions were collected. Peak fractions were assayed on a 12% SDS-PAGE gel to detect the 73-kDa HMGE monomer. Gel filtration molecular size markers (Sigma-Aldrich) were also passed over the same column under identical conditions at the following concentrations: 3 mg/ml carbonic anhydrase (33 kDa), 10 mg/ml albumin (66 kDa), 5 mg/ml alcohol dehydrogenase (150 kDa), and 4 mg/ml β -amylase (223 kDa). The elution volume of Blue Dextran (2,000 kDa) was used to determine the void volume (V_0) of 95 ml. The elution volume-to-void volume ratio (V_e/V_0) of each of the protein

molecular size standards was used to generate a calibration curve for the Sephacryl 200-S column.

BS³ cross-linking of EsaR NTD178. EsaR NTD178 (10 μ M) was cross-linked with 100 μ M BS³ (Thermo Fisher Scientific) in the absence or presence of 50 μ M AHL. The 15- μ l reactions were carried out in 20 mM HEPES, 500 mM NaCl, 10% glycerol (pH 7.4) at room temperature and quenched at time points up to 30 min by boiling in sample buffer. The protein was then visualized by 12% SDS-PAGE.

RESULTS:

EsaR is stable *in vivo* in the absence and presence of AHL. The majority of LuxR family members are known to be unstable/less stable in the absence of AHL (reviewed in reference 23), but very little is known about the actual mechanism of AHL responsiveness that stabilizes them. Comparative experiments in protease-proficient and-deficient *E. coli* strains revealed that the Clp and Lon proteases degraded TraR at a much higher rate when AHL was not present than when AHL was permitted to complex with the protein during translation. Thus, TraR does not accumulate to appreciable levels in the absence of AHL in protease-proficient *E. coli* (37). Using similar logic, it was hypothesized that EsaR might be less stable in its inactive state when associated with AHL. An *in vivo* analysis of cellular levels of EsaR in the native host, *P. stewartii*, from an OD₆₀₀ of 0.05 to an OD₆₀₀ of 1.6 via quantitative Western immunoblotting revealed that EsaR levels slowly increased from early to late exponential growth (Fig. 2.1A). A sample at low AHL/OD₆₀₀ clearly has less EsaR per mg total protein than a sample to which exogenous AHL was added (Fig. 2.1A). At low AHL/OD₆₀₀, EsaR is capable of

autorepressing its own expression. However, at a high AHL/OD₆₀₀, EsaR is inactivated and derepression of EsaR expression occurs. If AHL-triggered proteolytic degradation of EsaR were rapidly occurring, its levels would be anticipated to decrease at high AHL/OD₆₀₀. However, our experiments showed no net reduction in EsaR levels, even when excess AHL was supplemented in the growth medium (Fig. 2.1A). This suggests that extensive degradation by proteases is not the means by which EsaR is inactivated in the presence of AHL.

Pulse-chase experiments were performed in recombinant *E. coli* to compare the turnover rates of EsaR in the presence or absence of AHL in a more precise manner. EsaR has previously been shown to respond to AHL in *E. coli* in the same manner as in its native host (20, 28). EsaR was equally stable in the absence or presence of AHL for up to 60 min after synthesis of the protein (Fig. 2.1B). Therefore, both the Western immunoblot and pulse-chase experiments demonstrate that EsaR is not targeted for rapid proteolysis within the cell upon exposure to AHL.

A His-Maltose Binding Protein (MBP)-glycine linker-tagged EsaR construct (HMGE) is biologically active. The native form of EsaR has been purified (15), but the method is time-consuming and has not proven to be easily reproducible (S. B. von Bodman, personal communication). An N-terminal MBP fusion to EsaR was successfully used to study the dimeric structure of EsaR when it binds to DNA (15). To further analyze the activity of EsaR *in vitro*, we have improved our ability to rapidly purify EsaR using a His₆-MBP-glycine linker (Gly₅)-EsaR fusion protein (HMGE) expressed from an IPTG-inducible promoter. TEV protease was unable to completely cleave the His-MBP tag from EsaR, resulting in the production of mixed heterodimers (data not shown). To determine if full-length HMGE was biologically active, its

capacity to complement a chromosomal deletion of *esaR* was examined. Wild-type strain *P. stewartii* DC283 (9) expressed some EPS at high cell density on CPG medium (Fig. 2.2A) while a strain with a deletion of *esaR* and *esaI*, ESΔIR (29), without or with the vector control pDEST HisMBP (17), exhibited a hyper-muroid phenotype since EsaR is absent and *rcaA* is derepressed (Fig. 2.2A). When the ESΔIR strain is complemented with pSVB60 (15) (encoding the native EsaR protein) or with pHMGE, EPS production is noticeably reduced due to constitutive repression of *rcaA* (Fig. 2.2A). These strains regained a hyper-muroid phenotype in the presence of AHL due to inactivation of EsaR/HMGE and the subsequent derepression of *rcaA* (Fig. 2.2A). Thus, HMGE is biologically active *in vivo*, and it is capable of repressing the *rcaA* promoter in the absence of AHL and derepressing EPS production in the presence of the AHL ligand. Purified HMGE binds to the *esa* box target, the native EsaR binding site within the *esaR* promoter, in a manner similar to EsaR (15) as demonstrated by *in vitro* EMSAs (Fig. 2.2B). It is also able to associate with AHL *in vitro* enabling for an analysis of the responses of HMGE to the presence of ligand (see below).

Partial *in vitro* proteolysis reveals AHL-dependent protection and conformational changes in EsaR. Limited *in vitro* proteolytic digestions with HMGE were performed to further assess the effects of AHL binding on the conformation of EsaR. HMGE was purified in the absence or presence of 10 μM AHL, with the AHL added cotranslationally during growth (and present through protein purification) or posttranslationally after purification. Two different proteases (thermolysin and trypsin) were used to produce cleavage patterns of HMGE that were analyzed via SDS-PAGE. The activity of the two proteases, in the absence of EsaR, was not detectably

altered by the presence of AHL as determined through control digestions of purified bovine serum albumin (data not shown).

The highly stable His-MBP tag (45 kDa) was clearly seen in all of the HMGE samples digested with thermolysin (Fig. 2.3A) in the presence or absence of AHL, but no band of the predicted size for full-length EsaR was observed. However, two extra bands (~18 and 5 kDa) were observed when HMGE was incubated in the presence of AHL (either co- or posttranslationally) but not when HMGE was incubated without AHL (Fig. 2.3A). The bands were extracted, peptides were generated, and their minimal amino acid sequence was determined via MALDI-TOF/TOF (Virginia Tech-Mass Spectrometry Incubator). The bands produced from the thermolysin cleavage reactions were minimally comprised of EsaR amino acids 1 to 160 (the NTD of EsaR) and 23 to 74 (a region close to the putative AHL binding pocket) (Fig. 2.3C); there may be additional residues in the N or C termini of these protein fragments that were not detected. Both region 1 to 160 and region 23 to 74 of EsaR contain more than one thermolysin cleavage site, as predicted by PeptideCutter (ExPASy), suggesting that the presence of AHL produced a conformational shift that interfered with thermolysin cleavage. Subsequent purification of the EsaR NTD (amino acid residues 1 to 160) indicated that the polypeptide existed as a dimer (data not shown), which led to further analysis of the NTD.

Similar limited proteolytic digestion assays performed with trypsin produced the highly stable His-MBP tag (45 kDa) (Fig. 2.3B) and weak residual bands corresponding to the predicted size of EsaR (28 kDa) in all three samples \pm AHL. However, there was an extra band (~9 kDa) present in the samples with AHL. Through MALDI-TOF/TOF (Virginia Tech-Mass

Spectrometry Incubator) it was determined that this extra band corresponded minimally to amino acids 130 to 213 of EsaR (Fig. 2.3B). This region includes the predicted linker region between the NTD and CTD (Fig. 2.3C) and it contains more than one trypsin cleavage site, as predicted by PeptideCutter (ExPASy). The fact that cleavage did not occur in this region as efficiently in the presence of AHL suggests that interdomain conformational changes are occurring in response to AHL binding, a phenomenon that has long been speculated to occur among all LuxR family members (22) but has never before been biochemically demonstrated with a native ligand. In sum, it appears that HMGE, whose activity is inhibited by AHL, alters its conformation such that some proteolytic cleavage sites are less accessible in the presence than in the absence of AHL. Interestingly, the finding that AHL affords protection from proteases has also been observed with other members of the LuxR protein family that are stimulated by AHL (31, 37).

EsaR dimerizes in the absence and presence of AHL. Because EsaR was equally resistant to proteolytic digestion *in vivo* both in the presence and in the absence of AHL and more resistant to proteolytic digestion *in vitro*, another mechanism of AHL inactivation was considered. It is known that most LuxR homologues function as dimers when AHL is present (3, 26, 33, 37). Based on amino acid alignments, the corresponding dimerization interface for EsaR would be predicted to encompass residues 132 to 161. EsaR is known to bind to DNA as a dimer in the absence of AHL (15), but its quaternary structure in the presence of AHL has never been well defined. The effect of AHL on the multimeric state of EsaR was therefore determined through a combination of gel filtration chromatography and cross-linking experiments. During gel filtration experiments, HMGE exposed to 10 μ M AHL during growth and purification eluted with a single peak at 122 ml from a 320-ml volume column (Fig. 2.4A). Through the use of four known

molecular size markers, an apparent molecular size of 136 kDa was calculated for HMGE (Fig. 2.4B). The predicted monomeric molecular size of HMGE is 73 kDa, so a dimer would be ~146 kDa; these experiments suggest that HMGE is dimeric in the presence of AHL. Gel filtration chromatography was also performed on HMGE in the absence of AHL. The protein eluted with a single peak at 118 ml (Fig. 2.4A), just slightly earlier than the protein in the presence of AHL. An apparent molecular size of 155 kDa was calculated for HMGE (Fig. 2.4B). AHL had no effect on the protein standard calibration curve (data not shown). These *in vitro* results suggest that at the concentrations examined, HMGE exists as a dimer in both the absence and presence of AHL. The observation that HMGE has a slightly smaller calculated molecular size in the presence of AHL suggests that the ligand promotes a tighter conformation of the protein.

The NTD of EsaR binds AHL and is capable of dimerizing in the absence and presence of AHL. To further verify the finding that EsaR is capable of dimerizing in the presence of AHL, cross-linking experiments were performed in the absence or presence of AHL using only the NTD of EsaR from residues 1 to 178. The His-MBP tag was efficiently cleaved from the NTD using TEV protease; apparently the presence of the CTD hinders complete cleavage of HMGE by TEV. Limited proteolytic thermolysin digestion assays produced a similar banding pattern for the EsaR NTD in the presence of AHL (Fig. 2.5A) as had been observed with HMGE (Fig. 2.3A). MALDI-TOF/TOF analysis of the two EsaR NTD bands of highest molecular size determined that they were minimally comprised of amino acids 1 to 160 and 1 to 93. These regions encompass most of the NTD and the region around the AHL binding site; they appear to be protected from complete thermolysin digestion when AHL is present. Therefore, the EsaR

NTD appears to be capable of binding AHL, independent of the CTD (Fig. 2.5A), consistent with what has been observed in other LuxR homologues (3, 8,34).

The EsaR NTD protein was then exposed to the cross-linking agent BS³. Over a 30-min period, the EsaR NTD was cross-linked to a level similar to that observed in cross-linking experiments with full-length CarR, the LuxR-type activator from *Erwinia carotovora* (Fig. 2.5B) (31). The apparent molecular size of the cross-linked product suggests that the NTD of EsaR has a propensity to form dimers and that the CTD is not essential for this to occur. In addition, the EsaR NTD maintains a similar quaternary structure independent of the presence of ligand, further indicating that AHL binding does not significantly alter the multimeric state of the protein.

DISCUSSION:

EsaR is the best-understood member of a distinctive subclass of the LuxR family of proteins (23, 24). These proteins have been described as sharing several common attributes: they are produced by *Enterobacteriales*, they preferentially bind *N*-3-oxo-hexanoyl-L-homoserine lactone, they do not directly regulate their cognate AHL synthase genes, they can function as repressors and activators depending on the position of the recognition site in the DNA, and their genes are convergently transcribed with the genes for their respective AHL synthases. In addition, all of these proteins have an extended interdomain linker region and an extended CTD in comparison to the majority of LuxR homologues (24). They regulate gene expression using a reverse mechanism whereby in the absence of AHL they are capable of binding DNA but take on an inactive conformation in the presence of AHL. Structurally, EsaR and its closest relatives

deviate from most LuxR homologues because they are stable in the absence of their cognate AHL, making them amenable to *in vitro* analysis.

It has previously been demonstrated that EsaR is fully active as an apoprotein. In the absence of AHL, EsaR is capable of repressing transcription from the *esaR* and *rcaA* promoters (6, 14, 15) and activating transcription of an sRNA (20) at low cell density. AHL hinders the ability of EsaR to regulate transcription at high cell density. However, the molecular basis for inhibition of EsaR by AHL remains elusive. In this body of work, two possible ways that binding of AHL might modulate the level of active EsaR, an enhanced rate of proteolysis of the protein and an inability to dimerize, were examined.

This study established that EsaR does not appear to be extensively posttranslationally degraded by proteases *in vivo* in response to AHL binding. In *P. stewartii*, EsaR levels gradually rose from low cell density/low AHL to high cell density/high AHL, suggesting that rapid removal of the protein via proteases is not the manner in which the protein is inactivated in the presence of AHL. This is in stark contrast to the results of a similar analysis of TraR from *A. tumefaciens* in *E. coli*, which showed that apo-TraR is quickly degraded by proteases *in vivo*. Upon binding of AHL by TraR *in vitro*, the protein takes on an active conformation and in the process becomes more resistant to these proteases, as the half-life increases 20-fold (36, 37). Similarly, CarR from *E. carotovora* also exhibits enhanced protease resistance in the presence of AHL (31).

TraR is one of just a few members of the LuxR protein family for which detailed structural information is available. The structure of AHL-associated full-length TraR and the NTD of LasR

from *Pseudomonas aeruginosa* have been solved with their native ligands by X-ray crystallography (3, 27, 35, 38), and the structure of CviR from *Chromobacterium violaceum* bound to an antagonist is also known (8). The structure of the NTD of SdiA from *E. coli* was examined using nuclear magnetic resonance (NMR) analysis (34). No structural information exists for EsaR or any member of its subfamily. However, previous studies of EsaR using fluorescence spectroscopy revealed that AHL altered the intrinsic fluorescence emissions from tryptophan residues in the binding pocket (15). In addition, AHL enhanced the thermal stability of EsaR (15). The *in vitro* limited proteolytic digestion assay performed in this study reinforced the previous findings and further probed the structural differences between apo-EsaR and ligand-associated EsaR. AHL binding to EsaR resulted in altered patterns of protease susceptibility using two different proteases, thermolysin and trypsin.

In the presence of AHL, the ligand binding NTD of EsaR was less susceptible to thermolysin digestion (Fig. 2.3A). Thermolysin attacks hydrophobic regions, and binding of AHL most likely directly interfered with the ability of the protein to cleave target sites in the AHL binding pocket. In the case of assays with trypsin, a region spanning from the NTD through the linker region into the CTD of EsaR was found to be more resistant to the protease when AHL was present (Fig. 2.3B). This result is very intriguing because it suggests that AHL binding in the NTD may elicit a conformational change across both domains of the protein, resulting in a tighter conformation that protects the linker from degradation. For LuxR family proteins, it has long been proposed that AHL binding at the NTD leads to subsequent changes in the CTD that alter the DNA binding abilities of the protein (22). However, an inability to study LuxR proteins *in vitro* in the presence and absence of their native ligand has limited a structural analysis of this mechanism.

X-ray crystallography of CviR bound to an antagonist provides evidence in support of NTD-CTD interactions (8). It has been speculated that the antagonism of EsaR by its native AHL might work in a similar manner, resulting in a decreased affinity for the promoters it regulates.

In addition to intradomain interactions playing a role in the responsiveness of EsaR to AHL, changes in the interface between the two polypeptides in a homodimer may also be important. Binding of AHL may inhibit dimerization of the NTDs, leading to dissociation of EsaR into monomers and subsequent dissociation from DNA. Both gel filtration analysis of HMGE and *in vitro* cross-linking of the NTD demonstrate that EsaR has a propensity to form dimers at the concentrations examined and that the presence of AHL does not decrease the capacity for dimerization to occur. Further, only the EsaR NTD is required for both AHL binding and dimerization to occur. Thus, AHL does not appear to alter the multimeric state of EsaR.

A complete understanding of the mechanism by which AHL binds to the NTD of LuxR homologues and modulates the activity of the CTD remains an unresolved issue in the quorum-sensing field. Clearly, diverse mechanisms for AHL responsiveness exist within the LuxR family. Our report offers an explanation of the interaction between the AHL signal and its cognate EsaR receptor, a system that is the model for a unique subset of quorum-sensing regulators. In the case of EsaR, binding of AHL causes a conformational shift in the protein, in which the protein appears to take on a tighter, more stable and likely less flexible conformation. Under these conditions, EsaR is no longer able to make appropriate interactions with DNA, leading to its dissociation. Future structural studies of EsaR would provide valuable insights into the precise nature of this mechanism.

ACKNOWLEDGEMENTS

We thank M. Hughes and M. Reyes for technical assistance, A. Thode, D. Donham and M. Churchill for generating and sharing their homology model of EsaR, F. Schubot for advice on protein biochemistry, W. K. Ray and R. Helm at the Virginia Tech-Mass Spectrometry Incubator for MALDI-TOF/TOF analysis, S. B. von Bodman and S. Winans for providing strains, and A. Levchenko for his support of this project.

This work was funded by a National Institutes of Health GM0066786 subcontract and NSF grant MCB-0919984 to A.M.S.

REFERENCES:

1. **Atkinson S., Chang C. Y., Sockett R. E., Cámara M., Williams P.** 2006. Quorum sensing in *Yersinia enterocolitica* controls swimming and swarming motility. *J. Bacteriol.* **188**:1451–1461.
2. **Beck von Bodman S., Farrand S. K.** 1995. Capsular polysaccharide biosynthesis and pathogenicity in *Erwinia stewartii* require induction by an *N*-acylhomoserine lactone autoinducer. *J. Bacteriol.* **177**:5000–5008.
3. **Bottomley M. J., Muraglia E., Bazzo R., Carfi A.** 2007. Molecular insights into quorum sensing in the human pathogen *Pseudomonas aeruginosa* from the structure of the virulence regulator LasR bound to its autoinducer. *J. Biol. Chem.* **282**:13592–13600.
4. **Bradshaw-Rouse J. J., et al.** 1981. Agglutination of *Erwinia stewartii* strains with a corn allutinin: correlation with extracellular polysaccharide production and pathogenicity. *Appl. Environ. Microbiol.* **42**:344–350.
5. **Brosius J., Holy A.** 1984. Regulation of ribosomal RNA promoters with a synthetic *lac* operator. *Proc. Natl. Acad. Sci. U. S. A.* **81**:6929–6933.
6. **Carlier A. L., von Bodman S. B.** 2006. The *rcaA* promoter of *Pantoea stewartii* subsp. *stewartii* features a low-level constitutive promoter and an EsaR quorum-sensing-regulated promoter. *J. Bacteriol.* **188**:4581–4584.
7. **Castang S., Reverchon S., Gouet P., Nasser W.** 2006. Direct evidence for the modulation of the activity of the *Erwinia chrysanthemi* quorum-sensing regulator ExpR by acyl homoserine lactone pheromone. *J. Biol. Chem.* **281**:29972–29987.
8. **Chen G., et al.** 2011. A strategy for antagonizing quorum sensing. *Mol. Cell* **42**:199–209.
9. **Dolph P. J., Majerczak D. R., Coplin D. L.** 1988. Characterization of a gene cluster for exopolysaccharide biosynthesis and virulence in *Erwinia stewartii*. *J. Bacteriol.* **170**:865–871.
10. **Eberhard A., et al.** 1981. Structural identification of autoinducer of *Photobacterium fischeri* luciferase. *Biochemistry* **20**:2444–2449.
11. **Fuqua C., Parsek M. R., Greenberg E. P.** 2001. Regulation of gene expression by cell-to-cell communication: acyl-homoserine lactone quorum sensing. *Annu. Rev. Genet.* **35**:439–468.
12. **Gottesman S., Roche E., Zhou Y., Sauer R. T.** 1998. The ClpXP and ClpAP proteases degrade proteins with carboxy-terminal peptide tails added by the SsrA-tagging system. *Genes Dev.* **12**:1338–1347.

13. **Grant S. G., Jessee J., Bloom F. R., Hanahan D.** 1990. Differential plasmid rescue from transgenic mouse DNAs into *Escherichia coli* methylation-restriction mutants. Proc. Natl. Acad. Sci. U. S. A. **87**:4645–4649.
14. **Minogue T. D., Carlier A. L., Koutsoudis M. D., von Bodman S. B.** 2005. The cell density-dependent expression of stewartan exopolysaccharide in *Pantoea stewartii* ssp. *stewartii* is a function of EsaR-mediated repression of the *rcaA* gene. Mol. Microbiol. **56**:189–203.
15. **Minogue T. D., Wehland-von Trebra M., Bernhard F., von Bodman S. B.** 2002. The autoregulatory role of EsaR, a quorum-sensing regulator in *Pantoea stewartii* ssp. *stewartii*: evidence for a repressor function. Mol. Microbiol. **44**:1625–1635.
16. **Morohoshi T., et al.** 2007. The plant pathogen *Pantoea ananatis* produces *N*-acyl homoserine lactone and causes center rot disease of onion by quorum sensing. J. Bacteriol. **189**:8333–8338.
17. **Nallamsetty S., Austin B. P., Penrose K. J., Waugh D. S.** 2005. Gateway vectors for the production of combinatorially-tagged His6-MBP fusion proteins in the cytoplasm and periplasm of *Escherichia coli*. Protein Sci. **14**:2964–2971.
18. **Oinuma K., Greenberg E. P.** 2011. Acyl-homoserine lactone binding to and stability of the orphan *Pseudomonas aeruginosa* quorum-sensing signal receptor QscR. J. Bacteriol. **193**:421–428.
19. **Pinto U. M., Winans S. C.** 2009. Dimerization of the quorum-sensing transcription factor TraR enhances resistance to cytoplasmic proteolysis. Mol. Microbiol. **73**:32–42.
20. **Schu D. J., Carlier A. L., Jamison K. P., von Bodman S., Stevens A. M.** 2009. Structure/function analysis of the *Pantoea stewartii* quorum-sensing regulator EsaR as an activator of transcription. J. Bacteriol. **191**:7402–7409.
21. **Sjöblom S., Brader G., Koch G., Palva E. T.** 2006. Cooperation of two distinct ExpR regulators controls quorum sensing specificity and virulence in the plant pathogen *Erwinia carotovora*. Mol. Microbiol. **60**:1474–1489.
22. **Stevens A. M., Greenberg E. P.** 1999. Transcriptional activation by LuxR, p. 231–242. In Dunny G. M., Winans S. C. (ed.), Cell-cell signaling in bacteria. American Society for Microbiology, Washington, DC.
23. **Stevens A. M., Queneau Y., Soulere L., von Bodman S., Doutheau A.** 2011. Mechanisms and synthetic modulators of AHL-dependent gene regulation. Chem. Rev. **111**:4–27.
24. **Tsai C. S., Winans S. C.** 2010. LuxR-type quorum-sensing regulators that are detached from common scents. Mol. Microbiol. **77**:1072–1082.

25. **Tsai C. S., Winans S. C.** 2011. The quorum-hindered transcription factor YenR of *Yersinia enterocolitica* inhibits pheromone production and promotes motility via a small non-coding RNA. *Mol. Microbiol.* **80**:556–571.
26. **Urbanowski M. L., Lostroh C. P., Greenberg E. P.** 2004. Reversible acyl-homoserine lactone binding to purified *Vibrio fischeri* LuxR protein. *J. Bacteriol.* **186**:631–637.
27. **Vannini A., et al** 2002. The crystal structure of the quorum sensing protein TraR bound to its autoinducer and target DNA. *EMBO J.* **21**:4393–4401.
28. **von Bodman S. B., et al.** 2003. The quorum sensing negative regulators EsaR and ExpR *Ecc*, homologues within the LuxR family, retain the ability to function as activators of transcription. *J. Bacteriol.* **185**:7001–7007.
29. **von Bodman S. B., Majerczak D. R., Coplin D. L.** 1998. A negative regulator mediates quorum-sensing control of exopolysaccharide production in *Pantoea stewartii* subsp. *stewartii*. *Proc. Natl. Acad. Sci. U. S. A.* **95**:7687–7692.
30. **Waters C. M., Bassler B. L.** 2005. Quorum sensing: cell-to-cell communication in bacteria. *Annu. Rev. Cell Dev. Biol.* **21**:319–346.
31. **Welch M., et al.** 2000. N-acyl homoserine lactone binding to the CarR receptor determines quorum-sensing specificity in *Erwinia*. *EMBO J.* **19**:631–641.
32. **Whitehead N. A., Barnard A. M., Slater H., Simpson N. J., Salmond G. P.** 2001. Quorum-sensing in Gram-negative bacteria. *FEMS Microbiol. Rev.* **25**:365–404.
33. **Yang M., Giel J. L., Cai T., Zhong Z., Zhu J.** 2009. The LuxR family quorum-sensing activator MrtR requires its cognate autoinducer for dimerization and activation but not for protein folding. *J. Bacteriol.* **191**:434–438.
34. **Yao Y., et al.** 2006. Structure of the *Escherichia coli* quorum sensing protein SdiA: activation of the folding switch by acyl homoserine lactones. *J. Mol. Biol.* **355**:262–273.
35. **Zhang R. G., et al.** 2002. Structure of a bacterial quorum-sensing transcription factor complexed with pheromone and DNA. *Nature* **417**:971–974.
36. **Zhu J., Winans S. C.** 1999. Autoinducer binding by the quorum-sensing regulator TraR increases affinity for target promoters in vitro and decreases TraR turnover rates in whole cells. *Proc. Natl. Acad. Sci. U. S. A.* **96**:4832–4837.
37. **Zhu J., Winans S. C.** 2001. The quorum-sensing transcriptional regulator TraR requires its cognate signaling ligand for protein folding, protease resistance, and dimerization. *Proc. Natl. Acad. Sci. U. S. A.* **98**:1507–1512.

38. **Zou Y., Nair S. K.** 2009. Molecular basis for the recognition of structurally distinct autoinducer mimics by the *Pseudomonas aeruginosa* LasR quorum-sensing signaling receptor. *Chem. Biol.* **16**:961–970.

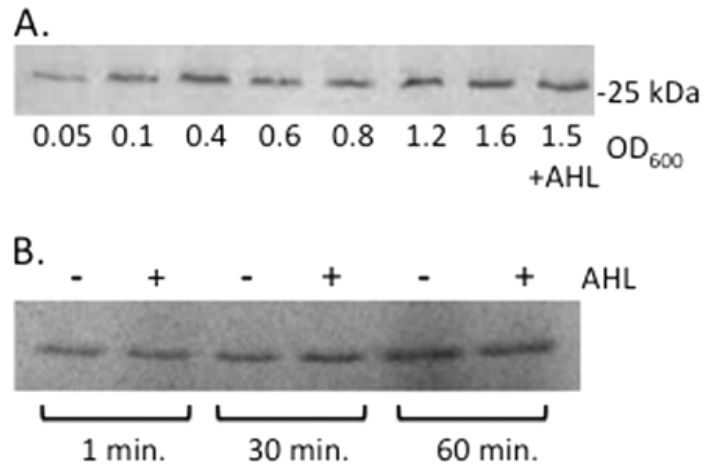


FIG 2.1. EsaR accumulation and stability *in vivo*. (A) Results from *in vivo* Western immunoblot experiments, in which EsaR accumulation was measured in *P. stewartii* DC283 at the indicated OD600 values with natural AHL levels, except for one sample where exogenous AHL was added as indicated. (B) Pulse-chase experiments, in which EsaR was labeled in *E. coli* SG22163 in the absence or presence of 10 μ M AHL. Stability was examined at time points up to 60 min. The images are representative of experiments performed in duplicate.

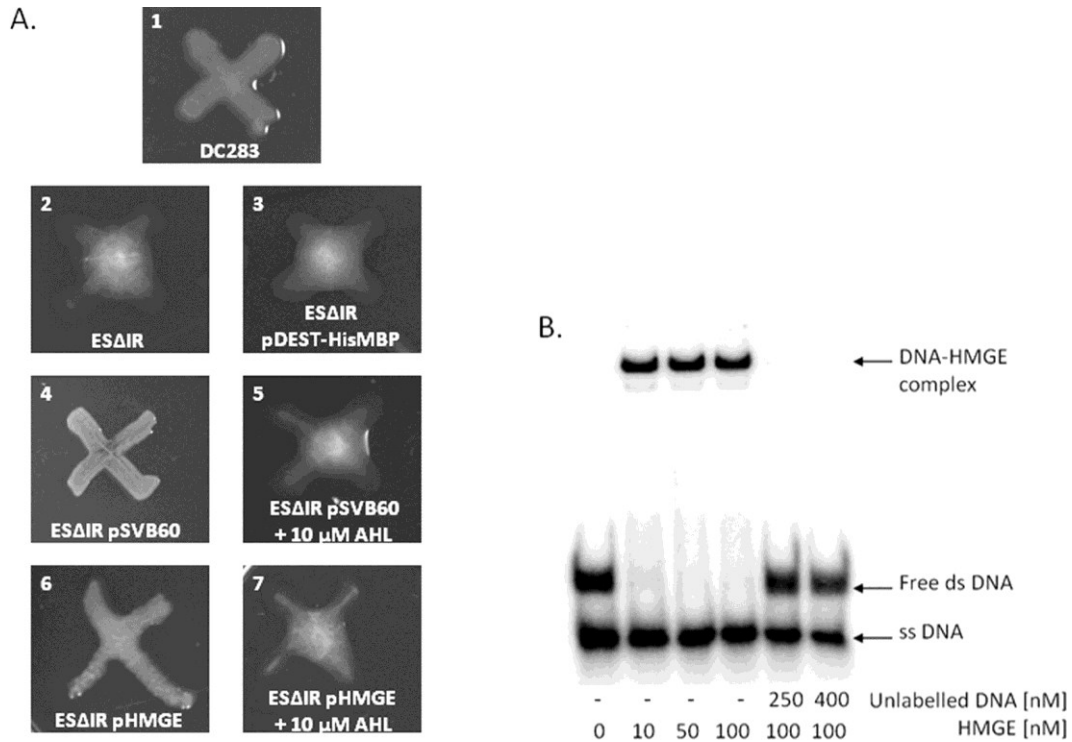


FIG. 2.2. HMGE activity assays. (A) Qualitative analysis of EPS production on CPG agar medium (4) (0.1% Casamino Acids, 1% peptone, 1% glucose, and 1.5% agar), with Ap (50 $\mu\text{g/ml}$) or tetracycline (Tc) (10 $\mu\text{g/ml}$) as appropriate, following incubation at 30°C for 48 h: 1, wild-type *P. stewartii* DC283 (9); 2, *esaR esaI* double-deletion strain *P. stewartii* ESΔIR (29), and 3, *P. stewartii* ESΔIR with the vector control pDEST HisMBP (Ap^r) (17); 4 and 5, *P. stewartii* ESΔIR pSVB60 (Tc^r) grown in the absence or presence of 10 μM AHL, respectively; 6 and 7, *P. stewartii* ESΔIR pHMGE (Ap^r) grown in the absence or presence of 10 μM AHL, respectively. (B) EMSA of HMGE with *PesaR28* DNA probe. Radiolabeled *PesaR28* DNA probe (2 nM) (lane 1) was incubated with various concentrations of HMGE as indicated (lanes 2, 3, and 4) and shown to produce a higher-molecular-size complex. Specificity of binding was verified by adding excess unlabeled *PesaR28*, which resulted in a downshift of the labeled probe (lanes 5, 6).

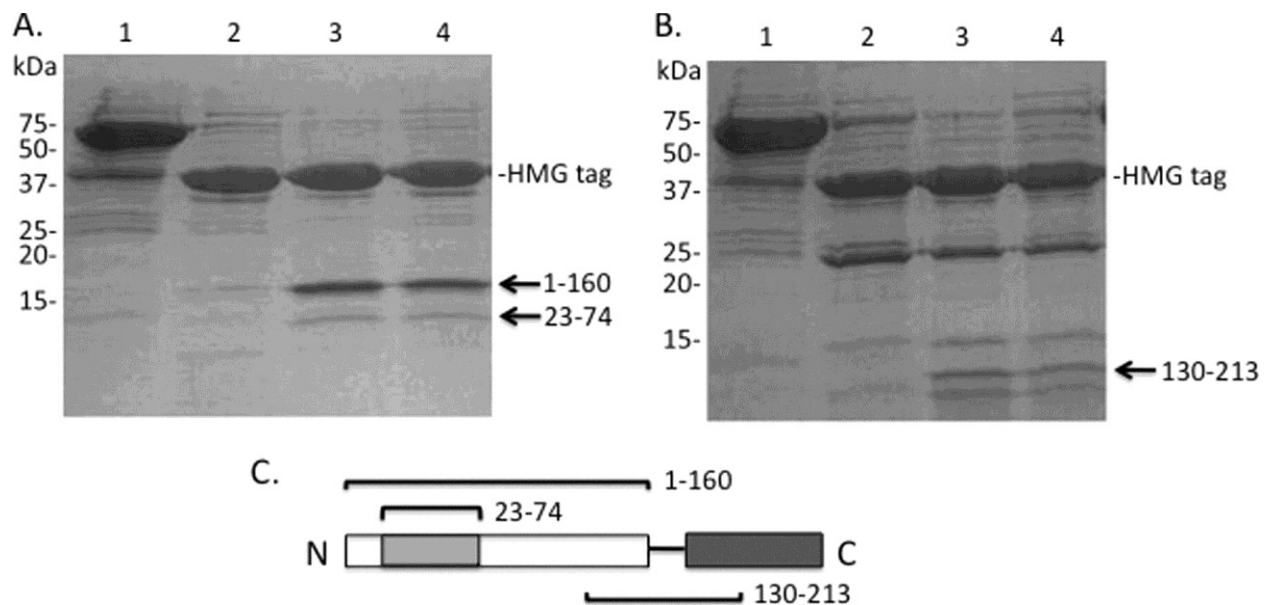


FIG. 2.3. Limited *in vitro* digestion of EsaR by thermolysin and trypsin. SDS-PAGE analysis of resistance of EsaR to (A) thermolysin and (B) trypsin \pm AHL. Purified HMGE was used at a final concentration of 13.5 μ M for all conditions (lanes 1 to 4) as follows: 1, no protease; 2, no AHL plus protease; 3, AHL present during growth and purification plus protease; 4, AHL added after purification plus protease. The dominant band in lanes 2 to 4 is the His-MBP tag (45 kDa). Arrows indicate EsaR-associated bands of interest, with the numbers providing the minimal number of residues present in the protein fragment. The images are representative of experiments performed in duplicate. (C) Cartoon model of the domain structure of EsaR. The AHL binding NTD is white, with the AHL binding pocket region in light gray and the DNA binding CTD in dark gray. Residues of EsaR found to be protected from thermolysin or trypsin digestion are labeled above or below the diagram, respectively.

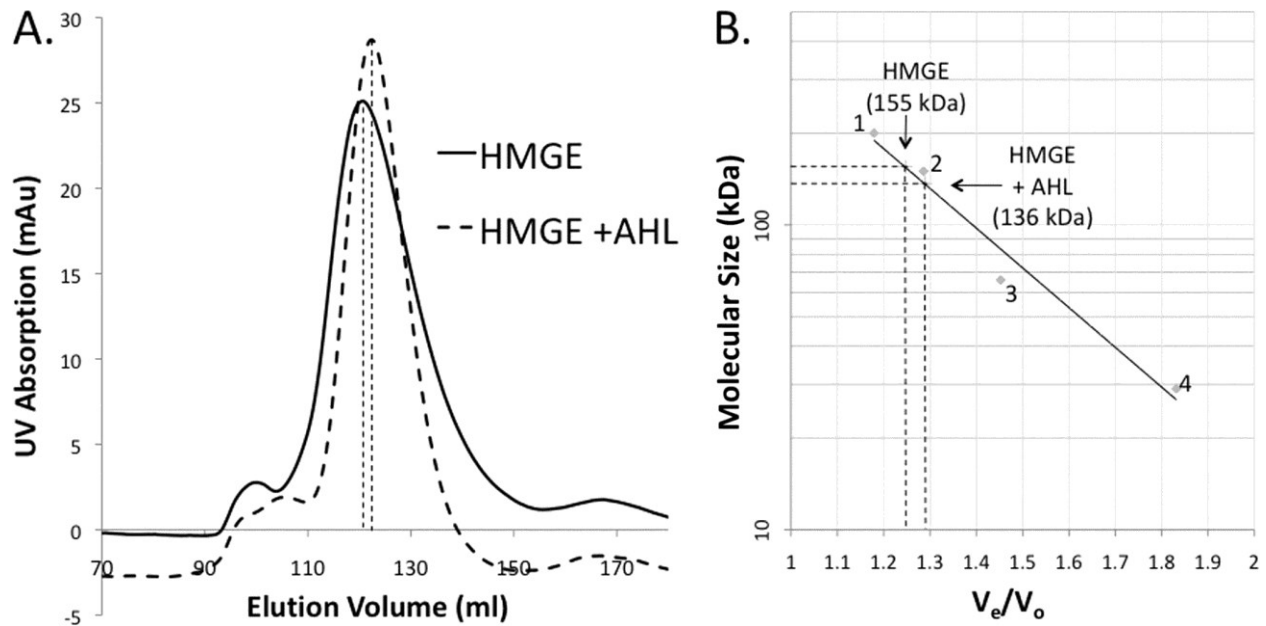


FIG. 2.4. Multimeric state of HMGE fusion protein in presence and absence of AHL. (A) UV absorption profiles (280 nm) of protein fractions containing HMGE eluted in the presence and absence of 10 μ M AHL over the 320-ml 26/60 Sephacryl 200-S gel filtration column (solid line, HMGE without AHL in buffer; dashed line, HMGE with AHL in buffer). HMGE without AHL eluted at 118 ml and HMGE with AHL at 122 ml. This corresponds to a molecular size of 155 kDa in the absence of AHL and 136 kDa in the presence of AHL, as determined by the calibration plot generated using the elution volumes of molecular size markers in panel B. The two additional minor peaks seen on the left and right of the major peak are aggregates and truncated HMGE, respectively, as determined through SDS-PAGE analysis. (B) The data points on the calibration plot represent the following: 1, β -amylase (200 kDa); 2, alcohol dehydrogenase (150 kDa); 3, albumin (66 kDa); and 4, carbonic anhydrase (29 kDa). Plots are representative of experiments performed in duplicate.

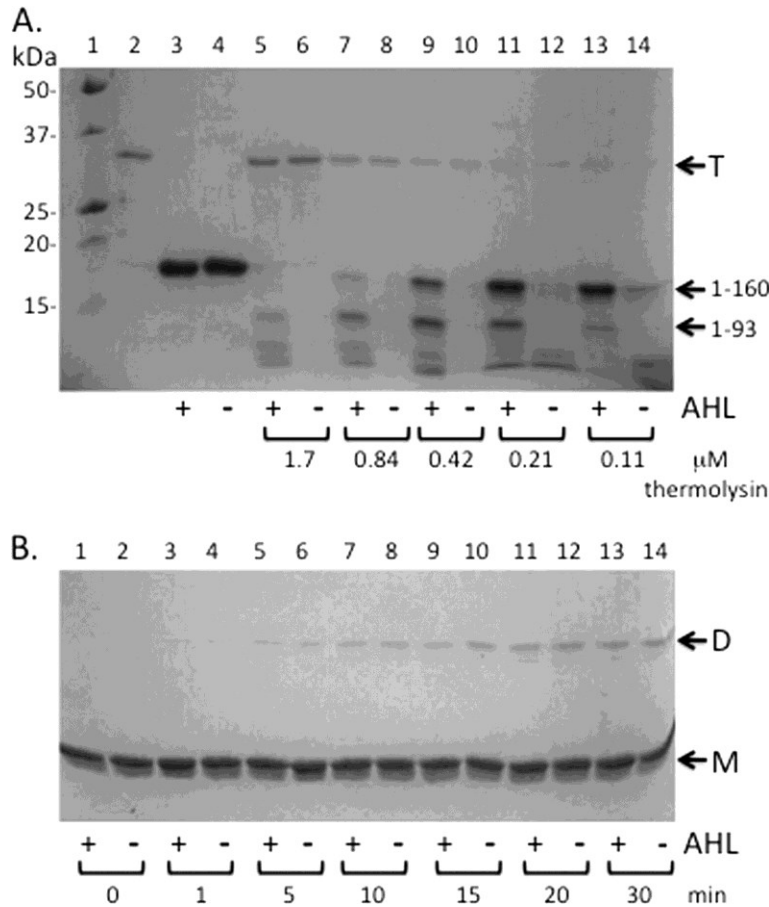


FIG. 2.5. Ability of EsaR NTD178 to resist proteolytic digestion and to form dimers. (A) Limited *in vitro* digestion of NTD178 by thermolysin. Purified NTD178 was used at a final concentration of 13.5 μM . Samples were as follows: 1, size standards; 2, thermolysin; 3 and 4, NTD178 with and without AHL (+ and –, respectively); 5 to 14, NTD178 with and without AHL and digested with the indicated concentration of thermolysin. Arrows indicate EsaR-associated bands of interest, with the numbers providing the minimal number of residues present in the protein fragment, and the mobility of thermolysin (T). (B) Time course of NTD178 cross-linking by BS³. NTD178 (10 μM) was exposed to 100 μM BS³ cross-linker in the presence (+) and absence (–) of AHL. Reaction pairs, left to right, correlate to 0, 1, 5, 10, 15, 20, and 30 min. The two arrows highlight the bands associated with the 42-kDa dimer (D) and 21-kDa monomer (M) of NTD178. The images are representative of experiments performed in duplicate.

Chapter Three

Proteomic Analysis of the Quorum-Sensing Regulon in *Pantoea stewartii* and Identification of Direct Targets of EsaR

Revathy Ramachandran and **Ann M. Stevens***. 2013. Proteomic Analysis of the Quorum-Sensing Regulon in *Pantoea stewartii* and Identification of Direct Targets of EsaR. Appl. Environ. Microbiol. doi:10.1128/AEM.01744-13. 79:6244-6252

*Corresponding author:

Department of Biological Sciences MC 0910
Life Sciences 1, Rm. 219, Virginia Tech
970 Washington St. SW
Blacksburg, VA 24061
Phone (540)-231-9378
FAX (540)-231-4043
Email ams@vt.edu

ABSTRACT:

The proteobacterium *Pantoea stewartii* subsp. *stewartii* causes Stewart's wilt disease in maize when it colonizes the xylem and secretes large amounts of stewartan, an exopolysaccharide. The success of disease pathogenesis lies in the timing of bacterial virulence factor expression through the different stages of infection. Regulation is achieved through a quorum-sensing (QS) system consisting of the acyl-homoserine lactone (AHL) synthase, EsaI, and the transcription regulator EsaR. At low cell densities, EsaR represses transcription of itself and of *rcaA*, an activator of the stewartan biosynthesis operon; it also activates *esaS*, which encodes a sRNA. Repression or activation ceases at high cell densities when EsaI synthesizes sufficient levels of the AHL ligand N-3-oxo-hexanoyl-L-homoserine lactone to bind and inactivate EsaR. This study aims to identify other genes activated or repressed by EsaR during the QS response. Proteomic analysis identified a QS regulon of more than 30 proteins. Electrophoretic mobility shift assays of promoters from genes encoding differentially expressed proteins distinguished direct targets of EsaR from indirect targets. Additional quantitative reverse transcription-PCR (qRT-PCR) and DNA footprinting analysis established that EsaR directly regulates the promoters of *dkgA*, *glpF* and *lrhA*. The proteins encoded by *dkgA*, *glpF*, and *lrhA* are a 2,5-diketogluconate reductase, glycerol facilitator, and transcriptional regulator of chemotaxis and motility, respectively, indicating a more global QS response in *P. stewartii* than previously recognized.

INTRODUCTION:

Quorum sensing (QS) is a cell density-dependent method of coordinating gene expression employed by bacteria to regulate various cellular processes. Proteobacteria commonly detect and respond to the concentration of a chemical signal, an acylated homoserine lactone (AHL), produced by an AHL synthase homologous to LuxI from *Vibrio fischeri*. This signal is sensed by an AHL-responsive transcription regulator homologous to LuxR (1). Thus, gene expression is altered in relation to cell density such that physiological processes, such as bioluminescence, virulence, and pigment or capsule production are affected (2, 3). QS is a central component in the regulatory networks of proteobacteria, and along with other bacterial regulatory systems, it allows the bacteria to colonize and grow efficiently in a particular environment or host-associated niche (4).

The proteobacterium *Pantoea stewartii* subsp. *stewartii* is a phytopathogen known to utilize QS to regulate virulence. *P. stewartii* is the causative agent of Stewart's wilt that affects maize cultivars, particularly sweet corn. It is found in the midgut of *Chaetocnema pulicaria*, the corn flea beetle where it overwinters. Within the plant, the bacterium colonizes the xylem after migrating there from the sites of insect feeding on the leaves and stalks of maize (5). Once in the xylem, *P. stewartii* forms a biofilm and overproduces an exopolysaccharide, stewartan, that obstructs the xylem and likely causes the vascular wilting associated with Stewart's wilt by blocking water transport (6, 7). *P. stewartii* also possesses a *hrp* and *wts* gene cluster encoding a Hrp type III secretion system and effector proteins (8). Affected seedlings wither (wilt phase), and affected mature plants develop necrotic lesions (leaf blight phase), leading to losses in the crop yield (9). Other pathogenic *Pantoea* species include *Pantoea ananatis*, which causes soft rot

of onions (10), and *Pantoea citrea*, which causes pink disease of pineapple (11). *Pantoea* species are also found symbiotically associated with leaf-cutter ants (12).

The expression of stewartan, a key virulence factor in *P. stewartii*, is controlled by the cell density-dependent QS system, consisting of EsaI/EsaR, a signaling molecule synthase and the cognate transcription regulator homologous to LuxI/LuxR (6). EsaI constitutively synthesizes a 3-oxo-hexanoyl-homoserine lactone (AHL) signal that accumulates at high cell densities. EsaR is a transcription factor that activates or represses expression of certain genes at low cell densities. Binding of the AHL ligand at high cell densities inactivates it. EsaR regulates virulence by repressing *rcaA*, an activator of the stewartan biosynthesis operon. RcsA in *P. stewartii* is functionally interchangeable with the RcsA regulator in *Escherichia coli* that controls capsular polysaccharide synthesis (13). Inactivation of EsaR at high cell densities by the AHL ligand permits the RcsAB heterodimer to activate stewartan synthesis (14). At low cell densities, EsaR also autorepresses itself and activates the expression of a small RNA of unknown function (15, 16). Mutants lacking *esaR* constitutively overproduce stewartan and are less virulent than the wild type, indicating that it is the temporal regulation of virulence factors during the stages of infection that lead to success in establishing disease in the host (14). However, the full extent of EsaR regulation and QS-controlled genes in *P. stewartii* is not known.

In this study, we have further defined the QS regulon using a proteomic approach. Two-dimensional (2D) SDS-PAGE experiments revealed more than 30 proteins that are differentially expressed in the presence of EsaR and, thus, are regulated by QS. Electrophoretic mobility shift assays (EMSAs) revealed several direct targets of EsaR in the regulon. Regulation of three of the

promoters at the level of transcription was confirmed through quantitative reverse transcription-PCR (qRT-PCR), and the binding sites of EsaR have been defined through DNase I footprinting and additional EMSA analysis. Identification of these regulated targets provides a more robust understanding of the QS regulon in *P. stewartii*.

MATERIALS AND METHODS:

Bacterial strains, plasmids, and growth conditions. A list of bacterial strains and plasmids utilized is provided in **Table 3.1**. Both *Pantoea stewartii* and *Escherichia coli* strains were grown in Luria-Bertani (LB) broth supplemented with ampicillin (100 µg/ml) or tetracycline (10 µg/ml) as required. *Pantoea* strains were grown at 30°C, and *E. coli* strains were grown at 37°C. Conjugation was performed using *E. coli* strain CC118λ*pir* carrying the conjugative helper plasmid pEVS104 to facilitate transfer of pSVB60 or pBBR1MCS-3 into *P. stewartii* ESΔIR (**17**) to generate an EsaR-complemented strain and the control with the same selectable marker.

Two-dimensional SDS-PAGE. To prepare cell extracts, *P. stewartii* strain ESN51 grown to stationary phase was used to inoculate 1 liter of LB broth alone or supplemented with 10 µM AHL [*N*-(β-ketocaproyl)-L-homoserine lactone (3-oxo-C₆-HSL)] (Sigma, St. Louis, MO) to an optical density (OD) at 600 nm of 0.05 and allowed to grow at 30°C with shaking to an OD at 600 nm of 0.5. The cells were harvested by centrifugation and stored at -80°C. The cell pellet was resuspended in 15 ml of cold 8 M urea plus 1% Triton buffer and lysed by passage through a French press twice at a cell pressure of 18,000 lb/in². The lysate was then centrifuged for 10 min at 5,000 × *g* at 4°C before being subjected to ultracentrifugation using a Ti70 rotor at 40,000 rpm at 4°C for 1 h to clarify the cell extract. Protein samples were similarly extracted from *P. stewartii* strains ESΔIR (pBBR1MCS-3) and ESΔIR (pSVB60).

2D gel electrophoresis was performed by the Virginia Bioinformatics Institute (VBI) Core Laboratory (Blacksburg, VA). Briefly, samples containing 150 µg of protein were focused in the first dimension using 17-cm, pH 3 to 10 NL immobilized pH gradient (IPG) strips (Bio-Rad, Hercules, CA) and then loaded along with Precision plus protein standard plugs (Bio-Rad) on 20-cm precast 12% SDS-polyacrylamide gels (Jule Inc., Milford, CT). The postelectrophoresis gels were stained with Coomassie staining solution (2.5 g Coomassie brilliant blue R250, 450 ml methanol, and 100 ml acetic acid per liter) and stored in 0.1% sodium azide. The gels were scanned on a GS-800 calibrated densitometer (Bio-Rad) to analyze the differentially expressed protein spots.

Mass spectrometry and protein identification. Differentially expressed proteins were identified by excising the spots of interest from the 2D gels, and their sequence was determined via matrix-assisted laser desorption/ionization tandem time of flight mass spectrometry (MALDI-TOF MS-MS) (Virginia Tech Mass Spectrometry Incubator, Blacksburg, VA) as described previously (18). Protein identifications were made by searching the peptide sequences obtained from mass spectrometry analysis against the supplied *P. stewartii* genome v5 from the ASAP database (19).

Purification of EsaR fusion protein. A His-tagged maltose-binding protein (MBP) fused to a glycine linker-tagged EsaR protein (HMGE) was purified as previously described (20) with the following modifications. To ensure that only DNA-binding competent protein was used in the EMSAs, the purified HMGE was passed through a HiTrap heparin HP column (GE Healthcare Life Sciences, Piscataway, NJ) and eluted using a gradient of 800 mM NaCl. HMGE was then

further purified in a HiPrep 26/60 Sephacryl 200-S (GE Healthcare Life Sciences) gel filtration column using the AKTAPrime fast-performance liquid chromatography (FPLC) system, equilibrated with 20 mM HEPES, 1 mM EDTA, 30 mM KCl, and 10% glycerol (pH 7.4).

EMSA analysis. Phusion DNA polymerase (Thermo Fisher Scientific Inc., Waltham, MA) was used to amplify upstream promoter regions from genes of interest with specific forward and reverse primers (IDT-DNA Inc., Coralville, IA) (see Table A.1 in the supplemental material). The resulting PCR fragments were subsequently purified using the QIAquick gel extraction kit (Qiagen, Valencia, CA). DNA fragments (2 to 10 pmol) were individually end labeled using [γ - 32 P]ATP (PerkinElmer, Waltham, MA) and T4 polynucleotide kinase (New England BioLabs, Ipswich, MA) and resuspended in distilled H₂O (dH₂O) to a final concentration of 20 nM. HMGE (0 to 100 nM) and 1 nM promoter DNA were incubated for 30 min in 20- μ l reaction mixtures with EMSA binding buffer at a final concentration in all samples of 20 mM HEPES, 1 mM EDTA, 30 mM KCl, 0.2% Tween 20, 10 mM (NH₄)₂SO₄, 50 ng/ μ l poly (dI-dC), 150 μ g/ml acetylated bovine serum albumin (BSA), and 10% glycerol (pH 7.4). The constituents of the EMSA reaction were based on previous experiments (14). The postincubation reactions were separated on 6% Tris-glycine-EDTA native PAGE minigels (Bio-Rad) at 80 V for 2 h. The entire apparatus was placed in an ice-packed container to maintain low temperatures. After electrophoresis, the gels were dried and exposed to a Fisher Biotech autoradiography cassette (Fisher Scientific, Pittsburgh, PA). The screen was then visualized using a Typhoon Trio variable-mode imager (GE Healthcare, Life Sciences).

Additional EMSAs performed to determine the precise bases essential for binding were performed in a similar fashion as described above except 10 nM 6-carboxyfluorescein (FAM)-labeled DNA fragments were used instead of radiolabeled fragments, but visualization was still achieved through a Typhoon Trio variable-mode imager.

qRT-PCR. *P. stewartii* ESΔIR (pBBR1MCS) and ESΔIR (pSVB60) grown to stationary phase were used to inoculate 5 ml LB supplemented with tetracycline (10 µg/ml) at an OD at 600 nm of 0.05 and allowed to grow to a final OD at 600 nm of 0.5. RNAprotect bacteria reagent (10 ml) (Qiagen) was used per the manufacturer's instructions to stabilize the RNA. The cell pellets were stored at -80°C prior to total RNA extraction using the RNeasy minikit (Qiagen) with an additional on-column DNase I digestion step using the RNase-free DNase set (Qiagen). RNA was quantified using a NanoPhotometer (Implen, Westlake Village, CA) and submitted to the VBI Core Laboratory Facility for analysis by an Agilent Bioanalyzer 2100 to check for quality. All RNA integrity number (RIN) values were above 9.7. The extracted RNA was converted to cDNA using the high-capacity cDNA reverse transcription kit (Life Technologies, Grand Island, NY) per the manufacturer's instructions. The cDNA was quantified using a NanoPhotometer and checked for purity by measuring absorbance ratios at 260/280 nm and 260/230 nm. The cDNA samples were used as the templates in a 7300 real-time PCR system (Applied Biosystems, now Life Technologies).

Primers were designed to enable amplification of coding regions of the EsrR targets *dkgA*, *fabF*, *glpF*, *lrhA*, *mglB*, and *rpsB* (see Table A.1 in the supplemental material). The amplified fragments were ligated into pGEM (Promega, Madison, WI), transformed into *E.*

coli Top10 cells (**Table 3.1**), and sequenced. They were then used as the template to optimize qRT-PCR primers within 100% ±10% efficiency. The primer pairs (Table A.1) for qRT-PCR analysis of all direct targets of EsaR determined by EMSAs were designed using Primer Express 3.0 (Life Technologies). The parameters for primer design were set as follows: 18 to 24 bp in length, melting temperature (T_m) of 60°C, and amplicon length of 80 to 120 bp. Template DNA (either plasmid or cDNA) was used at concentrations ranging from 10 ng to 0.001 ng per 25- μ l reaction mixture containing 300 nM (each) of the specific forward and reverse primer pair and 2 \times SYBR green PCR master mix (Life Technologies) diluted to a 1 \times concentration with dH₂O. Reactions were carried out in triplicate in a MicroAmp optical 96-well reaction plate (Life Technologies). The thermal cycler settings were programmed for 10 min at 95°C followed by 45 cycles consisting of 15 s at 95°C and 1 min at 60°C, which was also set as the data collection point. A dissociation stage was added at the end of the PCR run to confirm specific product amplification. The data obtained were analyzed through a 7300 system SDS RQ software v1.4 (Life Technologies) using an automated cycle threshold, and the relative expression was calculated using the PFAFFL method (**21**). In total, triplicate samples from two replicate experiments were analyzed.

DNase I footprinting analysis. A modified DNase I footprinting approach (**8**) involved the use of FAM-labeled and non-labeled primer pairs (see Table A.1 in the supplemental material) annealing to the promoter regions of *dkgA*, *glpF*, and *lrhA* to amplify the regions of interest. Fluorescently labeled DNA (50 ng) was incubated with 100 nM HMGE in 1 \times EMSA binding buffer (see above) supplemented with 5 mM MgCl₂ and 2 mM CaCl₂. The DNA was digested using 50 ng of DNase I (Worthington Biochemicals, Lakewood, NJ) for 5 min at room

temperature. The reaction was stopped by the addition of 125 mM EDTA and cleaned using the QIAquick gel extraction kit (Qiagen). A 10- μ l sample of DNA eluted in dH₂O was processed at VBI on the 3730 DNA analyzer (Life Technologies), with a G5 dye set, running an altered default genotyping module with increased injection time and injection voltage (8). The electropherograms of the probes generated from digestion in the presence of BSA and in the presence of HMGE were overlapped using Peak Scanner v1.0 (Life Technologies) to reveal bases that are protected from cleavage by DNase I. Simultaneous manual sequencing of the labeled probe was performed using the Thermo Sequenase cycle sequencing kit (Affymetrix, Santa Clara, CA) using specific FAM-labeled primers to generate 4 electropherograms for each dideoxynucleotide, which were then overlapped to yield sequencing electropherograms that could be compared to the DNase I-digested fragments.

RESULTS:

Identification of QS-regulated proteins. To identify proteins regulated by QS in *P. stewartii*, 2D gel electrophoresis was first performed using cell extracts from *P. stewartii* ESN51 (*esaI* mutant) with and without exogenously added AHL (see Fig. A.1 in the appendix). Several differentially expressed proteins were identified from this preliminary experiment. In order to identify additional proteins of the QS regulon, 2D gel electrophoresis was repeated twice using two other *P. stewartii* strains that exhibit an enhanced physiological response to QS, *P. stewartii* ES Δ IR carrying pBBR1MCS-3 or pSVB60. ES Δ IR is a DC283 Δ *esaR* Δ *esaI* strain that lacks the transcription regulator EsaR and the AHL synthase EsaI, making it completely deficient in QS. This QS defect is partially complemented by pSVB60, which carries the gene coding for EsaR with its expression driven from the native promoter. The vector pBBR1MCS-3

serves as a negative control. In the absence of the AHL synthase, EsaR is constitutively active, allowing for identification of proteins whose expression is activated by EsaR, as demonstrated by qualitatively higher protein levels in strain ESΔIR(pSVB60) versus ESΔIR(pBBR1MCS-3), while proteins that are repressed by EsaR are more highly expressed in ESΔIR(pBBR1MCS-3), since EsaR is completely absent (Fig. A.1). When plated on medium enhancing capsule production, the $\Delta esaR \Delta esaI$ mutant strain ESΔIR(pBBR1MCS-3) exhibits a hypermucoid appearance due to overproduction of capsule, whereas strain ESΔIR(pSVB60) appears dry and streaky due to constitutive repression of capsule production compared to the wild-type control (20). Over the 3 cumulative 2D SDS-PAGE trials (Fig. A.1 in the appendix), 34 proteins were observed twice or more to be differentially expressed, 22 EsaR-activated proteins and 12 EsaR-repressed proteins (Table 3.2). Interestingly, RcsA, a known repressed target of EsaR was not observed, highlighting an inherent drawback due to the limited sensitivity of the proteomic approach.

Identification of direct targets of EsaR. In an attempt to ascertain indirect versus direct targets among the 34 proteins identified from the 2D SDS-PAGE experiments (Table 3.2), the EsaR-regulated genes with 24 promoters putatively controlling 26 of these proteins were tested for direct regulation by EsaR via EMSAs utilizing 200- to 400-bp upstream promoter regions and the EsaR fusion protein HMGE (His-MBP-glycine linker-EsaR) (20). The eight proteins whose promoters were not subjected to EMSA analysis were encoded by genes located in the middle of operons such that no promoter regions were observed in proximity to support EsaR binding, and thus they were not analyzed by EMSA. EsaR directly binds to six promoters (Fig. 3.1), while the rest were established as indirect targets (see Fig. A.1 in the appendix). Specific binding was

demonstrated when labeled promoter probes were bound by HMGE and the shift was successfully competed using non-labeled promoter probes. The genes with the bound promoters are as follows: *dkgA*, encoding 2,5-diketo-D-gluconate reductase A; *fabF*, encoding 3-oxoacyl-(acyl carrier protein) synthase I; *glpF*, encoding glycerol facilitator (first in an operon consisting of *glpK* [glycerol kinase] and *glpX* [fructose 1,6-bisphosphatase II]); *lrhA*, encoding DNA-binding transcriptional repressor of flagellar, motility, and chemotaxis genes; *mglB*, encoding periplasmic binding component of a methyl-galactoside transporter (first in an operon with *mglA* [ATP-binding component] and *mglC* [membrane component] of the methyl-galactoside transporter); and *rpsB*, encoding 30S ribosomal subunit protein (Fig. 3.1). A noticeable difference was observed, though not quantified, in the intensity of the bound probe of *PdkgA* and *PlrhA* compared to the other probes, with *PdkgA* and *PlrhA* showing stronger, more-complete shifts. Furthermore, in initial EMSA trials, three additional promoters, for the genes CKS-5296, encoding putative lipoprotein, *galU*, encoding glucose-1-phosphate uridylyltransferase, and *fusA*, encoding GTP-binding protein chain elongation factor EF-G, were also seen to be weakly bound by HMGE but were unable to successfully compete with the same unlabeled probe (Fig. A.2 in the appendix) and hence they were not pursued further.

Verification of transcriptional control of *dkgA*, *glpF*, and *lrhA*. To quantify the fold change in expression of the six genes with promoters bound by EsaR, qRT-PCR was performed on RNA extracted from *P. stewartii* strain ESΔIR (pBBR1MCS-3) and ESΔIR (pSVB60) (Fig. 3.2). Relative mRNA expression of *glpF* and *lrhA* was increased nearly 4-fold in the presence of EsaR when normalized to the expression of a 16S rRNA gene. Expression of *dkgA* was repressed more than 5-fold in the presence of EsaR. Thus, the 2D SDS-PAGE, EMSA, and qRT-PCR results are

consistent for these three direct targets. Interestingly, the relative expression of *fabF*, *mglB*, and *rpsB* was not significantly altered in the two RNA samples. Although EsaR binds the promoters of these genes as demonstrated by EMSA and the protein encoded by the genes was differentially expressed in previous 2D SDS-PAGE experiments, the mRNA levels remain unchanged in the presence of EsaR.

Determination of the EsaR binding site at the *dkgA*, *glpF*, and *lrhA* promoters. A modified DNase I footprinting technique using fluorescently labeled probes and an automated capillary DNA fragment analysis instrument (8) was optimized for the 181-bp P_{dkgA} DNA fragment, 226-bp P_{glpF} DNA fragment, and the 284-bp P_{lrhA} DNA fragment (Fig. 3.3). Overlapping electropherograms generated from digestion in the presence of BSA and in the presence of HMGE revealed bases that are protected from cleavage by DNase I only in the presence of HMGE.

The binding site on P_{dkgA} is 48 bases upstream of the predicted ATG start codon. This binding site was further delineated by using EMSA analysis on probes that deleted two base pairs at a time until a loss of binding was observed (Fig. 3.4). This allowed us to narrow down the 20 bp that are essential for binding by considering similarity to previously known *esa* boxes (Fig. 3.5) (14, 16). The newly discovered EsaR binding site at *dkgA* is conserved in 11 of 20 bases of the previously known *esa* box in the *esaR* promoter (Fig. 3.5). The EsaR binding site is centered around -22 bp from the initiation site of transcription (based on unpublished RNA sequencing [RNA-Seq] data in A. M. Stevens' lab) and overlaps a putative -10 RNA polymerase binding site, consistent with the repressed nature of this promoter in the presence of EsaR.

A DNase I footprinting analysis of the EsaR-activated *glpF* promoter revealed two 20-bp protected regions ~275 bases upstream of the predicted ATG start site separated by 11 bases. The 51-bp region was protected by cleavage by DNase I in the presence of EsaR (Fig. 3.3). The binding sites were further delineated by using EMSA analysis on probes that deleted three base pairs at a time to identify bases essential for binding (Fig. 3.4). The 20-bp sites sharing the most homology with the *esa* box, with 8 and 9 out of 20 bases conserved with the *esa* box were identified (Fig. 3.5).

Similar analysis of the EsaR-activated *lrhA* promoter using a fluorescently labeled 284-bp upstream promoter DNA identified two distinct 20-bp binding sites separated by 2 bases (Fig. 3.3). EsaR binding at these two sites was confirmed using EMSA analysis of short probes that deleted three base pairs at a time until a loss of binding was observed (Fig. 3.4). The newly discovered EsaR binding sites, with the highest similarity to previously known *esaR* boxes, are conserved in 10 and 11 of 20 bases present in the *esa* box in the *esaR* promoter (Fig. 3.5). These sites are ~475 bp upstream of the predicted ATG start codon and centered at -170 bp from a predicted transcriptional start site (based on unpublished RNA-Seq data in A. M. Stevens' lab). The relative positions of the *esa* boxes in the promoters of EsaR direct targets are shown in Fig. A.3 in the appendix.

Analysis of EsaR binding sites. Previously, only two native binding sites for EsaR had been identified; the *esa* box in the promoter of *esaR* and the *esa* box in the promoter of *rcaA* (15). EsaR has also been shown to bind to the *lux* box in a recombinant *E. coli* harboring a *V. fischeri luxI* promoter in an *in vivo* experiment (16). Using these three known binding sites and the five

newly identified 20-bp EsaR binding sites identified via DNase I footprinting and EMSAs, an alignment was generated to identify a possible consensus sequence for EsaR binding, ACCTGTACTNNAGTACAGNT (where N is any nucleotide) (Fig. 3.5). This sequence is highly palindromic, similar to the conserved palindromes seen in other *lux* box-like sequences (14). Five bases, C3, T4, G5, C16, and A17, are similar to five of the six essential bases of LuxR-DNA interaction identified in the *lux* box of *V. fischeri* (22). The sixth residue at position 18 however, was not conserved, as both A and G residues were observed with similar frequencies. In addition, residues A1, A12, G13, T14, and T20 are also more conserved in the *esa* boxes and could be critical for EsaR-DNA interaction, distinguishing the consensus from the LuxR-binding consensus.

DISCUSSION:

In this study, we have completed a proteomic approach identifying and characterizing genes involved in the QS regulon of *P. stewartii*. Comparison of the differentially expressed proteins in the strains proficient and deficient in QS allowed the identification of over 30 proteins that were previously not known to be regulated by EsaR (Table 3.2). These proteins were observed to play possible roles in capsular synthesis, fatty acid metabolism, and virulence, indicating a more-global cell density-dependent regulation of cellular functions in *P. stewartii* than previously known. While establishing the physiological function of the newly discovered QS-regulated proteins and definitively making connections to virulence in *P. stewartii* is beyond the scope of this study, plausible roles for some of the EsaR-regulated proteins are discussed below.

Two proteins essential in capsule production and previously shown to be not regulated by *rcaA* have been shown to be repressed by EsaR. The genes encoding these two proteins, GalE (UDP-galactose-4-epimerase) and GalF (a putative regulatory subunit for GalU), are found in an operon downstream of the *wceI* operon needed for stewartan production (23). Another repressed protein, GalU (glucose-1-phosphate uridylyltransferase), sometimes found in a complex with GalF (24), is a limiting factor in the production of exopolysaccharide. Thus, by repressing expression of these three proteins, EsaR further inhibits steps in the biosynthesis of stewartan at low cell densities. Interestingly, another previously identified repressed target of EsaR, RcsA, which activates the capsule operon (14), was not observed via 2D SDS-PAGE analysis. This may be due to the specific growth conditions used here or the fact it was simply below the limits of detection. However, OsmC, an osmotically induced membrane protein known to be activated by the Rcs phosphorelay in *E. coli*, was observed to be repressed by EsaR (25). Thus, the proteomic approach has revealed additional possible connections to the regulation of capsule production but has likely still not provided a complete list of the involved factors.

In this study, six promoters that are directly regulated by EsaR were identified and the EsaR binding sites in three of the promoters of the *dkgA*, *glpF*, and *lrhA* genes (Fig. 3.3 and 3.4) were fully characterized. DkgA belongs to the aldo-keto reductase (AKR) family that constitutes NADPH-dependent oxidoreductases with broad substrate ranges. DkgA is hypothesized to catalyze the conversion of 2,5-diketogluconate to 2-keto-L-gluconate in *Erwinia* species (26), and it has been linked to furfural tolerance and ascorbic acid biosynthesis in *E. coli* (27, 28). In *Tatumella citrea*, formerly *Pantoea citrea* (29), the production of 2,5-diketogluconate, is directly responsible for the intense coloration characteristic of pink disease of pineapple (11), presumably

due to pathways containing DkgA-like enzymes. While it is unknown whether *T. citrea* possesses a *dkgA* gene and a QS system similar to those of *P. stewartii* and whether a similar regulation is observed, it is interesting to speculate that DkgA may play a role in causing Stewart's wilt similar to its importance in causing the pink disease of pineapple.

The *glpF* gene codes for a glycerol facilitator in the inner membrane and facilitates transport of glycerol. It is the first gene in a tricistronic operon consisting of *glpK* and *glpX*, which code for a glycerol kinase and a fructose biphosphatase, respectively. Glycerol is found in the mid-guts of beetles in winter, so activating the glycerol utilization operon at low cell densities may be relevant, as a response to *P. stewartii* overwintering in hibernating beetles (30). The *glpFKX* operon is regulated by other transcriptional regulators in *E. coli*, GlpR and the cyclic AMP (cAMP)-cAMP receptor protein (CRP) regulator (31). Potential GlpR and CRP binding sites were observed 87 and 406 bases upstream of the ATG start site, respectively, suggesting similar repressor and activator functions by the two proteins in *P. stewartii*.

LrhA is an indirect repressor of the chemotaxis, motility, and flagellar biosynthesis operon and also represses the expression of genes involved in the synthesis of type 1 fimbriae and the expression of the master regulator FlhDC, through which it indirectly regulates many other genes in *E. coli* (32, 33). In *E. coli*, the expression of *lrhA* is activated by itself and indirectly repressed by the RcsCDB phosphorelay system and FtsK, the DNA motor protein (34). LrhA in *P. stewartii* shares 69% identity with HexA from *Pectobacterium carotovora*, where it is known to negatively regulate the small RNA *rsmB* and RpoS levels (35). In *P. stewartii*, motility at low cell density from the initial site of plant inoculation to the xylem would logically seem to be

necessary. However, the swarming motility exhibited by *P. stewartii* is more critical during biofilm formation within the xylem (36). Swarming motility requires synthesis of capsule, which occurs at high cell density once EsaR is inactive, and when LrhA would also be deactivated. In addition, it is also possible that LrhA-mediated repression of fimbrial expression prevents attachment at low cell density. It is interesting to note that the identified EsaR binding site in P_{lrhA} was more than 475 bases upstream of the ATG start site. This is not unusual however, as the known *esa* box documented on the promoter of *rcaA* is more than 400 bases upstream of the ATG start site. The presence of two sites so far upstream of the start site for translation could be due to the presence of a long 5' untranslated region, indicating the possibility of further regulatory elements such as small noncoding RNAs.

Three additional possible direct targets of EsaR were also found in the EMSA analysis but not by qRT-PCR. The apparent absence of transcriptional control of EsaR of these three targets is inconsistent with the proteomic and EMSA results and could be due to secondary methods of regulation, such as posttranscriptional control by small noncoding RNAs. It is also possible that transcriptional control occurred at an earlier stage of growth with differential protein expression being maintained over a longer period of time. The *fabF* gene, at the end of a fatty acid biosynthesis operon, codes for a 3-oxoacyl-(acyl carrier protein) synthase. Acyl carrier proteins are acyl donors for AHLs and the sugars involved in capsule synthesis. FabF also regulates fatty acid composition of the membrane phospholipids in response to cold in *E. coli* (37). The *mglB* gene is part of a tricistronic operon coding for components of methyl-galactoside transporter and functions as a galactose chemoreceptor and the periplasmic binding component for the transporter in *E. coli* (38). Galactose is an important component of stewartan (39).

The *rpsB* gene codes for a 30S ribosomal subunit protein S2p. There is one report describing elevated levels of RpsB in biofilms of *Listeria monocytogenes*, wherein it was hypothesized to serve as a sensor of physical and chemical changes in the surrounding environment (40). RpsB may serve a similar role in *P. stewartii*.

Complete analysis of the QS regulon and the interactions of various other pathways with QS could illustrate how the cumulative effect of subtle changes in gene expression confers physiological benefits to the bacterium. Therefore, a transcriptomic approach would aid in recognizing the complete picture of additional indirect and direct targets of EsaR. The detailed analysis of the EsaR binding site in the promoters of *dkgA*, *lrhA*, and *glpF* has allowed the development of a more robust consensus sequence for EsaR binding that may prove useful to identify other EsaR-regulated genes using bioinformatic approaches. Deletion analysis of each EsaR direct target individually would aid in understanding the precise roles of these genes in plant pathogenesis and the necessity of regulation by QS in *P. stewartii*. It is probable that the temporal regulation afforded by QS helps the bacterium in adapting to different physiological conditions during colonization and infection.

ACKNOWLEDGEMENTS:

We thank the laboratory of S. von Bodman (University of Connecticut) for providing us with plasmids and strains and sharing unpublished results and W. K. Ray and R. Helm at the Virginia Tech (VT) Mass Spectrometry Incubator for MALDI-TOF MS-MS analysis.

This work is supported by the National Science Foundation grant MCB-0919984, Virginia Tech GSA GRDP award cycle II in 2012 and 2013, and the 2012-2013 Biological Sciences GSDA fellowship.

REFERENCES:

1. **Fuqua C, Winans SC, Greenberg EP.** 1996. Census and consensus in bacterial ecosystems: the LuxR-LuxI family of quorum-sensing transcriptional regulators. *Annu. Rev. Microbiol.* **50**:727–751.
2. **Waters CM, Bassler BL.** 2005. Quorum sensing: cell-to-cell communication in bacteria. *Annu. Rev. Cell Dev. Biol.* **21**:319–346.
3. **Stevens AM, Schuster M, Rumbaugh KP.** 2012. Working together for the common good: cell-cell communication in bacteria. *J. Bacteriol.* **194**:2131–41.
4. **Withers H, Swift S, Williams P.** 2001. Quorum sensing as an integral component of gene regulatory networks in Gram-negative bacteria. *Curr. Opin. Microbiol.* **4**:186–193.
5. **Pataky J.** 2003. Stewart's wilt of corn. doi:10.1094/APSnetFeature-2003-0703.
6. **Beck von Bodman S, Farrand SK.** 1995. Capsular polysaccharide biosynthesis and pathogenicity in *Erwinia stewartii* require induction by an N-acyl homoserine lactone autoinducer. *J. Bacteriol.* **177**:5000–8.
7. **von Bodman SB, Majerczak DR, Coplin DL.** 1998. A negative regulator mediates quorum-sensing control of exopolysaccharide production in *Pantoea stewartii* subsp. *stewartii*. *Proc. Natl. Acad. Sci.* **95**:7687–7692.
8. **Merighi M, Majerczak DR, Zianni M, Tessanne K, Coplin DL.** 2006. Molecular characterization of *Pantoea stewartii* subsp. *stewartii* HrpY, a conserved response regulator of the Hrp type III secretion system, and its interaction with the *hrpS* promoter. *J. Bacteriol.* **188**:5089–100.
9. **Roper MC, Wilt SS.** 2011. *Pantoea stewartii* subsp. *stewartii*: lessons learned from a xylem-dwelling pathogen of sweet corn. *Mol. Plant Pathol.* 1–10.
10. **Coutinho TA, Venter SN.** 2009. *Pantoea ananatis*: an unconventional plant pathogen. *Mol. Plant Pathol.* **10**:325–335.
11. **Pujol CJ, Kado CI.** 2000. Genetic and biochemical characterization of the pathway in *Pantoea citrea* leading to pink disease of pineapple. *J. Bacteriol.* **182**:2230–2237.
12. **Aylward FO, Currie CR, Suen G.** 2012. The evolutionary innovation of nutritional symbioses in leaf-cutter ants. *Insects* **3**:41–61.
13. **Torres-Cabassa A, Gottesman S, Frederick RD, Dolph PJ, Coplin DL.** 1987. Control of extracellular polysaccharide synthesis in *Erwinia stewartii* and *Escherichia coli* K-12: a common regulatory function. *J. Bacteriol.* **169**:4525–4531.

14. **Minogue TD, Carlier AL, Koutsoudis MD, Bodman SB von.** 2005. The cell density dependent expression of stewartan exopolysaccharide in *Pantoea stewartii* ssp. *stewartii* is a function of EsaR-mediated repression of the *rcaA* gene. *Mol. Microbiol.* **56**:189–203.
15. **Minogue TD, Wehland-von Trebra M, Bernhard F, von Bodman SB.** 2002. The autoregulatory role of EsaR, a quorum-sensing regulator in *Pantoea stewartii* ssp. *stewartii*: evidence for a repressor function. *Mol. Microbiol.* **44**:1625–35.
16. **Schu DJ, Carlier AL, Jamison KP, von Bodman SB, Stevens AM.** 2009. Structure/function analysis of the *Pantoea stewartii* quorum-sensing regulator EsaR as an activator of transcription. *J. Bacteriol.* **191**:7402–9.
17. **Koutsoudis MD, Tsaltas D, Minogue TD, von Bodman SB.** 2006. Quorum-sensing regulation governs bacterial adhesion, biofilm development, and host colonization in *Pantoea stewartii* subspecies *stewartii*. *Proc. Natl. Acad. Sci.* **103**:5983–5988.
18. **Gilbert ER, Williams PM, Ray WK, Li H, Emmerson DA, Wong EA, Webb KE.** 2010. Proteomic evaluation of chicken brush-border membrane during the early posthatch period. *J. Proteome Res.* **9**:4628–4639.
19. **Glasner JD.** 2003. ASAP, a systematic annotation package for community analysis of genomes. *Nucleic Acids Res.* **31**:147–151.
20. **Schu DJ, Ramachandran R, Geissinger JS, Stevens AM.** 2011. Probing the impact of ligand binding on the acyl-homoserine lactone-hindered transcription factor EsaR of *Pantoea stewartii* subsp. *stewartii*. *J. Bacteriol.* **193**:6315–22.
21. **Pfaffl MW.** 2001. A new mathematical model for relative quantification in real-time RTPCR. *Nucleic Acids Res.* **29**:e45.
22. **Antunes LCM, Ferreira RBR, Lostroh CP, Greenberg EP.** 2008. A mutational analysis defines *Vibrio fischeri* LuxR binding sites. *J. Bacteriol.* **190**:4392–7.
23. **Carlier A, Burbank L, von Bodman SB.** 2009. Identification and characterization of three novel EsaI/EsaR quorum-sensing controlled stewartan exopolysaccharide biosynthetic genes in *Pantoea stewartii* ssp. *stewartii*. *Mol. Microbiol.* **74**:903–13.
24. **Marolda CL, Valvano MA.** 1996. The GalF protein of *Escherichia coli* is not a UDP glucose pyrophosphorylase but interacts with the GalU protein possibly to regulate cellular levels of UDP-glucose. *Mol. Microbiol.* **22**:827–840.
25. **Sturny R, Cam K, Gutierrez C, Conter A.** 2003. NhaR and RcsB independently regulate the *osmCp1* promoter of *Escherichia coli* at overlapping regulatory sites. *J. Bacteriol.* **185**:4298–4304.
26. **Yum DY, Lee BY, Pan JG.** 1999. Identification of the *yqhE* and *yafB* genes encoding two 2, 5-diketo-D-gluconate reductases in *Escherichia coli*. *Appl. Environ. Microbiol.* **65**:3341–6.

27. **Turner PC, Miller EN, Jarboe LR, Baggett CL, Shanmugam KT, Ingram LO.** 2011. YqhC regulates transcription of the adjacent *Escherichia coli* genes *yqhD* and *dkgA* that are involved in furfural tolerance. *J. Ind. Microbiol. Biotechnol.* **38**:431–9.
28. **Jeudy S, Monchois V, Maza C, Claverie J-M, Abergel C.** 2006. Crystal structure of *Escherichia coli* DkgA, a broad-specificity aldo-keto reductase. *Proteins* **62**:302–7.
29. **Brady CL, Venter SN, Cleenwerck I, Vandemeulebroecke K, De Vos P, Coutinho T.** 2010. Transfer of *Pantoea citrea*, *Pantoea punctata* and *Pantoea terrea* to the genus *Tatumella* emend. as *Tatumella citrea* comb. nov., *Tatumella punctata* comb. nov. and *Tatumella terrea* comb. nov. and description of *Tatumella morbirosei* sp. nov. *Int. J. Syst. Evol. Microbiol.* **60**:484–94.
30. **Cohen E.** 2012. Roles of aquaporins in osmoregulation, desiccation and cold hardiness in insects. *Entomol. Ornithol. Herpetol.* S1:001.doi:10.4172/2161-0983.S1-001.
31. **Weissenborn DL, Wittekindt N, Larson TJ.** 1988. Structure and regulation of the *glpFK* operon encoding glycerol diffusion facilitator and glycerol kinase of *Escherichia coli* K-12. *J. Biol. Chem.* **263**:2409–2416.
32. **Blumer C, Kleefeld A, Lehnen D, Heintz M, Dobrindt U, Nagy G, Michaelis K, Emödy L, Polen T, Rachel R, Wendisch VF, Uden G.** 2005. Regulation of type 1 fimbriae synthesis and biofilm formation by the transcriptional regulator LrhA of *Escherichia coli*. *Microbiology.* **151**:3287–3298.
33. **Lehnen D, Blumer C, Polen T, Wackwitz B, Wendisch VF, Uden G.** 2002. LrhA as a new transcriptional key regulator of flagella, motility and chemotaxis genes in *Escherichia coli*. *Mol. Microbiol.* **45**:521–532.
34. **Peterson CN, Carabetta VJ, Chowdhury T, Silhavy TJ.** 2006. LrhA regulates *rpoS* translation in response to the Rcs phosphorelay system in *Escherichia coli*. *J. Bacteriol.* **188**:3175–3181.
35. **Mukherjee a, Cui Y, Ma W, Liu Y, Chatterjee a K.** 2000. HexA of *Erwinia carotovora* ssp. *carotovora* strain Ecc71 negatively regulates production of RpoS and *rsmB* RNA, a global regulator of extracellular proteins, plant virulence and the quorum-sensing signal, N-(3-oxohexanoyl)-L-homoserine. *Environ. Microbiol.* **2**:203–15.
36. **Herrera CM, Koutsoudis MD, Wang X, Bodman SB von.** 2008. *Pantoea stewartii* subsp. *stewartii* exhibits surface motility, which is a critical aspect of Stewart's wilt disease development on maize. *Mol. Plant Microbe Interact.* **21**:1359–1370.
37. **Garwin JL, Klages AL, Cronan JE.** 1980. Beta-ketoacyl-acyl carrier protein synthase II of *Escherichia coli*. Evidence for function in the thermal regulation of fatty acid synthesis. *J. Biol. Chem.* **255**:3263–3265.

38. **Harayama S, Bollinger J, Iino T, Hazelbauer GL.** 1983. Characterization of the *mgl* operon of *Escherichia coli* by transposon mutagenesis and molecular cloning. *J. Bacteriol.* **153**:408–415.
39. **Wang X, Yang F, von Bodman SB.** 2012. The genetic and structural basis of two distinct terminal side branch residues in stewartan and amylovoran exopolysaccharides and their potential role in host adaptation. *Mol. Microbiol.* **83**:195–207.
40. **Trémoulet F, Duché O, Namane A, Martinie B, Labadie JC.** 2002. Comparison of protein patterns of *Listeria monocytogenes* grown in biofilm or in planktonic mode by proteomic analysis. *FEMS Microbiol. Lett.* **210**:25–31.
41. **Crooks GE, Hon G, Chandonia J-M, Brenner SE.** 2004. WebLogo: a sequence logo generator. *Genome Res.* **14**:1188–1190.
42. **Dolph PJ, Majerczak DR, Coplin DL.** 1988. Characterization of a gene cluster for exopolysaccharide biosynthesis and virulence in *Erwinia stewartii*. *J. Bacteriol.* **170**:865-871.
43. **Grant SG, Jessee J, Bloom FR, Hanahan D.** 1990. Differential plasmid rescue from transgenic mouse DNAs into *Escherichia coli* methylation-restriction mutants. *Proc. Natl. Acad. Sci.* **87**:4645–4649.
44. **Herrero M, De Lorenzo V, Timmis KN.** 1990. Transposon vectors containing non antibiotic resistance selection markers for cloning and stable chromosomal insertion of foreign genes in gram-negative bacteria. *J. Bacteriol.* **172**:6557–6567.
45. **Kovach ME, Elzer PH, Hill DS, Robertson GT, Farris M a, Roop RM, Peterson KM.** 1995. Four new derivatives of the broad-host-range cloning vector pBBR1MCS, carrying different antibiotic-resistance cassettes. *Gene* **166**:175–6.
46. **Stabb, E.V. and Ruby E.** 2002. RP4-based plasmids for conjugation between *Escherichia coli* and members of the Vibrionaceae. *Meth. Enzymol.* **358**:413–426.

Table 3.1: Plasmids and strains used in this study

Bacterial strain or plasmid	Relevant Information ^a	Reference
<i>P. stewartii</i> strains		
DC283	Wild-type SS104; Nal ^r	(42)
ESΔIR	DC283 Δ <i>esaR</i> Δ <i>esaI</i> mutant	(7)
ESΔIR (pBBR1MCS-3)	DC283 Δ <i>esaR</i> Δ <i>esaI</i> mutant with vector control	This study
ESΔIR (pSVB60)	DC283 Δ <i>esaR</i> , Δ <i>esaI</i> mutant with <i>esaR</i> expressed from native promoter	(14)
ESN51	DC283, AHL deficient, <i>esaI</i> ::Tn5seqN51	(6)
<i>E. coli</i> strains		
Top 10	F- <i>mcrA</i> Δ(<i>mrr-hsdRMS-mcrBC</i>) Ø 80 <i>dlacZ</i> ΔM15 Δ <i>lacX74 deoR recAI araD139</i> Δ(<i>ara-leu</i>)7697 <i>galU galK rpsL</i> (Str ^r) <i>endA1 nupG</i>	(43)
CC118λ <i>pir</i>	Δ(<i>ara-leu</i>), <i>araD</i> , Δ <i>lacX74</i> , <i>galE</i> , <i>galK</i> , <i>phoA20</i> , <i>thi-1</i> , <i>rpsE</i> , <i>rpoB</i> , <i>argE</i> (Am), <i>recA1</i> , λ <i>pir</i>	(44)
Plasmids		
pBBR1MCS-3	Broad host range vector; Tet ^r	(45)
pEVS104	Conjugative helper plasmid; <i>tra trb</i> Kn ^r	(46)
pSVB-60	pBBR1MCS-3 with <i>esaR</i> controlled by native P _{<i>esaR</i>} ; Tet ^r	(15)
pHMGE	P _{<i>lac</i>} promoter-controlled HisMBP-GLY5- <i>EsaR</i> ; Ap ^r	(16)

^a Ap^r, Ampicillin resistance; Nal^r, naldixic acid resistance; Tet^r, tetracycline resistance; Kn^r, kanamycin resistance

Table 3.2: The QS regulon of *Pantoea stewartii* regulated by EsaR

Category	Gene ^a	Protein ^b
EsaR-activated genes/proteins	CKS-1750	N-acetylmuramoyl-L-alanine amidase
	CKS-5296	Lipoprotein, putative
	<i>accA</i> *	Acetyl-CoA carboxylase, carboxytransferase, alpha subunit
	<i>aceF</i> *	Pyruvate dehydrogenase, dihydrolipoyltransacetylase component E2
	<i>ahpF</i>	Alkyl hydroperoxide reductase, F52a subunit, FAD/NAD(P) binding
	<i>degP</i>	Serine endoprotease (protease Do), membrane-associated
	<i>fabF</i>	3-oxoacyl-(acyl-carrier-protein) synthase
	<i>fabI</i>	Enoyl-(acyl-carrier-protein) reductase, NADH-dependent
	<i>fkpA</i>	FKBP-type peptidyl-prolyl <i>cis-trans</i> isomerase (rotamase)
	<i>fusA</i>	Protein chain elongation factor EF-G, GTP-binding
	<i>glmU</i>	Fused <i>N</i> -acetyl glucosamine-phosphate uridylyltransferase acetyl transferase
	<i>glpK</i>	Glycerol kinase
	<i>hslU</i> *	Molecular chaperone of HslUV protease
	<i>lrhA</i>	DNA-binding transcriptional repressor of flagellar, motility and chemotaxis genes
	<i>mglB</i>	Methyl-galactoside transporter subunit periplasmic-binding component of ABC superfamily
	<i>nemA</i>	<i>N</i> -Ethylmaleimide reductase, FMN-linked
	<i>ompA</i>	Predicted outer membrane lipoprotein
	<i>pheT</i>	Phenylalanine tRNA synthetase, β -subunit
	<i>rpsB</i>	30S ribosomal subunit protein S2
	<i>rplA</i> *	50S ribosomal subunit protein L1
<i>rplC</i> *	50S ribosomal subunit protein L3	
<i>rplF</i> *	50S ribosomal subunit protein L6	
EsaR-repressed genes/proteins	CKS-2738	UDP-glucose dehydrogenase
	<i>accC</i>	Acetyl-CoA carboxylase, biotin carboxylase subunit
	<i>dkgA</i>	2,5-diketo-D-gluconate reductase A
	<i>galE</i>	UDP-galactose-4-epimerase
	<i>galF</i>	Predicted regulatory subunit of GalU
	<i>galU</i>	Glucose-1-phosphate uridylyltransferase
	<i>htpG</i>	Chaperone protein HtpG
	<i>osmC</i> *	Osmotically inducible, stress-inducible membrane protein
	<i>osmY</i>	Periplasmic protein
	<i>pgm</i>	Phosphoglucomutase
	<i>tetR</i>	Predicted TetR-family transcriptional regulator
<i>atpA</i> *	F1 sector of membrane-bound ATP synthase	

^a Genes not analyzed in EMSA analysis are indicated by an asterisk.

^b CoA, coenzyme A; FKBP, FK506-binding protein; FMN, flavin mononucleotide.

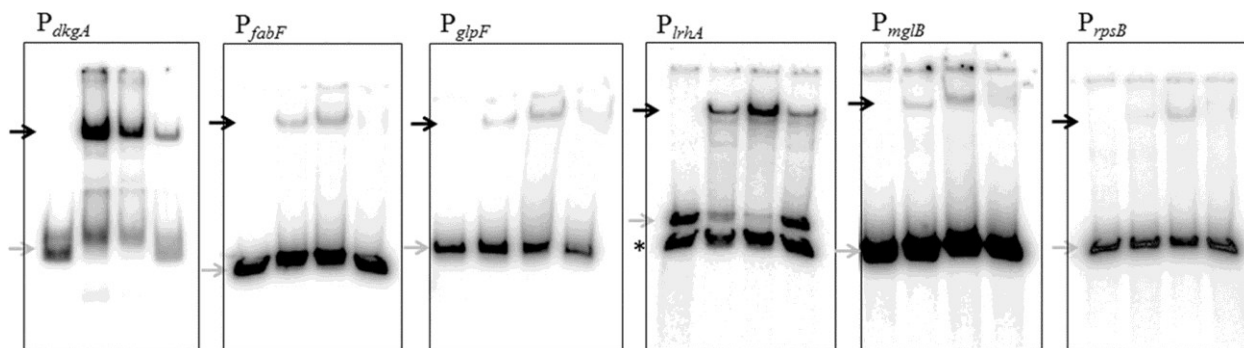


FIG 3.1. Electrophoretic mobility shift assays of putative QS regulon promoters with the His-MBP-glycine linker-EsaR fusion protein, HMGE (20). Gray arrows indicate free, unbound probe; black arrows indicate probe bound by HMGE. The black asterisk to the left of the P_{lrhA} gel indicates a DNA fragment not bound by EsaR that was produced during PCR amplification of P_{lrhA} . The concentration of DNA probe in all lanes is 1 nM. The lanes within each panel consist of the following: from left to right, DNA probe, DNA probe with 50 nM HMGE, DNA probe with 100 nM HMGE, and DNA probe with 100 nM HMGE plus 100 nM unlabeled DNA probe. From left to right, the gene promoters analyzed are P_{dkgA} ($dkgA$ encodes 2,5-diketo-D-gluconate reductase A), P_{fabF} ($fabF$ encodes 3-oxoacyl-[acyl carrier protein] synthase I), P_{glpF} ($glpF$ encodes glycerol facilitator), P_{lrhA} ($lrhA$ encodes a DNA-binding transcriptional repressor of flagellar, motility, and chemotaxis genes), P_{mglB} ($mglB$ encodes a periplasmic binding component of ABC superfamily methyl-galactoside transporter), and P_{rpsB} ($rpsB$ encodes 30S ribosomal subunit protein).

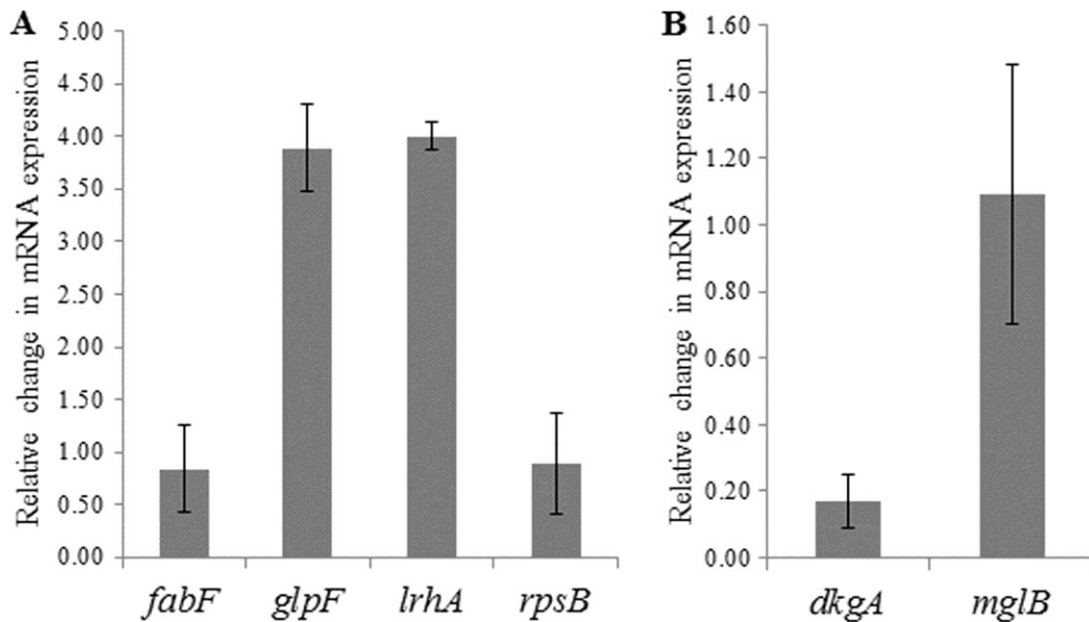


FIG 3.2. Relative change in mRNA expression in *P. stewartii* ESAIR (pSVB60) versus ESAIR (pBBR1MCS-3). Genes activated (A) or repressed (B) by EsaR. Error bars were calculated from triplicate samples obtained from two replicate experiments. All values are normalized with respect to the change in mRNA expression of 16S rRNA which was set at 1.

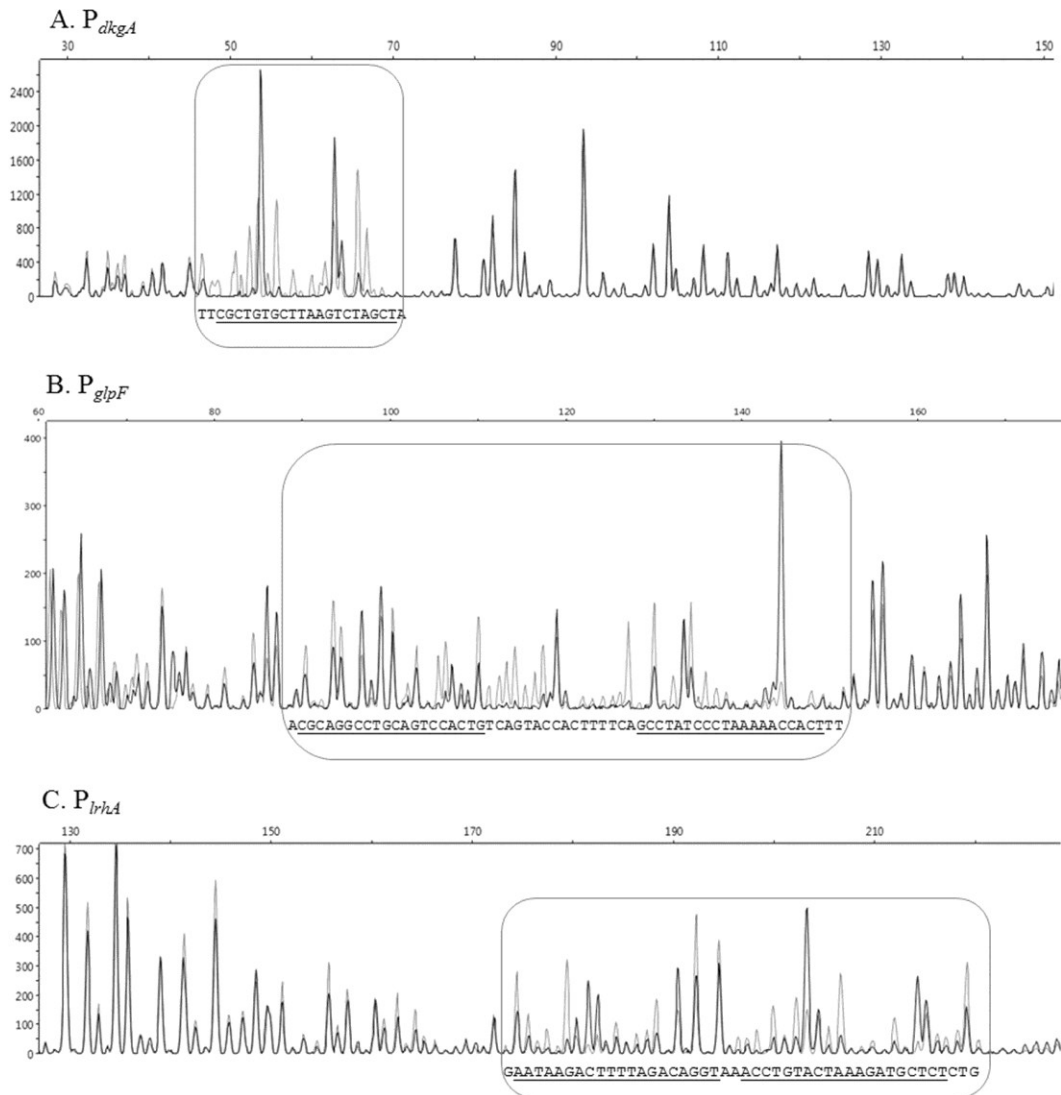


FIG 3.3. DNase I footprinting assay of EsaR binding sites in the noncoding strand of P_{dkgA} , coding strand of P_{glpF} , and noncoding strand of P_{lrhA} . (A to C) Capillary electrophoresis of FAM-labeled DNA fragments P_{dkgA} (A), P_{glpF} (B), and P_{lrhA} (C) from DNase I protection assays in the presence (black) and absence (gray) of HMGE, demonstrating that HMGE binds to specific sequences in the three promoter regions and protects against DNase I digestion. The rounded rectangles highlight the binding regions. The protected sequences are shown at the bottom of the rounded rectangles, and the bases believed to be the 20-bp binding site determined through EMSAs are indicated by underlining. The x axis denotes size in base pairs, and the y axis denotes relative fluorescence units.

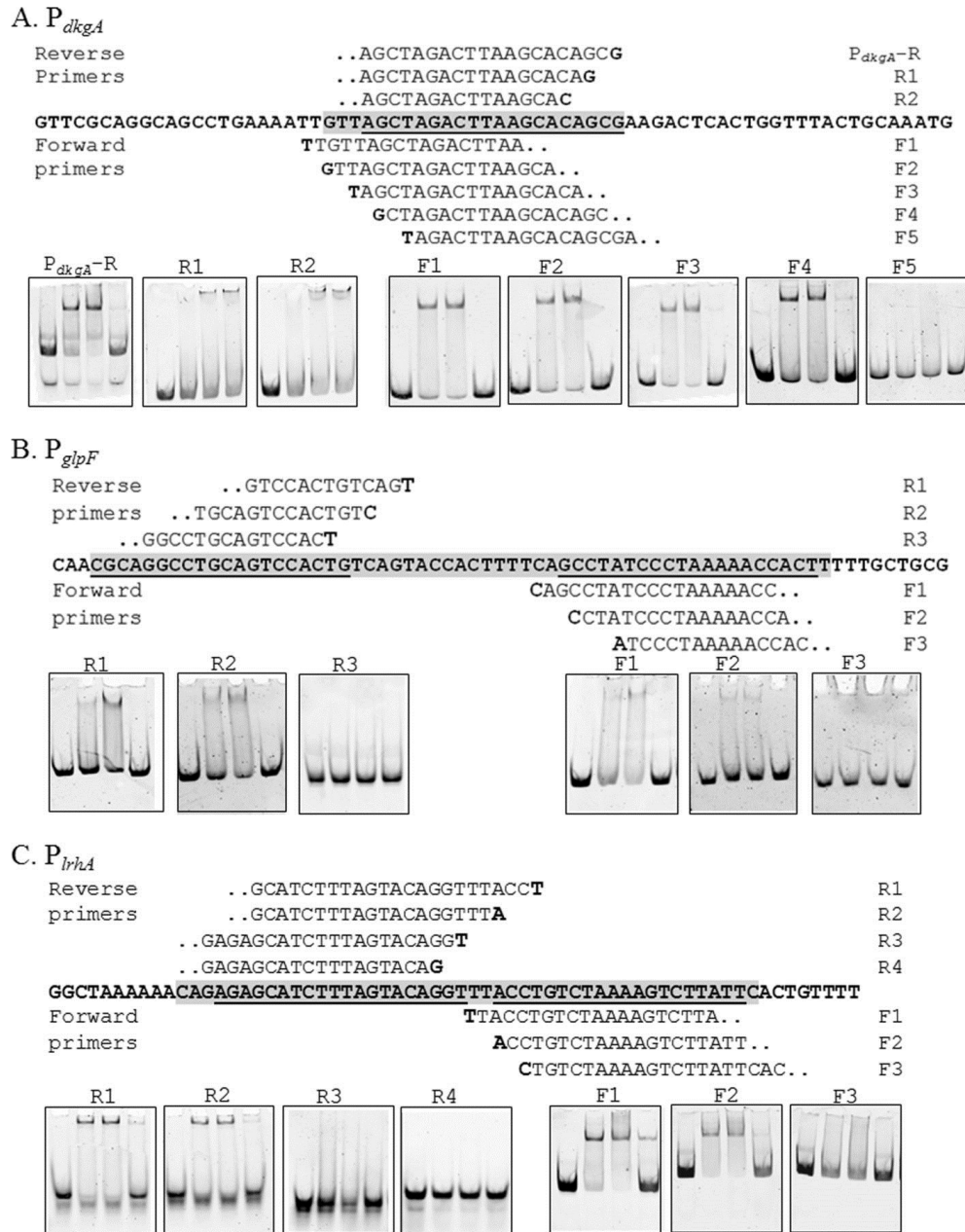


FIG 3.4. Nested deletion EMSA analysis of EsaR direct targets. (A to C) The region protected by DNase I digestion in P_{dkgA} (A), P_{glpF} (B), and P_{lrhA} (C) is the gray-shaded sequence (5' to 3'), and the underlined bases are the 20-bp EsaR binding sites. Sequences above and below the bold sequence are forward and reverse primers used to identify the required bases, and the bold letters in the primer sequence indicate the 5' start base for the primer. EMSAs in boxes denote the point where binding by EsaR is lost upon removing flanking bases of the EsaR binding site. The concentration of DNA probe in all lanes is 10 nM. Lanes within each panel consist of the following (from left to right): DNA probe, DNA probe with 50 nM HMGE, DNA probe with 100 nM HMGE, and DNA probe with 100 nM HMGE plus 100 nM unlabeled DNA probe.

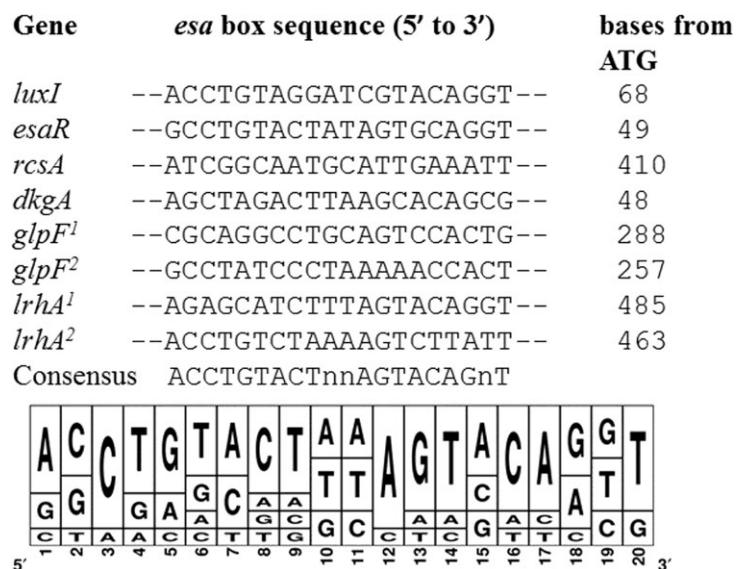


FIG 3.5. Alignment of *esa* boxes recognized by EsaR in *P. stewartii*. The distances of the *esa* box elements from the translational start sites of the downstream open reading frames are indicated. EsaR binds to *esa* boxes on the *esaR* and *rcaA* promoter and to the *lux* box on the *luxI* promoter in *in vitro* assays (14, 16). The five newly discovered *esa* boxes were added to the alignment to generate a consensus sequence. In the consensus sequence, n denotes either one of four nucleotides. The sequence logo was constructed using Weblogo 3.0 (41).

Chapter Four

Transcriptome-based Analysis of the Quorum-Sensing Regulon in

Pantoea stewartii

MANUSCRIPT-IN-PREPARATION

Revathy Ramachandran¹, Alison Kernell Burke¹, Guy Cormier², Roderick V. Jensen¹ and Ann M. Stevens^{1*}

¹Dept. of Biological Sciences, Virginia Tech, Blacksburg, VA 24061

²University of Georgia, Georgia Advanced Computing Resource Center and Institute of Bioinformatics, Athens, GA 30602

*Corresponding author:

Department of Biological Sciences MC 0910
970 Washington St. SW / Rm. 219 Life Sciences 1
Virginia Tech
Blacksburg, VA 24061
Phone (540)-231-9378
FAX (540)-231-4043
Email: ams@vt.edu

Revathy Ramachandran generated the data shown in Table 4.1, Table 4.2, Figure 4.2, Figure 4.4 and Figure 4.5 and contributed to Figure 4.1.

ABSTRACT:

Pantoea stewartii subsp. *stewartii* is a proteobacterium that causes Stewart's wilt disease in corn plants. The bacteria form a biofilm in the xylem of infected plants and produce capsule that blocks water transport, eventually causing wilt. At low cell densities, the quorum-sensing (QS) regulatory protein EsaR represses expression of the capsule, *esaR* itself and *dkgA*, encoding a 2, 5-diketogluconate reductase. Under these conditions, EsaR also functions as an activator and directly enhances expression of *esaS* that encodes a small non-coding RNA, *glpFKX* that encodes the glycerol utilization operon and *lrhA* that encodes a repressor of chemotaxis, motility and adhesion. At high bacterial cell-densities, this regulation is relieved by the binding of EsaR to the acylated homoserine lactone (AHL) signal which is synthesized constitutively over growth. QS-dependent gene expression is critical for the establishment of disease in the plant. However, the identity of the complete set of genes controlled by EsaR/QS is incomplete. A proteomic approach previously identified around 30 proteins in the QS regulon. In this study, a whole transcriptome, next-generation sequencing analysis of rRNA-depleted RNA from QS proficient and deficient *P. stewartii* strains was performed to identify additional targets of EsaR. A qRT-PCR analysis of differentially expressed genes was also used to confirm EsaR-dependent transcriptional regulation of a subset of genes. Eleven newly identified promoters were shown to be directly bound by EsaR using EMSA assays. Overall, the QS regulon of *P. stewartii* orchestrates three major physiological responses; capsule & cell wall biosynthesis, surface motility & adhesion and stress response.

INTRODUCTION:

Stewart's wilt is a disease affecting maize cultivars caused by the proteobacterium *Pantoea stewartii* subsp. *stewartii*. Transmission to plants is possible through an insect vector, the corn flea beetle *Chaetocnema pulicaria* that carries the bacterium in its alimentary canal and transmits bacteria during feeding (1). *P. stewartii* possesses hypersensitivity response and pathogenicity (*hrp/hrc*) type III secretion system (T3SS) and water-soaking effector (*wts*) gene clusters that encode proteins responsible for water-soaked lesions in leaves during the early stages of infection (2). In the later stages of infection, the bacteria colonize the xylem and form a biofilm by secreting the exopolysaccharide stewartan. The formation of biofilm blocks water flow and leads to wilting, necrosis, and possible death, causing severe reductions in crop yield (3). Stewart's wilt is a serious concern for susceptible sweet corn hybrids (1). Bacterial wilt diseases that cause disease by blockage of the vascular systems are seen in many other economically important plant species, such as the bacterial wilt of cucurbit by *Erwinia tracheiphila* (4), black rot of cruciferous plants by *Xanthomonas campestris* (5), Pierce disease of grapes caused by *Xylella fastidiosa* (6) and the broad host-ranged plant pathogen *Ralstonia solanacearum* (7).

In *P. stewartii*, the production of stewartan is controlled by quorum sensing (QS) via the DNA-binding regulatory protein EsaR (8). EsaR controls stewartan production at low cell densities by repressing expression of *rcsA*, which encodes a DNA-binding transcriptional activator of the capsular synthesis operon (9). EsaR senses changes in cell density by recognizing an acylated homoserine lactone (AHL) signal, 3-oxo-hexanoyl-L-homoserine lactone, which is synthesized by the cognate AHL synthase, EsaI. Production of the diffusible AHL is constitutive during

growth in *P. stewartii*, thus the concentration of AHL in the surrounding medium serves as an indicator of population density. In the absence of AHL, EsaR binds to specific 20-bp regulatory sequences in promoter regions called *esa* boxes and affects transcription of downstream genes (8). At high cell density, AHL binds to EsaR leading to derepression or deactivation of downstream gene expression.

Previous studies using a proteomic approach have shown that the QS regulon in *P. stewartii* consists of at least 30 proteins. The production of three other proteins is known to be directly regulated by EsaR; DkgA, 2, 5-diketogluconate reductase that is repressed at low cell densities and LrhA, a repressor of chemotaxis, adhesion & motility, and GlpFKX, glycerol utilization proteins that are activated at low cell-densities (10). Proteomic approaches suffer from a limitation of detection of the protein product. Thus, in this study a high-throughput RNA-Seq analysis was used as a screen for the identification of additional genes involved in the QS regulon of *P. stewartii*. Bioinformatics, qRT-PCR, and electrophoretic mobility shift assays were employed during the analysis of select targets in the regulon. Eleven newly identified promoters were shown to be directly regulated by EsaR. Importantly, it has been shown that the regulation of three physiological functions, capsule production, surface motility/adhesion and stress response appear to be coordinately controlled by EsaR.

MATERIALS AND METHODS:

RNA purification and rRNA depletion for RNA-Seq. Cultures of *P. stewartii* DC283 ESΔIR (pBBR1MCS-3) and DC283 ESΔIR (pSVB60) (10) grown overnight at 30° C were used to inoculate 5 ml RM medium (1x M9 salts, 2% casamino acids, 1 mM MgCl₂ (8)) supplemented with tetracycline (10 μg/ml) and grown to an OD₆₀₀ of 0.5. Ten ml RNA protect Reagent (Qiagen, Valencia, CA) was added and incubated with cells for 5 min at room temperature to stabilize mRNA, before samples were centrifuged for 10 min at 5000 x g. Cell pellets were resuspended in 200 μl TE buffer (10 mM Tris-HCl, 1 mM EDTA, pH 7.0) supplemented with 15 mg/ml lysozyme (Qiagen) and 30 mAU/ml proteinase K (Qiagen). QIAzol lysis reagent was then added and the total RNA harvested using a miRNeasy kit (Qiagen) per the manufacturer's protocol. Quantity and quality of total RNA was assessed on an Agilent Bioanalyzer 2100 at the Virginia Bioinformatics Institute (VBI, Blacksburg, VA). Total RNA of each sample was depleted for ribosomal RNA using the Ribo-zero rRNA removal kit for Gram-negative bacteria (Epicentre, Madison, WI) per the manufacturer's protocol. The rRNA depleted sample was assessed for quality a second time prior to sample processing for Illumina sequencing (VBI) with single-paired read ends of 75-bp length.

Processing of Illumina sequencing data. The *P. stewartii* subsp. *stewartii* transcriptome sequencing read files in FASTQ format were transformed into FASTA format using the SeqIO module of BioPython (11) v.1.63 (www.biopython.org) through Python 2.7.6 on a dual 4-core Opteron workstation with 64GB of RAM running the OpenSUSE 12.3 Linux distribution. Then the standalone BLAST+ suite (12, 13) v.2.2.29

(<ftp://ftp.ncbi.nlm.nih.gov/blast/executables/blast+/2.2.29/>) was used to align the reads to the partially assembled version v5b *P. stewartii* DC283 genome sequence provided on the ASAP website (14). First, a BLAST database and its index were created using the FASTA files for each of the samples using the `makeblastdb` and `makembindex` BLAST+ routines. Second, for each sample, standalone `blastn` queries were performed using the nucleotide sequences for the *P. stewartii* DC283 protein coding genes against the BLAST databases for each sample. In `blastn` a *wordsize* of 16 and a maximum *e-value* of 1.e-10 were chosen for alignment. The table format output (*-outfmt 6*) of each `blastn` query was subsequently processed using an awk-based shell script to count and list the total number of `blastn` hits for each of the protein-coding genes in the *P. stewartii* subspecies *stewartii* data set. Subsequent data processing was done using Microsoft Excel and Lasergene (DNASTAR Inc., Madison, WI). Analysis of +1 transcription start sites was performed by viewing the alignment on reads for presence of a sharp cliff of at least 10 reads, when view in the Megalign (Lasergene) browser. The analysis described above was repeated for the updated genome version v8 made available on the ASAP website. The data for both analyses, using versions of the genome v5b and v8, have been deposited in the NCBI sequence read archive (SRA database) (BioProject identification [ID] PRJNA236462).

EMSA analysis. 6-carboxyfluorescein (FAM)-labeled forward and unlabeled reverse primers (IDT-DNA Inc., Coralville, IA) (Table B.1) were used to generate FAM-labeled DNA fragments. A His-Maltose Binding Protein-Glycine linker tagged EsaR protein (HMGE) was purified as previously described (15) with the following modifications. To ensure only DNA-binding competent protein was used in the EMSA assays, the purified HMGE was passed through a HiTrap Heparin HP Column (GE Healthcare Life Sciences, Piscataway, NJ) and eluted

using 10mM NaH₂PO₄ buffer with a gradient of 0 to 800 mM NaCl. HMGE was then transferred into the EMSA binding buffer (20 mM Hepes, 1 mM EDTA, 30 mM KCl and 10% glycerol, pH 7.4) using a 5 ml desalting column (GE Healthcare Life Sciences). HMGE (0-100 nM) was incubated with 5 nM of FAM-labeled DNA for 30 minutes in EMSA reaction buffer (20 mM Hepes, 1 mM EDTA, 30 mM KCl, 0.2% Tween 20, 10 mM (NH₄)₂SO₄, 50 ng/μl Poly d(I-C), 150 μg/ml acetylated BSA, 10% glycerol, pH 7.4) in a total reaction volume of 20 μl. The post-incubation reactions were separated on pre-chilled 4.5% Tris-Glycine-EDTA native PAGE mini-gels (Bio-Rad, Hercules, CA) at 80 V for 2 hrs. Visualization was achieved through a TYPHOON Trio Variable Mode Imager (GE Healthcare, Life Sciences) using the blue laser.

Quantitative Real-Time PCR (qRT-PCR). *P. stewartii* DC283 ESΔIR (pBBR1MCS-3) and DC283 ESΔIR (pSVB60) cells were grown, treated with RNA protect (Qiagen) and harvested as described above for RNA-Seq. RNA was quantified using a NanoPhotometer (Implen, Westlake Village, CA) and checked for quality using an Agilent Bioanalyzer 2100 (VBI). All RNA integrity number (RIN) values were 10.0. The extracted RNA was converted to cDNA using the High Capacity cDNA Reverse Transcription Kit (Life Technologies, Grand Island, NY) per the manufacturer's instruction. The cDNA was quantified using a NanoPhotometer (Implen) and checked for purity by measuring absorbance ratios at 260/280 nm and 260/230 nm. The cDNA samples were used as templates in a 7300 Real-Time PCR system (Applied Biosystems, now Life Technologies). The primer pairs (Table B.1) for qRT-PCR analysis were designed using Primer Express 3.0 (Life Technologies) and optimized to 100 ± 10% efficiency using cloned coding regions of each gene as template. Primers used for cloning template regions are listed in Table B.1. Parameters for qRT-PCR primer design were set as: 18-24 bp in length, T_m of 64°C

and amplicon length of 80-120 bp. Template DNA (either plasmid or cDNA) was used at concentrations ranging from 80 ng to 0.001 ng per 25 μ l reaction containing 300 nM each of the specific forward and reverse primer pair and 2x SYBR green PCR master mix (Life Technologies) diluted to a 1x concentration with dH₂O. Reactions were carried out in triplicate in a MicroAmp Optical 96-well Reaction Plate (Life Technologies) on samples from two separate experiments. The thermal cycler settings were programmed for 95^oC for 10 min, 45 cycles of 95^oC for 15 sec and either 60^oC, 62^oC or 64^oC for 1 min depending on the primer pair (Table B.1), which was also set as the data collection point. A dissociation stage was added at the end of the PCR run to confirm specific product amplification. The data obtained was analyzed through 7300 system SDS RQ software v1.4 (Life Technologies) using an automated cycle-threshold and the relative expression calculated using the PFAFFL method (16).

RESULTS:

RNA-Seq analysis of the QS regulon in *P. stewartii*. A RNA-Seq analysis was performed as a screen to identify genes in the EsaR regulon using ribosomal-RNA depleted RNA from the QS proficient *esaR*⁺/*esaI* strain DC283 ESΔIR (pSVB60) and the QS deficient *esaR*⁻/*esaI* strain DC283 ESΔIR (pBBR1MCS-3) described previously (10). Thirty million reads of 75-bp length were obtained for each sample that aligned with nearly 100 x coverage for most genes, when aligned to the v5b *P. stewartii* DC283 genes available at the ASAP database. The genome of *P. stewartii* contains 30 identical transposases, which were excluded from the analysis during normalization of reads. Insertion sequence IS66 Orf2, genes coding for hypothetical proteins and putative protein products were also excluded. From the refined dataset of 3125 genes, roughly

200 genes were observed to be differentially regulated two-fold or higher in the two strains (Table B.2). Approximately 150 genes were seen to be repressed and around 60 genes were activated (Table B.2, Figure 4.1). The mRNA transcripts for the EsaR-repressed *rcsA* gene were five-fold higher in DC283 ESΔIR (pBBR1MCS-3) (the *esaR*, *esaI* deletion strain) whereas the *esaR* gene was 3.6-fold higher in DC283 ESΔIR (pSVB60) (the *esaR/esaI* deletion strain with *esaR* complemented in multicopy). Two previously identified EsaR direct targets, *dkgA* and *lrhA* were seen to be repressed seven-fold and activated three-fold, respectively, consistent with published results (10). However, no change in expression was observed in the expression of the *glpFKX* operon, another directly activated target of EsaR (Table B.2). Some mRNA reads were seen to align to non-coding regions of the genome, indicating the presence of possible non-coding sRNAs and additional regulatory systems. EsaS, the sRNA activated by EsaR (15) was found to be activated nearly ten-fold in DC283 ESΔIR (pSVB60). The mapped transcriptome also allows for visualization of 5' untranslated regions, aiding in prediction of transcriptional start sites, upstream regulatory elements and genome assembly.

Bioinformatic approach to identify direct targets of EsaR. To identify genes that are directly regulated by the master QS regulator EsaR, a bioinformatics approach was first attempted. Such an approach was attractive, as it helps in reducing the number of possible targets in the large amounts of data available from high-throughput analyses like RNA-Seq. A position specific weight matrix (PSWM) was constructed using the alignment of eight published 20-bp EsaR binding sites (*esa* boxes) (10). Using the PATSER program (17) the entire *P. stewartii* database was scanned to identify promoters that possess an *esa* box with similarity to the PSWM. This list was next cross-referenced with the list of differentially expressed mRNAs determined through

RNA-Seq to identify genes that were regulated at least two-fold. Ten genes were identified including three previously known genes, *esaR*, *dkgA* and *lrhA*, which possessed high-scoring *esa* boxes in the PATSER program (Table 4.1). EMSA analysis was carried out on the promoters of the seven remaining genes. Two promoters, P_{CKS-5453} and P_{CKS-0678} were shown to be bound by the His-MBP-Glycine linker-EsaR fusion protein (HMGE) (15) and the shift was successfully competed by the specific competitor, the 28-bp PesaR28 DNA fragment (8) (Figure 4.2). As positive and negative controls, the 181-bp P_{dkgA} promoter probe (10) and a 32-bp MCS from pUC18 generated by annealing complementary primers were used, respectively (Figure 4.2). The remaining four promoters were found to be not bound by EsaR, despite possessing very high-scoring predicted *esa* boxes. Additionally, one promoter, P_{uspB} showed very weak binding by EsaR. Analysis of the region upstream revealed a divergently transcribed gene *uspA*, repressed 2.3 times by EsaR in the RNA-Seq data and possessing a lower-scoring *esa* box in its promoter, possibly shared with *uspB*. EMSA analysis revealed that this promoter, P_{uspA}, is strongly bound by EsaR, possibly regulating both *uspA* and *uspB* (Figure 4.2). Taken together, these findings suggest that the scoring and sorting of potential targets based on a predicted PSWM scores was not highly effective, possibly due to the limitations of the bioinformatics tools applied or the consensus sequence utilized.

Validating transcriptional control and identifying putative direct targets. A second set of criteria was established to broaden the potential list of predicted direct targets of EsaR from among the differentially expressed genes seen in the RNA-Seq analysis. Promoters of the most differentially regulated genes that possessed a clear transcriptional start site (+1) and a possible EsaR binding site in or around the +1 were analyzed. This approach placed less emphasis on the

scoring of the possible *esa* boxes. Twenty-six genes that were differentially expressed four-fold or higher in the presence of EsaR were studied for predicted +1 sites. A potential +1 was characterized by a sharp rise in the number of aligned reads at a particular nucleotide residue upstream of the ATG start codon. The +1 of previously known direct targets of EsaR showed similar sharp rises. The putative EsaR binding sites were identified by using the PATSER program as described above (18). Of the 26 genes regulated four-fold or higher, eight genes did not possess a clear +1 and were not analyzed further. Four other genes were targets seen previously, *esaI*, *esaR*, *rcaA*, and *dkgA*. The remaining 14 genes, putatively controlled by 12 promoters, were analyzed further (Table 4.2). Quantitative RT-PCR was performed to validate the changes in gene expression observed in the Illumina sequencing. Two separate RNA samples extracted independently of the sample generated for RNA-Seq analysis were used. The 16S rRNA coding region was used as reference to normalize expression of other genes. All genes showed fairly similar levels of regulation as seen in RNA-Seq analysis, except CKS-3373 and *elaB* which appears to be minimally regulated and *wceG2*, which was down regulated 14-fold in the presence of EsaR in the qRT-PCR assays, but only four-fold in RNA-Seq. Although the ratios of change in expression obtained via RNA-Seq and qRT-PCR differed slightly, all genes displayed similar trends in regulation (activation vs. repression) (Figure 4.3).

EMSA analysis on putative targets: The 12 putative EsaR-controlled promoters (Table 4.2) were subsequently analyzed for direct binding using EMSA analysis with the same positive and negative controls described above. Eight promoters were shown to bind the His-MBP-Glycine linker-EsaR fusion protein (HMGE) (15) and the shift was successfully outcompeted in the presence of a specific competitor, the 28-bp PesaR28 DNA fragment (8) (Figure 4.4). Three

promoters did not successfully bind HMGE. However a fourth promoter, P_{yjbE} , did exhibit weak binding at the highest concentration of HMGE used. The promoter of CKS-3373 which failed to show any regulation in the qRT-PCR assays also did not seem to be bound by EsaR. However, the promoter of *elaB* showed strong binding to the EsaR fusion protein, despite the lack of transcriptional regulation seen in qRT-PCR assays. This difference in assay output between EMSA and qRT-PCR has been observed previously for *glpF* (10).

DISCUSSION:

RNA-Seq analysis was performed on strains of *P. stewartii* proficient and deficient in QS to broaden the defined EsaR regulon. Transcriptome data consisting of 30 million reads from a single RNA-Seq experiment was generated and aligned to 66 contigs and for nearly 3000 gene, allowing the visualization of the alignment of overlapping reads for each mRNA fragment. The alignment of reads to the genome allowed for estimation of putative +1 transcriptional start sites, a read pile-up profile of the mRNA and the presence of any 3' or 5' untranslated sequence. Subsequent validation and confirmation of genes directly regulated by EsaR, the master QS regulator in *P. stewartii*, was performed using qRT-PCR and EMSA assays respectively. In total, 11 promoters were newly identified as direct targets of EsaR. All of the promoters are repressed by EsaR, which could be the result of a bias during the selection process for putative targets. The genes putatively controlled by these promoters can be broadly classified into the functional categories of cell wall and capsule biosynthesis (*WceG2*, *WceL*, *YjbE*, CKS-5453), surface motility & adhesion (CKS-0458, CKS-0459, CKS-0461) and stress response (*YciF*, *ElaB*, CKS-1103, *OsmY*, CKS-088, *UspA*, *UspB*) (Figure 4.5). With the addition of *UspA* as a directly

regulated target, EsaR controls three regulators RcsA, LrhA and UspA for each of the 3 broad functional classifications under which the directly regulated genes lie.

EsaR indirectly represses the expression of stewartan via the RcsA-dependent pathway (19). Here it is shown that EsaR directly regulates four additional genes involved in synthesis of capsule, *wceG2*, *wceL*, *yjbE* and *CKS-5453*. WceL, a UDP-glucose-4-epimerase and WceG2, undecaprenyl-phosphate UDP-galactose phosphotransferase, are two proteins expressed by genes in the stewartan I cluster (20) by promoters independent of the RcsA-controlled promoter. Interestingly, *wceG2* possesses a nearly 100-bp untranslated region in the RNA-Seq read alignment with considerably higher expression than the coding region, suggesting the presence of a small regulatory RNA that would add to the complexity of regulation by EsaR. Regulation of capsule production in *P. stewartii* appears to be an example of a coherent feedforward loop, in which a master transcription factor EsaR regulates a downstream regulator RcsA and genes at the end of the cascade concurrently (21). Such kinetics is critical for filtering out noisy inputs in an environment, while yet achieving rapid response. In *P. stewartii*, this multi-layered control could help in varying the amounts of capsule produced by fine tuning the expression of each target when appropriate environmental cues are received.

P. stewartii mutants of *wceL* are deficient in EPS and proficient in adhesion (22). Synthesis of stewartan begins with WceG2, which has redundant function with WceG1 (23). Another EsaR target, CKS-5453 codes for N-acetylmuramyl-L-alanine amidase, and is homologous to *ampD* from *E. coli*. The role of CKS_5453 in capsule biosynthesis is less clear, but it is involved in cell wall degradation that could release by-products utilizable in stewartan synthesis (24). P_{yjbE} ,

although only weakly bound by EsaR, is still interesting to study. YjbE is a predicted protein thought to play a role in exopolysaccharide production and overexpression of the *yjbEFGH* operon. These genes influence colony morphology and production of a non-colanic acid polysaccharide (25). *P. stewartii* possesses an intact *yjbEFGH* operon which is seen to be repressed by EsaR in our RNA-Seq experiments. Coincidentally, in *E. coli*, the heterodimer RcsAB also binds to and activates the expression from P_{*yjbE*}, giving further evidence to a possible coherent feed forward regulatory mechanism adopted by EsaR (25).

Three of the most highly regulated genes seen in the RNA-Seq data belong to a sigma-fimbriae operon, whose expression is repressed in the presence of EsaR (Figure 4.5). It is interesting to note that EsaR activates *lrhA*, a predicted repressor of chemotaxis, motility and fimbriae expression (10). The timed expression of fimbriae may be critical to biofilm formation or adhesion in the xylem since both LrhA and EsaR seem to work together to ensure repression at low cell density. *P. stewartii* utilizes surface motility at high cell densities to form a biofilm and spread systematically in the xylem. Its motility is dependent on expression of flagella and stewartan (26). Perhaps the expression of the sigma-fimbriae operon at high cell-density within the xylem aids in adhesion of the biofilm to the lumen. Of the many flagella-associated proteins that *P. stewartii* possesses, levels of *fliC* (flagellin subunit), *fliD* (flagellar hook-associated protein) and *fliR* (flagellar biosynthesis protein) are repressed more than 2-fold at low cell-densities in the presence of EsaR in the RNA-Seq data, further supporting this hypothesis.

The majority of the genes seen to be directly regulated by EsaR are involved in stress response. UspA, the universal stress response regulator was repressed, along with five other proteins involved in stress response of which *yciF*, *elaB*, CKS1103 and *osmY* are part of the alternative

sigma factor for stress, σ^S , regulon. How EsaR affects the expression of σ^S is not known. However, *rpoS*, was seen to be nearly 2-fold repressed in the RNA-Seq dataset. It would be interesting to further elucidate this mechanism and study the effect of deletion of *uspA* and *rpoS* in *P. stewartii* pathogenesis. ElaB is an inner membrane protein associated with the ribosomes whose function is unknown (27). Interestingly, *elaB* expression is under regulation by QS in another plant-associated microbe. A moderate effect in expression of *elaB* in response to C8-HSL induced QS regulation in *Burkholderia ambifaria*, a bacterium found normally in the pea rhizosphere, has been observed (28). YciF is an uncharacterized protein belonging to the DUF892 family that is putatively involved in stress response and part of the σ^S regulon (29). Expression of *yciF* was repressed in a mutant of the master QS regulator MqsR in *E. coli*, although via an autoinducer 2 dependent pathway which *P. stewartii* is not known to possess (30). OsmY was seen to be repressed by EsaR in previously carried out proteomic studies (10). OsmY is a periplasmic protein that is induced under hyperosmotic stress and is under complex regulation by many global regulators in *E. coli* (31). CKS-1103 is a 55 aa long peptide that is induced in response to stress and shares 71% identity with YciG of *E. coli*. CKS-0881 is another stress induced protein that shares 35% identity with YhcN, a hydrogen peroxide stress-induced protein of *E. coli*. Independent of the RpoS regulon, *uspA* codes for the universal stress global response regulator and is divergently transcribed from *uspB*, encoding the predicted universal stress response protein B. Universal stress proteins (USPs) are overproduced in response to a variety of stresses and afford the organism a mechanism to survive in unsuitable conditions, though by unknown pathways (32). EsaR represses production of UspA and other genes at low cell-density, tamping down the apparent stress response of *P. stewartii* when it's present in the leaf tissue during early stages of infection.

The studies described in this manuscript were performed on the then-available version 5b (v5b) of the *P. stewartii* DC283 genome on the ASAP website (14). During the course of the analysis, a newer, more complete version of the *P. stewartii* genome was released. Version 8 (v8) consists of 4490 protein coding genes. Upon repeating the analysis with the newly available version v8 of the genome additional putative direct targets have been identified that this study may have missed. After aligning the Illumina sequencing reads to the v8 database, normalization was performed and the transposases and IS66 Orf2 elements were excluded similar to analysis using v5b. However, the hypothetical genes were included in the later analysis using v8 due to their large numbers. The new alignment mapped to 4440 genes, and around 400 genes were seen to differentially regulated two-fold or higher (BioProject ID PRJNA236462). Most of these regulated genes (around 200) are annotated to code for hypothetical proteins. Four newly annotated genes seen to be regulated four-fold or higher were discovered, that were not analyzed in this study and maybe of interest. CKS-4376 coding for a putative transcriptional regulator and CKS-2108 coding for a putative type I secretion protein are repressed by EsaR and CKS-2806 coding for a putative formate dehydrogenase oxidoreductase protein and *yebE* coding for an uncharacterized DUF533 family protein are activated by EsaR.

In summary, genes relevant to three physiologically responses, capsule & cell wall biosynthesis, surface motility & adhesion and stress response were seen to be regulated by QS in *P. stewartii*. Eleven promoters were identified to be direct targets of EsaR, considerably broadening the defined QS regulon of *P. stewartii*. Three second-tier regulators may be involved in controlling the three major physiological responses that are directly regulated by EsaR. Additionally, some of the genes downstream of these regulators are also direct targets of EsaR suggesting a coherent

feedforward mechanism of regulation control that may permit a fine-tuned response to different environmental inputs. Further analysis into the function of each direct target will elucidate the role, if any, in plant pathogenesis. Such information could be useful in the development of disease prevention strategies in maize, and perhaps be adaptable to other important crops affected by bacterial wilt diseases.

ACKNOWLEDGEMENTS:

We would like to thank the Susanne von Bodman for providing strains and plasmids, members of the *Pantoea stewartii* subsp. *stewartii* DC283 whole genome shotgun (WGS) project at the University of Wisconsin for making the genome sequence available prior to publication and Blakely Sproles for technical assistance in plasmid construction.

This work is supported by National Science Foundation grant MCB- 0919984 (AMS), Virginia Tech Graduate Student Association Graduate Research Development Program (GSA GRDP) award (RR) and a Biological Sciences Graduate Student Development Award (GSDA) fellowship (RR).

REFERENCES:

1. **Pataky J.** 2003. Stewart's wilt of corn. doi:10.1094/APSnet Feature-2003-0703.
2. **Ham JH, Majerczak D, Ewert S, Sreerekha M-V, Mackey D, Coplin D.** 2008. WtsE, an AvrE-family type III effector protein of *Pantoea stewartii* subsp. *stewartii*, causes cell death in non-host plants. *Mol. Plant Pathol.* **9**:633–643.
3. **Roper MC.** 2011. *Pantoea stewartii* subsp. *stewartii*: lessons learned from a xylem-dwelling pathogen of sweet corn. *Mol. Plant Pathol.* **12**:628–37.
4. **Sasu MA, Seidl-Adams I, Wall K, Winsor JA, Stephenson AG.** 2010. Floral transmission of *Erwinia tracheiphila* by cucumber beetles in a wild *Cucurbita pepo*. *Environ. Entomol.* **39**:140–148.
5. **Crossman L, Dow JM.** 2004. Biofilm formation and dispersal in *Xanthomonas campestris*. *Microbes Infect.* **6**:623–629.
6. **Nunney L, Yuan X, Bromley R, Hartung J, Montero-Astúa M, Moreira L, Ortiz B, Stouthamer R.** 2010. Population genomic analysis of a bacterial plant pathogen: novel insight into the origin of Pierce's disease of grapevine in the U.S. *PLoS One* **5**:e15488.
7. **Peeters N, Guidot A, Vailliau F, Valls M.** 2013. *Ralstonia solanacearum*, a widespread bacterial plant pathogen in the post-genomic era. *Mol. Plant Pathol.* **14**:651–62.
8. **Minogue TD, Wehland-von Trebra M, Bernhard F, von Bodman SB.** 2002. The autoregulatory role of EsaR, a quorum-sensing regulator in *Pantoea stewartii* ssp. *stewartii*: evidence for a repressor function. *Mol. Microbiol.* **44**:1625–35.
9. **Beck von Bodman S, Farrand SK.** 1995. Capsular polysaccharide biosynthesis and pathogenicity in *Erwinia stewartii* require induction by an N-acylhomoserine lactone autoinducer. *J. Bacteriol.* **177**:5000–8.
10. **Ramachandran R, Stevens AM.** 2013. Proteomic analysis of the quorum-sensing regulon in *Pantoea stewartii* and identification of direct targets of EsaR. *Appl. Environ. Microbiol.* **79**:6244–52.
11. **Cock PJA, Antao T, Chang JT, Chapman BA, Cox CJ, Dalke A, Friedberg I, Hamelryck T, Kauff F, Wilczynski B, de Hoon MJL.** 2009. Biopython: freely available Python tools for computational molecular biology and bioinformatics. *Bioinformatics* **25**:1422–1423.
12. **Altschul SF, Gish W, Miller W, Myers EW, Lipman DJ.** 1990. Basic local alignment search tool. *J. Mol. Biol.* **215**:403–410.

13. **Camacho C, Coulouris G, Avagyan V, Ma N, Papadopoulos J, Bealer K, Madden TL.** 2009. BLAST+: architecture and applications. *BMC Bioinformatics* **10**:421.
14. **Glasner JD.** 2003. ASAP, a systematic annotation package for community analysis of genomes. *Nucleic Acids Res.* **31**:147–151.
15. **Schu DJ, Carlier AL, Jamison KP, von Bodman SB, Stevens AM.** 2009. Structure/function analysis of the *Pantoea stewartii* quorum-sensing regulator EsaR as an activator of transcription. *J. Bacteriol.* **191**:7402–9.
16. **Pfaffl MW.** 2001. A new mathematical model for relative quantification in real-time RT-PCR. *Nucleic Acids Res.* **29**:e45.
17. **Hertz GZ, Stormo GD.** 1999. Identifying DNA and protein patterns with statistically significant alignments of multiple sequences. *Bioinformatics* **15**:563–577.
18. **Thomas-Chollier M, Sand O, Turatsinze J-V, Janky R, Defrance M, Vervisch E, Brohée S, Van Helden J.** 2008. RSAT: regulatory sequence analysis tools. *Nucleic Acids Res.* **36**:W119–W127.
19. **Carlier AL, von Bodman SB.** 2006. The *rcaA* promoter of *Pantoea stewartii* subsp. *stewartii* features a low-level constitutive promoter and an EsaR quorum-sensing-regulated promoter. *J. Bacteriol.* **188**:4581–4.
20. **Wang X, Yang F, von Bodman SB.** 2012. The genetic and structural basis of two distinct terminal side branch residues in stewartan and amylovoran exopolysaccharides and their potential role in host adaptation. *Mol. Microbiol.* **83**:195–207.
21. **Mangan S, Zaslaver A, Alon U.** 2003. The coherent feedforward loop serves as a sign-sensitive delay element in transcription networks. *J. Mol. Biol.* **334**:197–204.
22. **Koutsoudis MD, Tsaltas D, Minogue TD, von Bodman SB.** 2006. Quorum-sensing regulation governs bacterial adhesion, biofilm development, and host colonization in *Pantoea stewartii* subspecies *stewartii*. *Proc. Natl. Acad. Sci. U. S. A.* **103**:5983–5988.
23. **Carlier A, Burbank L, von Bodman SB.** 2009. Identification and characterization of three novel EsaI/EsaR quorum-sensing controlled stewartan exopolysaccharide biosynthetic genes in *Pantoea stewartii* ssp. *stewartii*. *Mol. Microbiol.* **74**:903–13.
24. **Jacobs C, Joris B, Jamin M, Klarsov K, Van Beeumen J, Mengin-Lecreux D, van Heijenoort J, Park JT, Normark S, Frère JM.** 1995. AmpD, essential for both beta-lactamase regulation and cell wall recycling, is a novel cytosolic N-acetylmuramyl-L-alanine amidase. *Mol. Microbiol.* **15**:553–559.

25. **Ferrieres L, Aslam SN, Cooper RM, Clarke DJ.** 2007. The *yjbEFGH* locus in *Escherichia coli* K-12 is an operon encoding proteins involved in exopolysaccharide production. *Microbiology* **153**:1070–1080.
26. **Herrera CM, Koutsoudis MD, Wang X, Bodman SB Von.** 2008. *Pantoea stewartii* subsp. *stewartii* exhibits surface motility, which is a critical aspect of Stewart's wilt disease development on maize. *Mol. Plant-Microbe Interact.* **21**:1359–1370.
27. **Yoshida H, Maki Y, Furuike S, Sakai A, Ueta M, Wada A.** 2012. YqjD is an inner membrane protein associated with stationary-phase ribosomes in *Escherichia coli*. *J. Bacteriol.* **194**: 4178-4183
28. **Chapalain A, Vial L, Laprade N, Dekimpe V, Perreault J, Déziel E.** 2013. Identification of quorum sensing-controlled genes in *Burkholderia ambifaria*. *Microbiologyopen* **2**:226–42.
29. **Weber H, Polen T, Heuveling J, Wendisch VF, Hengge R.** 2005. Genome-wide analysis of the general stress response network in *Escherichia coli*: σ S-dependent genes, promoters, and sigma factor selectivity. *J. Bacteriol.* **187**:1591–1603.
30. **González Barrios AF, Zuo R, Hashimoto Y, Yang L, Bentley WE, Wood TK.** 2006. Autoinducer 2 controls biofilm formation in *Escherichia coli* through a novel motility quorum-sensing regulator (MqsR, B3022). *J. Bacteriol.* **188**:305–316.
31. **Yim HH, Brems RL, Villarejo M.** 1994. Molecular characterization of the promoter of *osmY*, an *rpoS*-dependent gene. *J. Bacteriol.* **176**:100–107.
32. **Tkaczuk KL, A Shumilin I, Chruszcz M, Evdokimova E, Savchenko A, Minor W.** 2013. Structural and functional insight into the universal stress protein family. *Evol. Appl.* **6**:434–49.

Table 4.1: Genes in the RNA-Seq dataset that possess high-scoring predicted *esa* boxes in their upstream promoter regions and are differentially expressed two-fold or higher.

Accession no.	Gene name	Protein Product	Fold regulation ^a	Predicted EsaR binding sequence	^b <i>esa</i> box score	Promoter bound by EsaR
^c ACV-0290094	<i>esaR</i>	Quorum-sensing transcriptional activator EsaR	5.39 (A)	GCCTGTAC TATAGTGC AGGT	14.87	Yes (8)
^c ACV-0290502	<i>dkgA</i>	2,5-diketo-D-gluconate reductase A	6.73 (R)	AGCTAGAC TTAAGCAC AGCG	11.58	Yes (10)
ACV-0288416	<i>uspB</i>	Universal stress protein B	2.39 (R)	ACCGGCAC CGCAGAAC AGTG	10.58	Yes
ACV-0287730	<i>CKS-5453</i>	N-acetylmuramoyl-L-alanine amidase AmpD	2.04 (R)	ACAGGGAC GAAAATGC AGCT	9.07	Yes
^c ACV-0285895	<i>lrhA</i>	LysR family transcriptional regulator <i>lrhA</i>	3.15 (A)	AGAGCATC TTTAGTAC AGGT	8.89	Yes (10)
ACV-0289544	<i>wceG1</i>	Undecaprenol-phosphate galactose-phosphotransferase /O-antigen transferase	3.29 (R)	GGCTCAAC ATCAGTAC TGTT	8.84	No
ACV-0290308	<i>CKS-0678</i>	Pyridoxal-5'-phosphate-dependent enzyme, β -subunit	2.59 (A)	CCCTGCCC GGCAATAC TGGG	8.5	Yes
ACV-0291078	<i>CKS-1289</i>	Endoribonuclease L-PSP	2.15 (A)	ACCTATCC GGTATTGC AGAT	8.41	No
ACV-0286411	<i>hrpN</i>	Elicitor of the hypersensitivity reaction HrpN	2.15 (A)	AGCGGCAC TTAATAAA AGCT	8.1	No
ACV-0288415	<i>uspA</i>	Universal stress global response regulator	2.3 (R)	GCATTGCC TGTATTGC AGGT	7.36	Yes

^a (A) denotes fold activation, (R) denotes fold repression by EsaR as seen in the RNA-Seq data.

^b Score generated using PATSER program (http://rsat.ulb.ac.be/rsat/patsr_form.cgi) and consensus published previously.

^c Previously identified direct targets of EsaR, not analyzed by EMSA assays in this study.

Table 4.2: Genes in the RNA-Seq dataset differentially expressed four-fold or higher that possess a clear +1 and a possible *esa* box nearby.

Accession number	Gene name	Protein Product	Fold regulation ^a	Promoter bound by EsaR?
ACV-0290526	<i>CKS_0458</i>	Sigma-fimbriae uncharacterized paralogous subunit	11.47 (R)	Yes
ACV-0289766	<i>spy</i> [<i>CKS_3373</i>]	Envelope stress induced periplasmic protein	9.55 (A)	No
ACV-0288878	<i>yjbE</i>	Secreted protein	7.69 (R)	Weakly
ACV-0287180	<i>CKS_1103</i>	Conidiation-specific protein, stress-induced	6.68 (R)	Yes
ACV-0290380	<i>yciF</i>	Uncharacterized DUF892 family protein	5.76 (R)	Yes
ACV-0288895	<i>CKS_4689</i>	Conjugative transfer protein	5.75 (R)	No
ACV-0288505	<i>CKS_0881</i>	Uncharacterized DUF1471 family protein	5.67 (R)	Yes
ACV-0289538	<i>wceL</i>	Exopolysaccharide biosynthesis protein	4.67 (R)	Yes
ACV-0289613	<i>lysP</i>	Lysine-specific permease	4.36 (R)	No
ACV-0287610	<i>osmY</i>	Osmotically inducible protein	4.31 (R)	Yes
ACV-0286879	<i>wceG2</i>	Undecaprenyl-phosphate galactose phosphotransferase	4.19 (R)	Yes
ACV-0287347	<i>elaB</i>	Protein of unknown function DUF883	4.03 (R)	Yes

^a (A) denotes fold activation, (R) denotes fold repression seen in the RNA-Seq data.

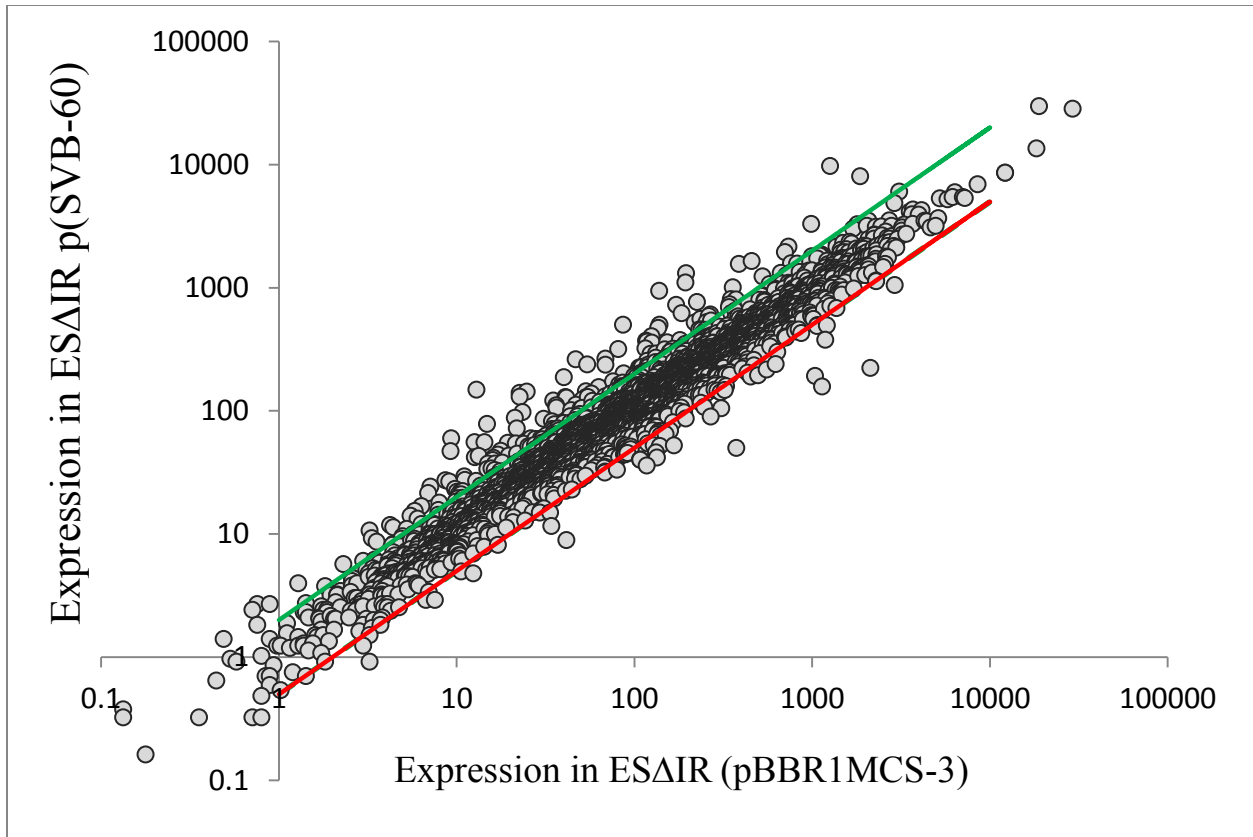


Figure 4.1: Comparison of mRNA expression. Whole transcriptome data of two *P. stewartii* strains, DC283 ESΔIR (pBBR1MCS-3) and DC283 ESΔIR (pSVB60) was obtained from RNA-sequencing. Each filled circle represents an mRNA. Change of expression of most genes fall around a line of slope of 1 indicating that they are equally expressed in both strains. The expression of gene transcripts that fall above the green threshold line is activated two-fold or higher by EsaR. The expression of genes that fall below the red threshold line is repressed two-fold or higher by EsaR in the RNA-Seq data.

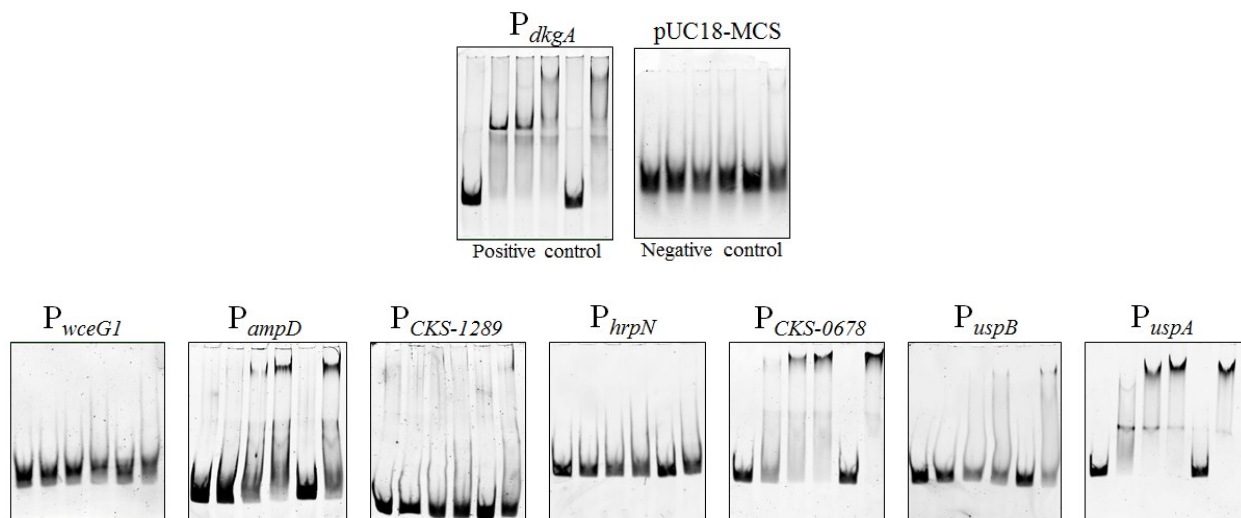


Figure 4.2: EMSA analysis to confirm direct binding by EsaR. Promoters of potential direct targets of EsaR identified via a bioinformatic approach were analyzed for binding by the EsaR fusion protein, HMGE. The promoter of *dkgA* (10) was used as positive control, and a 32-bp pUC18 MCS DNA fragment used as negative control. The concentration of FAM-labeled DNA probe in all lanes is 5 nM. The lanes within each panel consist of the following (left to right): DNA probe, DNA probe with 100 nM HMGE, DNA probe with 200 nM HMGE, DNA probe with 400 nM HMGE, DNA probe with 400 nM HMGE and 1 μ M specific competitor PesaR28 DNA fragment, DNA probe with 400 nM HMGE and 1 μ M non-specific pUC18 MCS DNA fragment.

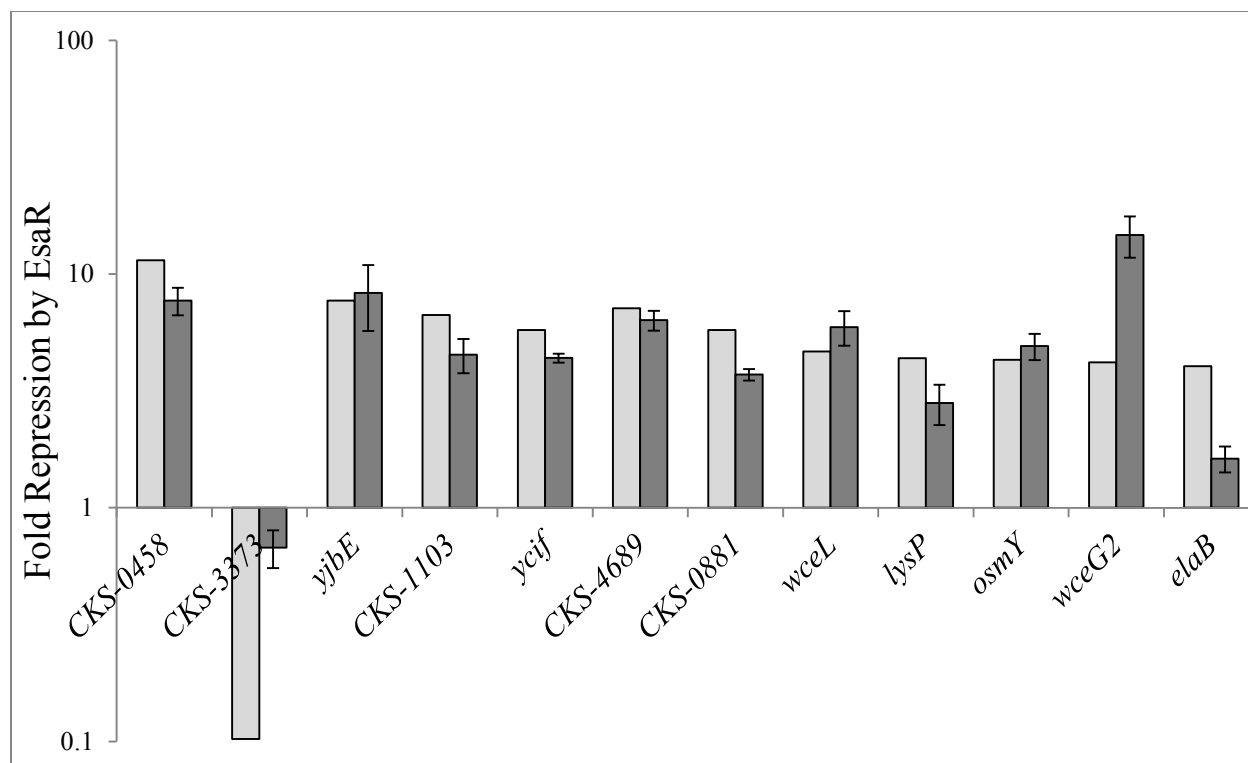


Figure 4.3: Validating transcriptional control of putative EsaR direct targets. Comparison of change in gene expression seen in RNA-Seq analysis (light grey) versus qRT-PCR assays (dark grey) of the 12 potential targets of EsaR assayed for direct regulation. Y-axis represents the fold repression (>1) or activation (<1) in the presence of EsaR. CKS-3373 is the only gene seen to be activated in the subset. Data represents two experimental samples analyzed in triplicate. Error bars denote standard error.

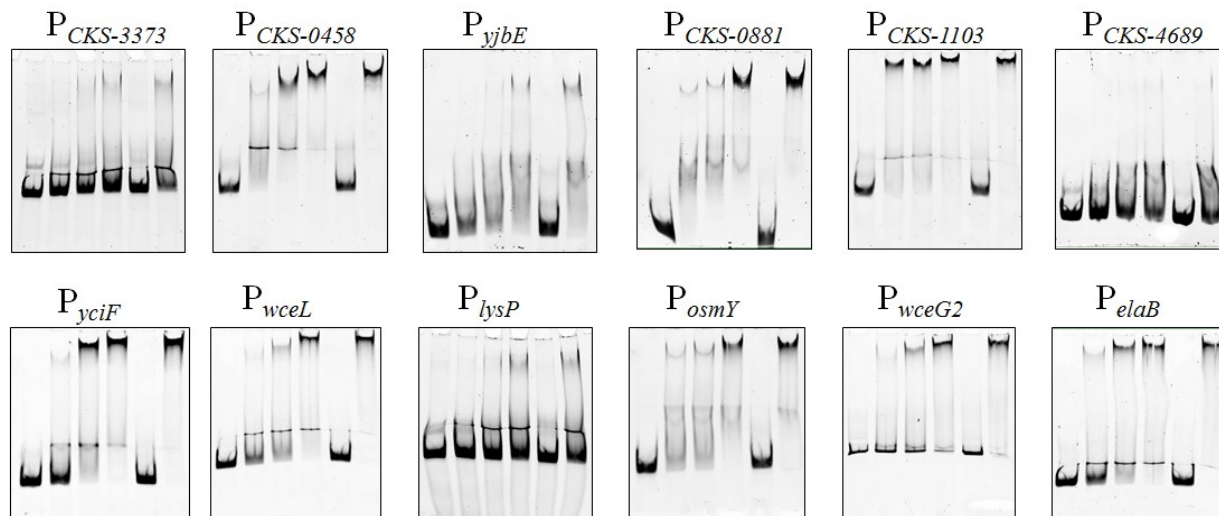


Figure 4.4: EMSA analysis to test direct binding of 12 promoters by EsaR. EMSA assays were performed with EsaR fusion protein, HMGE, The promoter of *dkgA* (10) was used as positive control, and a 32-bp pUC18 MCS DNA fragment used as negative control. The concentration of FAM-labeled DNA probe in all lanes is 5 nM. The lanes within each panel consist of the following (L to R): DNA probe, DNA probe with 100 nM HMGE, DNA probe with 200 nM HMGE, DNA probe with 400 nM HMGE, DNA probe with 400 nM HMGE and 1 μ M specific competitor PesaR28 DNA fragment, DNA probe with 400 nM HMGE and 1 μ M non-specific pUC18 MCS DNA fragment.

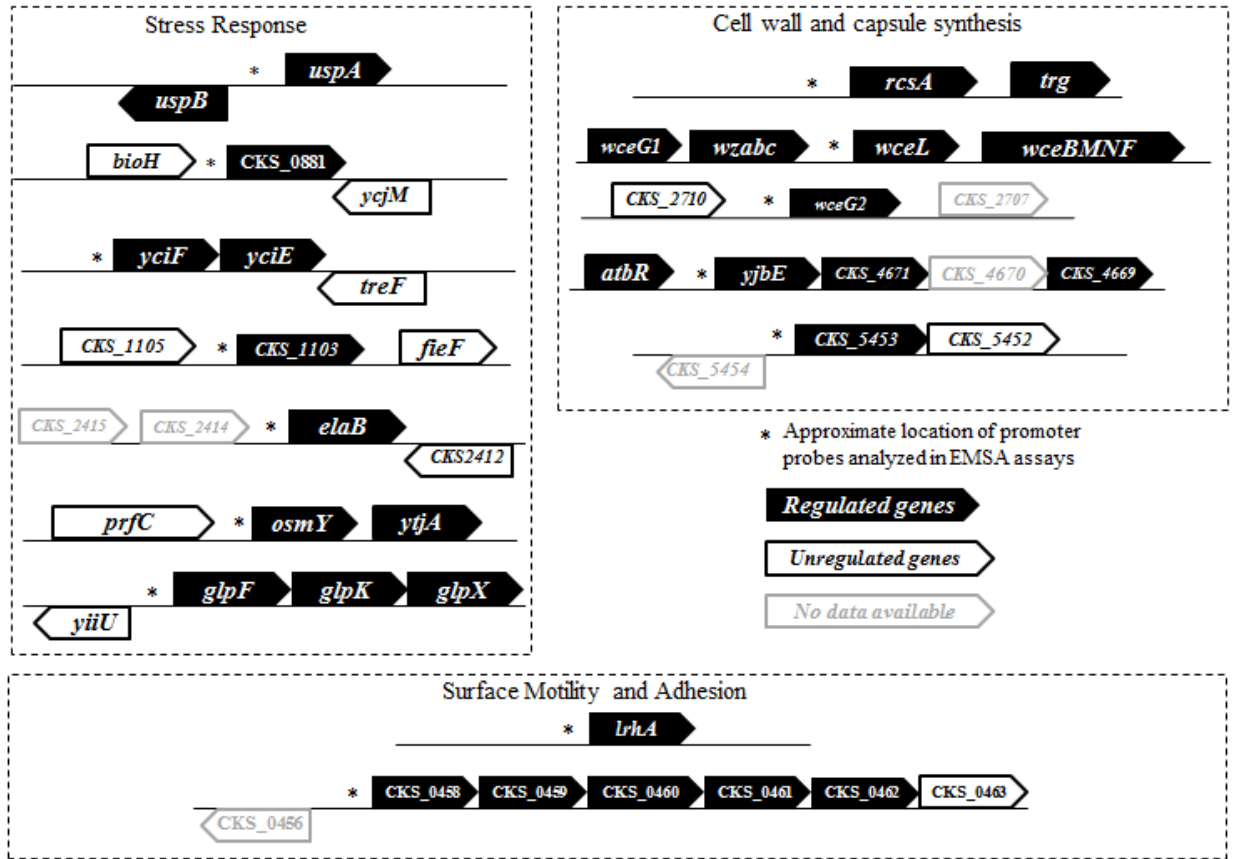


Figure 4.5: Genetic organization of the gene loci of *P. stewartii* directly regulated by EsaR.

Gene architectures near the 11 promoters assayed for direct binding by EsaR fusion protein in this study and 2 promoters identified in previous studies (*lrhA* and *rcsA*). Two EsaR direct targets with unknown physiological function, *esaS* encoding a small RNA and *dkgA* encoding a 2, 5-diketo gluconate reductase, are not included in the above diagram. Star denotes approximate location of promoter probes upstream of genes analyzed for direct binding. Differentially regulated genes from the RNA-Seq data are colored black, unregulated genes are colored in white and genes for which no transcriptome data is available are outlined in grey.

Chapter Five

Role of Two Quorum-Sensing Controlled Genes, *dkgA* and *lrhA*, in the Virulence of the Phytopathogen *Pantoea stewartii* subsp. *stewartii*

ABSTRACT:

The proteobacterium *Pantoea stewartii* subsp. *stewartii* causes Stewart's wilt disease in corn. *P. stewartii* is transmitted to plants during feeding by the corn flea beetle, *Chaetocnema pulicaria*. Once within the plants, the bacteria migrate to the xylem and secrete large amounts of stewartan, an exopolysaccharide, causing blockage of water transport and wilting of the plant. Production of stewartan is under control of the quorum-sensing (QS) regulator EsaR, which represses production of stewartan in the early stages of infection. At low cell-densities EsaR represses or activates expression of its regulon. Derepression or deactivation occurs at high cell densities when EsaR is bound by the acylated homoserine lactone (AHL) signal that is synthesized constitutively during growth by the cognate AHL synthase, EsaI. EsaR is known to directly regulate expression from 17 promoters. Two such directly regulated genes, *dkgA*, encoding 2, 5 diketo-D-gluconate reductase and *lrhA*, encoding a repressor of chemotaxis, motility & adhesion, were studied for their role in plant virulence. Phenotypically, the DC283 $\Delta lrhA$ strain has less capsule production and reduced motility in comparison to the wild type, whereas the DC283 $\Delta dkgA$ strain showed no changes in mucoidy or motility. Deletion of *dkgA* (DC283 $\Delta dkgA$) resulted in a loss of virulence in *in planta* assays and was complemented by expressing DkgA *in trans*. Similar plant virulence assay on DC283 $\Delta lrhA$ remain to be performed. Thus, these two QS regulated proteins appear to play a role in plant pathogenesis.

INTRODUCTION:

Stewart's wilt of *Zea mays* is caused by a *Pantoea stewartii* subsp. *stewartii* infection. The bacterium is transmitted to plants via the corn flea beetle, *Chaetocnema pulicaria*, within which it overwinters (1). *P. stewartii* is an agriculturally relevant pathogen that caused severe reductions in crop yields during the 1930s and still remains a concern for susceptible varieties of sweet corn. Severity of Stewart's wilt depends on the survival of the insect vector during winter and is directly proportional to the severity of the winter (2). Other plant pathogenic *Pantoea* species include *P. ananatis*, known to cause soft-rot in onions and a similarly related *Tatumella citrea* (previously *Pantoea citrea*) that causes pink rot of Pineapples (3, 4). The *Pantoea* genus is similar to the plant pathogenic *Erwinia* and *Pectobacterium* genera. *Erwinia amylovora* causes fire blight in apples and pears and *Pectobacterium carotovora* causes bacterial soft rot in a wide variety of plants (5, 6).

P. stewartii is carried in the mid-gut of the corn flea beetle and forms lifelong associations. Springtime feeding by the beetles deposits the bacterium directly into wounds on leaf tissue (1). Once within the plants, the bacteria expresses a Hrp-Hrc1 (hypersensitive response and pathogenicity-HR and conserved) Type 3 secretion system that secretes effector proteins and causes tissue water-soaking (7). The bacteria then migrate to the xylem where they grow to high cell densities and secrete an exopolysaccharide, stewartan, forming a biofilm (8). Mutants that do not produce stewartan are avirulent, but interestingly, mutants that overproduce stewartan are non-virulent in plant assays as well (9). Different proteins are required to successfully allow the bacterium to survive in the mid-gut of the beetle, the leaf tissue and eventually in the xylem as a

biofilm. *P. stewartii* utilizes quorum sensing (QS) to temporally regulate the expression of critical genes.

QS is a form of bacterial communication wherein the bacteria synchronize expression of certain genes and their encoded proteins (10). Two important proteins are necessary for QS in *P. stewartii*. EsaR, a transcriptional regulator, binds to certain promoters and alters gene expression based on cell density. An acylated homoserine lactone (AHL) synthase, EsaI, constitutively produces a chemical signal, 3-oxo-C6-HSL, that is sensed by EsaR as an indicator of cell density (11). At low cell-densities, dimeric EsaR binds to 20-bp palindromic sequences upstream of promoter regions where it either represses or activates transcription of downstream genes. At high cell-densities and correspondingly higher concentrations of AHL, EsaR is inactivated upon ligand binding, leading to loss of DNA binding and hence derepression or deactivation (12).

While the identity of some of the genes regulated by EsaR is known, the function of their protein products is less understood. Two genes, *dkgA* which codes for 2, 5-diketo-D-gluconate reductase, and *lrhA* which encodes a repressor of chemotaxis, motility & adhesion, were studied for their role in plant pathogenesis. Both genes are annotated in the genomes of *Pantoea*, *Erwinia*, *Xylella* and *Pectobacterium* genera. Identification of their role in virulence and the mechanism of action would aid in developing intervention strategies that could prevent the progression of disease in these agriculturally relevant crop pathogens.

MATERIALS AND METHODS:

Bacterial strains, plasmids and growth conditions. A list of bacterial strains and plasmids utilized is provided in Table 5.1. Both *P. stewartii* and *Escherichia coli* strains were grown in Luria-Bertani broth supplemented with antibiotics nalidixic acid (30 µg/ml), ampicillin (100 µg/ml), kanamycin (50 µg/ml), tetracycline (10 µg/ml), chloramphenicol (20 µg/ml), streptomycin (100 µg/ml) or gentamycin (20 µg/ml) as required. *P. stewartii* strains were grown at 30°C and *E. coli* strains at 37°C, respectively. The specific growth media used for phenotypic assays are described below.

Construction of unmarked DC283 $\Delta dkgA$ and DC283 $\Delta lrhA$. The Gateway cloning kit (Life Technologies, Gran Island, NY) (13) was used to generate unmarked deletions of *dkgA* or *lrhA*. Primers were used to amplify 1000-bp DNA fragments flanking the coding sequences (Table 5.2). Overlapping complementary sequences in the primers were used to anneal the two 1 kb sequences together, generating a 2 kb deletion fragment with flanking *attB* sites. The deletion fragment was cloned into pGEM vector and verified by sequencing (Virginia Bioinformatics Institute (VBI), Blacksburg, VA). A BP reaction was used to move the deletion fragment from pGEM to pDONR201, followed by an LR reaction to insert the deletion fragment into pKNG101::*attR-ccdB-Cm^R* (pAUC40). pAUC40 is a suicide-vector in *P. stewartii* (14). The resulting plasmid was transformed into competent *E. coli* S-17 λ *pir* cells (15). Conjugation was used to transfer this suicide vector into *P. stewartii* DC283 (16) using *E. coli* strain CC118 λ *pir* carrying the conjugative helper plasmid pEVS104 to facilitate suicide vector transfer (9). Double recombinants were selected using 5% sucrose, 0% salt LB plates as counter selection and screened via colony PCR utilizing primers (Table 5.2) that amplify fragments spanning the

deleted region. The resulting PCR fragment spanning the deleted gene was sequenced at VBI core laboratory (Blacksburg, VA) to verify accuracy.

Generation of complementation strains. The deletions of *lrhA* or *dkgA* in *P. stewartii* were complemented using the native gene promoters and coding sequences cloned into pBBR1MCS-3 and pBBR1MCS-5, respectively. Briefly, primers (Table 5.2) were used to amplify the required region and ligated into pGEM-T vector (Promega, Madison, WI). Purified plasmid DNA sequence was verified by sequencing (VBI). Plasmid was digested with restriction enzymes *SpeI* and *SacI* generating the desired promoter and gene DNA fragment. The pBBR1MCS vectors were similarly digested and ligated with the appropriate DNA fragments. The resulting recombinant vector was subsequently conjugated into *P. stewartii* DC283 Δ *dkgA* and DC283 Δ *lrhA* strains respectively. Screening of successful conjugants was performed by colony PCR utilizing the same primer pairs that were used to amplify the required region described above (Table 5.2).

Capsule production assays. Qualitative capsule production was examined on agar plates consisting of 0.1% casamino acids, 1% peptone and 1% glucose (CPG) plates (17). Cells grown to an optical density (OD) at 600 nm of 0.5 were used to streak plates using a sterile loop. Capsule production was qualitatively assessed after incubation at 30°C for 48 hours by the amount of mucoidy observed on the surface of the cross streaks.

Surface motility assays. Swarming motility assays were conducted as previously described (18). Cells were grown to an OD at 600 nm of 0.5 and 1 ml of the culture was harvested and washed

with 1x PBS buffer (phosphate buffered saline, 137 mM NaCl, 2.7 mM KCl, 10 mM Na₂HPO₄ and 1.8 mM KH₂PO₄, pH 7.4). The cells were then resuspended in 1 ml of 1x PBS and 5 µl of this was spotted on the center of a swarming agar plate (LB supplemented with 0.4% agar, 0.4% glucose) and incubated at 30°C for 2 days prior to observation of growth patterns.

Plant infection assays. The procedure for studying virulence of *P. stewartii* strains in *Zea mays* seedlings was adapted from published literature (19) with the following modifications. Sweet corn seedlings (*Zea mays* cv. Jubilee, 2bseeds, Broomfield, CO) were grown in Sunshine mix soil in an incubator at 28 °C, 80% relative humidity, 16 h light and 8 h dark cycle, 100 µE m⁻² s⁻¹ light intensity. Plants were inoculated 5 days after germination with 5 µl of bacterial suspension in PBS containing roughly 10⁷ cells. 1 cm long incisions approximately 1 mm deep were made 1 cm above the soil line using a sterile needle, and the bacterial suspension was inoculated into the wounds. 10 plants were inoculated for each strain tested. Symptom severity was rated 10 days post inoculation on the following scale (17): 0 = no symptoms; 1 = few scattered lesions; 2 = scattered water soaking symptoms; 3 = numerous lesions and slight wilting; 4 = moderately severe wilt; 5 = death.

RESULTS

Phenotypic analysis of *P. stewartii* DC283 $\Delta dkgA$ and DC283 $\Delta lrhA$. Unmarked single deletions were successfully generated individually in *dkgA* and *lrhA* in *P. stewartii* DC283 respectively (Figure 5.1). The plasmids pBBR3-PdkgA+ and pBBR5-PL+ expressing *dkgA* and *lrhA* from their native promoters were conjugated into DC283 $\Delta dkgA$ or DC283 $\Delta lrhA$ respectively to generate the complementation strains. DC283 $\Delta dkgA$ was analyzed for phenotypic changes as compared to wild-type DC283. No difference was seen in capsule production between the wild-type and the mutant on plating on casamino-peptone-glucose (CPG) plates and motility was not altered on 0.4% agar plates (Figure 5.2) (18). The DC283 $\Delta lrhA$ strain qualitatively showed reduced capsule production when compared to wild type and was deficient in motility as indicated by growth on 0.4% agar plates. Surface motility in *P. stewartii* is dependent on the production of stewartan, so the lack of motility in DC283 $\Delta lrhA$ may be due to the absence of capsule, or it could be due to another unknown mechanism (9). The DC283 $\Delta lrhA$ (pBBR5-PL+) complementation strain showed excess mucoidy. However, DC283 $\Delta lrhA$ (pBBR5-PL+) was unable to complement the motility defect. The presence of a *lac* promoter upstream of the multiple cloning site in pBBR1MCS-5 could contribute to higher levels of expression of *lrhA* on the multi-copy plasmid, resulting in an altered phenotype.

Role of *dkgA* in *P. stewartii* virulence. The severity of Stewart's wilt in *Zea mays* caused by *P. stewartii* strains DC283 (pBBR1MCS-3), DC283 $\Delta dkgA$ (pBBR1MCS-3) and DC283 $\Delta dkgA$ (pBBR3-PdkgA+) was quantified by a plant infection assay. The empty vector pBBR1MCS-3 was conjugated into DC283 and DC283 $\Delta dkgA$ as a control. Seedlings were manually inoculated by mimicking insect scratches on the stalk and the virulence was blindly rated by two individuals

independently, 10 days after inoculation. The wild-type strain was virulent with an average severity of 2.8 under the conditions tested (Figure 5.3). The DC283 $\Delta dkgA$ mutant was reduced in virulence and failed to cause wilt in the seedlings. The DC283 $\Delta dkgA$ (pBBR3-PdkgA+) complementation strain was able to overcome the defect and successfully establish disease, with an average severity rating of 2.8. Similar assays with DC283 $\Delta lrhA$ are planned.

DISCUSSION:

QS is a global regulatory system in *P. stewartii* that regulates production of genes dependent on cell density, including genes that may play a role in plant virulence (20). In this study, the role of two QS regulated genes, *dkgA* and *lrhA*, has been analyzed with regard to the establishment of a successful infection in *Zea mays*. The results contribute to understanding how these genes affect virulence and could also facilitate in developing strategies for preventing disease in plants.

DkgA is a 2, 5- diketo-D-gluconate reductase that belongs to the aldo-keto reductase (AKR) family constituting NADPH-dependent oxidoreductases with broad substrates ranges. The enzyme catalyzes the conversion of 2, 5 diketo-D-gluconate to 2 keto-L-gluconate in *Erwinia* species (21). Interestingly in plant virulence assays, no DC283 $\Delta dkgA$ cells were recovered from the xylem of infected seedlings 10 days after post-inoculation, whereas the wild type and the complementation strains were isolated with ease (data not shown). It seems that the deletion of *dkgA* causes a deficiency in the ability of *P. stewartii* to establish a viable infection in the xylem. Since DkgA is a metabolic enzyme, perhaps it is required to assimilate nutrients from the breakdown of the xylem during infection. Production of 2, 5-diketo-D-gluconate is directly responsible for the intense coloration characteristic of pink disease of pineapple caused by *Tatumella citrea* (22). It is not known whether *T. citrea* possesses a *dkgA*-like gene or a similar

QS system, but it is interesting to speculate that DkgA or its products may play a similar role in the xylem of *Zea mays* as in pink disease of pineapple (23).

LrhA is a LysR-type transcriptional repressor of chemotaxis, motility and adhesion seen in many gamma-proteobacteria. In *P. carotovora*, a homologous protein HexA is responsible for repressing motility and suppressing exoenzymes production (24). LrhA shares 69% amino acid identity with HexA (23). Virulence in *P. carotovora* is dependent on cell-density as well, and it is possible that HexA is under control of CarR, the homologous QS regulator (25). Similarly, PecT, another LysR-type regulator in *P. chrysanthemi* regulates production of pectinase (26). In *E. coli*, LrhA is the indirect repressor of chemotaxis, motility and the flagellar synthesis operon. Expression of *lrhA* is indirectly repressed by the RcsCDB phosphorelay system and FtsK, the DNA motor protein (27). It is possible that such regulation is seen in *P. stewartii* as well, along with the added regulation by EsaR. *P. stewartii* possess flagellar genes and exhibits a stewartan-dependent surface motility phenotype. Motility is not critical for the bacterium for movement from the leaf to the xylem, since this occurs passively. However, surface motility is critical for the establishment of a biofilm once in the xylem (18). It is possible that LrhA is activated at low cell densities by QS to ensure that the bacterium moves passively to the xylem. Once in the xylem, deactivation of LrhA could allow the bacterium to spread basipetally (against the flow of water) and colonize the entire xylem. The QS control of motility seems to be multi-tiered in *P. stewartii*. First, EsaR directly represses production of RcsA at low cell densities, blocking production of capsule which is needed for surface motility (12). Second, EsaR directly activates *lrhA* causing further repression of motility. Final, RcsA-B is known to repress expression of *flhDC* in *E. coli*, adding another level of possible indirect QS regulation in *P. stewartii* on motility, since the RcsAB system is fairly similar between *E. coli* and *P. stewartii* (28, 29).

Completion of plant virulence assays would determine the effect of *lrhA* in the virulence of *P. stewartii*.

A transposon-insertion in *lrhA* was previously generated by collaborator Susanne von Bodman (unpublished data) and sheds some light on the possible function of *lrhA* in *P. stewartii*. Briefly, the mutant was generated using transposon mutagenesis and insertion of a kanamycin resistance cassette within the coding sequence of the *lrhA* gene. The $\Delta lrhA::Kn^r$ strain showed similarly abolished mucoidy when grown on CPG plates, consistent with the DC283 $\Delta lrhA$ phenotype examined in this study. Capsule production was restored by expression of *wceO*, encoding a β -1,6-glucosyltransferase, *in trans*. LrhA was shown to directly bind and repress expression of *wceO*, but not other genes in the capsule-producing loci in *P. stewartii*, *wceI* and *wceII* (unpublished data, data not shown). Preliminary plant virulence assays of $\Delta lrhA::Kn^r$ performed at Virginia Tech suggest a decrease in virulence, however statistically significant replicates need to be performed.

Cumulatively, this study examines the effect of deletion of two genes directly regulated by EsaR on plant virulence. Given that these genes are fairly conserved in other plant pathogenic bacteria known to possess QS regulatory systems, the results from this study may be translated to other agriculturally-relevant plant diseases, especially bacterial wilt.

ACKNOWLEDGEMENTS:

We would like to thank the laboratory of Susanne von Bodman for providing strains and sharing unpublished data, Thomas Kuhar, Department of Entomology, Virginia Tech for providing *Zea mays* seeds, undergraduate students Audrey Robbins and Hunter Brigman for technical assistance and Sherry Hildreth and Brenda Winkel for assistance with the plant infection assays including access to plant incubator chambers.

This work is supported by National Science Foundation grant MBC- 0919984 (AMS), Virginia Tech Graduate Student Association's Graduate Research Development Programs (GSA GRDP) award (RR) and a Biological Sciences Graduate Student Development Award (GSDA) fellowship (RR).

REFERENCES:

1. **Roper MC.** 2011. *Pantoea stewartii* subsp. *stewartii*: Lessons learned from a xylem-dwelling pathogen of sweet corn. *Mol. Plant Pathol.* **12**:628–37.
2. **Cook KA, Weinzierl RA, Pataky JK, Esker PD, Nutter FW.** 2005. Population densities of corn flea beetle (Coleoptera: Chrysomelidae) and incidence of Stewart's wilt in sweet corn. *J. Econ. Entomol.* **98**:673–682.
3. **Coutinho TA, Venter SN.** 2009. *Pantoea ananatis*: an unconventional plant pathogen. *Mol. Plant Pathol.* **10**:325–335.
4. **Brady CL, Venter SN, Cleenwerck I, Vandemeulebroecke K, De Vos P, Coutinho T.** 2010. Transfer of *Pantoea citrea*, *Pantoea punctata* and *Pantoea terrea* to the genus *Tatumella* emend. as *Tatumella citrea* comb. nov., *Tatumella punctata* comb. nov. and *Tatumella terrea* comb. nov. and description of *Tatumella morbirosei* sp. nov. *Int. J. Syst. Evol. Microbiol.* **60**:484–94.
5. **Molina L, Rezzonico F, Défago G, Duffy B.** 2005. Autoinduction in *Erwinia amylovora*: evidence of an acyl-homoserine lactone signal in the fire blight pathogen. *J. Bacteriol.* **187**:3206–3213.
6. **Ma B, Hibbing ME, Kim H-S, Reedy RM, Yedidia I, Breuer J, Breuer J, Glasner JD, Perna NT, Kelman A, Charkowski AO.** 2007. Host range and molecular phylogenies of the soft rot enterobacterial genera *Pectobacterium* and *Dickeya*. *Phytopathology* **97**:1150–1163.
7. **Merighi M, Majerczak DR, Stover EH, Coplin DL.** 2003. The HrpX/HrpY two-component system activates *hrpS* expression, the first step in the regulatory cascade controlling the Hrp regulon in *Pantoea stewartii* subsp. *stewartii*. *Mol. Plant-Microbe Interact. MPMI* **16**:238–248.
8. **Minogue TD, Carlier AL, Koutsoudis MD, Bodman SB von.** 2005. The cell density-dependent expression of stewartan exopolysaccharide in *Pantoea stewartii* ssp. *stewartii* is a function of EsaR-mediated repression of the *rcsA* gene. *Mol. Microbiol.* **56**:189–203.
9. **Koutsoudis MD, Tsaltas D, Minogue TD, von Bodman SB.** 2006. Quorum-sensing regulation governs bacterial adhesion, biofilm development, and host colonization in *Pantoea stewartii* subspecies *stewartii*. *Proc. Natl. Acad. Sci. U. S. A.* **103**:5983–5988.
10. **Ng W-L, Bassler BL.** 2009. Bacterial quorum-sensing network architectures. *Annu. Rev. Genet.* **43**:197–222.

11. **Minogue TD, Wehland-von Trebra M, Bernhard F, von Bodman SB.** 2002. The autoregulatory role of EsaR, a quorum-sensing regulator in *Pantoea stewartii* ssp. *stewartii*: evidence for a repressor function. *Mol. Microbiol.* **44**:1625–35.
12. **Carlier AL, von Bodman SB.** 2006. The *rcaA* promoter of *Pantoea stewartii* subsp. *stewartii* features a low-level constitutive promoter and an EsaR quorum-sensing-regulated promoter. *J. Bacteriol.* **188**:4581–4.
13. **Choi K-H, Schweizer HP.** 2005. An improved method for rapid generation of unmarked *Pseudomonas aeruginosa* deletion mutants. *BMC Microbiol.* **5**:30.
14. **Carlier A, Burbank L, von Bodman SB.** 2009. Identification and characterization of three novel EsaI/EsaR quorum-sensing controlled stewartan exopolysaccharide biosynthetic genes in *Pantoea stewartii* ssp. *stewartii*. *Mol. Microbiol.* **74**:903–13.
15. **Herrero M, De Lorenzo V, Timmis KN.** 1990. Transposon vectors containing non-antibiotic resistance selection markers for cloning and stable chromosomal insertion of foreign genes in gram-negative bacteria. *J. Bacteriol.* **172**:6557–6567.
16. **Dolph PJ, Majerczak DR, Coplin DL.** 1988. Characterization of a gene cluster for exopolysaccharide biosynthesis and virulence in *Erwinia stewartii*. *J. Bacteriol.* **170**:865–871.
17. **von Bodman SB, Majerczak DR, Coplin DL.** 1998. A negative regulator mediates quorum-sensing control of exopolysaccharide production in *Pantoea stewartii* subsp. *stewartii*. *Proc. Natl. Acad. Sci. U. S. A.* **95**:7687–7692.
18. **Herrera CM, Koutsoudis MD, Wang X, Bodman SB von.** 2008. *Pantoea stewartii* subsp. *stewartii* exhibits surface motility, which is a critical aspect of Stewart's wilt disease development on maize. *Mol. Plant-Microbe Interact.* **21**:1359–1370.
19. **Wang X, Yang F, von Bodman SB.** 2012. The genetic and structural basis of two distinct terminal side branch residues in stewartan and amylovoran exopolysaccharides and their potential role in host adaptation. *Mol. Microbiol.* **83**:195–207.
20. **von Bodman SB, Willey JM, Diggle SP.** 2008. Cell-cell communication in bacteria: united we stand. *J. Bacteriol.* **190**:4377–4391.
21. **Yum DY, Lee BY, Pan JG.** 1999. Identification of the *yqhE* and *yafB* genes encoding two 2, 5-diketo-D-gluconate reductases in *Escherichia coli*. *Appl. Environ. Microbiol.* **65**:3341–6.
22. **Pujol CJ, Kado CI.** 2000. Genetic and biochemical characterization of the pathway in *Pantoea citrea* leading to pink disease of pineapple. *J. Bacteriol.* **182**:2230–2237.

23. **Ramachandran R, Stevens AM.** 2013. Proteomic analysis of the quorum-sensing regulon in *Pantoea stewartii* and identification of direct targets of EsaR. *Appl. Environ. Microbiol.* **79**:6244–52.
24. **Harris SJ, Shih YL, Bentley SD, Salmond GP.** 1998. The *hexA* gene of *Erwinia carotovora* encodes a LysR homologue and regulates motility and the expression of multiple virulence determinants. *Mol. Microbiol.* **28**:705–717.
25. **Pemberton CL, Whitehead N a, Sebaihia M, Bell KS, Hyman LJ, Harris SJ, Matlin a J, Robson ND, Birch PRJ, Carr JP, Toth IK, Salmond GPC.** 2005. Novel quorum-sensing-controlled genes in *Erwinia carotovora* subsp. *carotovora*: identification of a fungal elicitor homologue in a soft-rotting bacterium. *Mol. Plant. Microbe. Interact.* **18**:343–53.
26. **Surgey N, Robert-Baudouy J, Condemine G.** 1996. The *Erwinia chrysanthemi pecT* gene regulates pectinase gene expression. *J. Bacteriol.* **178**:1593–1599.
27. **Peterson CN, Carabetta VJ, Chowdhury T, Silhavy TJ.** 2006. LrhA regulates *rpoS* translation in response to the Rcs phosphorelay system in *Escherichia coli*. *J. Bacteriol.* **188**:3175–3181.
28. **Torres-Cabassa A, Gottesman S, Frederick RD, Dolph PJ, Coplin DL.** 1987. Control of extracellular polysaccharide synthesis in *Erwinia stewartii* and *Escherichia coli* K-12 : a common regulatory function. *J. Bacteriol.* **169**:4525–4531.
29. **Francez-Charlot A, Laugel B, Van Gemert A, Dubarry N, Wiorowski F, Castanié-Cornet M-P, Gutierrez C, Cam K.** 2003. RcsCDB His-Asp phosphorelay system negatively regulates the *flhDC* operon in *Escherichia coli*. *Mol. Microbiol.* **49**:823–832.
30. **Labes M, Puhler A, Simon R.** 1990. A new family of RSF1010-derived expression and *lac*-fusion broad-host-range vectors for Gram-negative bacteria. *Gene* **89**:37–46.
31. **Grant SG, Jessee J, Bloom FR, Hanahan D.** 1990. Differential plasmid rescue from transgenic mouse DNAs into *Escherichia coli* methylation-restriction mutants. *Proc. Natl. Acad. Sci. U. S. A.* **87**:4645–4649.
32. **Stabb, E.V. and Ruby E.** 2002. RP4-based plasmids for conjugation between *Escherichia coli* and members of the Vibrionaceae. *Methods Enzymol.* **358**:413–426.
33. **Kovach ME, Elzer PH, Hill DS, Robertson GT, Farris M a, Roop RM, Peterson KM.** 1995. Four new derivatives of the broad-host-range cloning vector pBBR1MCS, carrying different antibiotic-resistance cassettes. *Gene* **166**:175–6.

Table 5.1: Strains and plasmids utilized in this study

Strains	Genotype and notes ^a	References
<i>Pantoea stewartii</i> strains		
DC283	Wild-type strain; Nal ^r	(16)
DC283 $\Delta dkgA$	Unmarked deletion of <i>dkgA</i> coding sequence; Nal ^r	This study
DC283 $\Delta lrhA$	Unmarked deletion of <i>lrhA</i> coding sequence; Nal ^r	This study
DC283 $\Delta lrhA::Knr$	DC283 transposon mutant with Kn ^r cassette inserted between coding region of <i>lrhA</i> ; Nal ^r , Kn ^r	SVB, Unpublished data
<i>E. coli</i> strains		
CC118 λpir	$\Delta(ara-leu)$, <i>araD</i> , $\Delta lacX74$, <i>galE</i> , <i>galK</i> , <i>phoA20</i> , <i>thi-1</i> , <i>rpsE</i> , <i>rpoB</i> , <i>argE(Am)</i> , <i>recA1</i> , λpir	(15)
S17-1 λpir	<i>recA pro hsdR RP4-2-Tc::Mu-Km::Tn7</i>	(30)
Top 10	F- <i>mcrA</i> $\Delta(mrr-hsdRMS-mcrBC)$ \emptyset 80dlacZ Δ M15 $\Delta lacX74$ <i>deoR recA1 araD139</i> $\Delta(ara-leu)$ 7697 <i>galU galK rpsL (Strr) endA1 nupG</i>	(31)
Plasmids		
pGEM-T	Cloning vector	Promega
pDONR201	Entry vector in the Gateway system	Life Technologies
pAUC40	pKNG101:: <i>attR-ccdB-Cm^R</i> ; Cm ^r , Sr ^r	(14)
pEVS104	Conjugative helper plasmid, <i>tra trb</i> ; Kn ^r	(32)
pBBR1MCS-3	Broad host range vector; Tet ^r	(33)
pBBR1MCS-3	Broad host range vector; Tet ^r	(33)
pBBR3-PdkgA+	pBBR1MCS-3 with P _{<i>dkgA</i>} and <i>dkgA</i> ligated into SacI and SpeI sites; Tet ^r	This study
pBBR5-PL+	pBBR1MCS-5 with P _{<i>lrhA</i>} and <i>lrhA</i> ligated into SacI and SpeI sites; Gm ^r	This study

^a Ap^r, Ampicillin resistance; Nal^r, nalidixic acid resistance; Tet^r, tetracycline resistance; Kn^r, kanamycin resistance; Gm^r, gentamycin resistance; Cm^r, chloramphenicol; Sr^r, streptomycin

Table 5.2: Primers utilized in this study

Primers	Sequence (5' to 3')	Used for
DUPF	GTCGACACTTCCTCACCCGGC	Amplify 1 kb upstream region of <i>dkgA</i>
DUPR	AGTGGAAATATAGGCGGCCGCTTTTCAGGCTGCCTG	
DDNF	GCGGCCGCCTATATTCCACTTACGGGCGCATC	Amplify 1 kb downstream region of <i>dkgA</i>
DDNR	GGATCCCTGTGGGTATACGTGCGGGA	
DkgA-1kbUPF-attB1:	GGGACAAGTTTGTACAAAAAAGCAGGCTGTGACGTCACGCCAAAGTAGCGCTTAAAC	Amplify 2 kb deletion fragment of <i>dkgA</i> with flanking <i>attB</i> sites
DKGA-1kbDNR-attB2:	GGGGACCACTTTGTACAAGAAAGCTGGGTGGATCCGGAAAGGCGTACATCCACA	
PdkgA-F	GCTGACACAGTAAGTCGTGG	Screen for potential deletion mutants
DkgA-RTR	GCTTTTGACCAGGCCTTGTTGC	
DkgA-Seq-R	ATCTGCTGCCATGGAAGGT	
DkgA-F-EcoR	GAATTCGATATGGCAGACCAACC	Amplify coding region of <i>dkgA</i> , and screening conjugants
DkgA-R-Sma	CCCGGGCTATTAGCCGTTAAACG	
LrhA-UPF	GTCGACATTGTCCAGTTTGCCGG	Amplify 1 kb upstream region of <i>lrhA</i>
LrhA-UPR	AGTGGAAATATAGGCGGCCGCTTCACTTATTAGAG	
LrhA-DNF	GCGGCCGCCTATATTCCACTATCCCGTCTTC	Amplify 1 kb upstream region of <i>lrhA</i>
LrhA-DNR	GGATCCCCAATGCGCACCAG	
LrhA-1kbUPF-attB1	GGGGACAAGTTTGTACAAAAAAGCAGGCTGTCGACGTTTGCCGGATTTATCAATTTG	Amplify 2 kb deletion fragment of <i>lrhA</i> with flanking <i>attB</i> sites
LrhA-1kbDNR-attB2	GGGGACCACTTTGTACAAGAAAGCTGGGTGGATCCGCGCACCAGATAAACCAGGC	
UP-LrhA-SeqF	GTATGACAGACCCATTTACCCCG	Sequencing of mutants for deletion of <i>lrhA</i>
IN-LrhA-SeqF	GCGATCCCTCTGGTATTGCTGG	
DN-LrhA-SeqR	GCC CTG TTG GCC AGA GTA TG	
Spe1-LrhA-F	ACTAGTCATAGCGTAAGTAGGGTGTGAC	Amplify promoter and coding region of <i>lrhA</i> , and for screening conjugants
Sac1-LrhA-R	GAGCTCCTATTACTCTTCATCGTCCAGCAG	

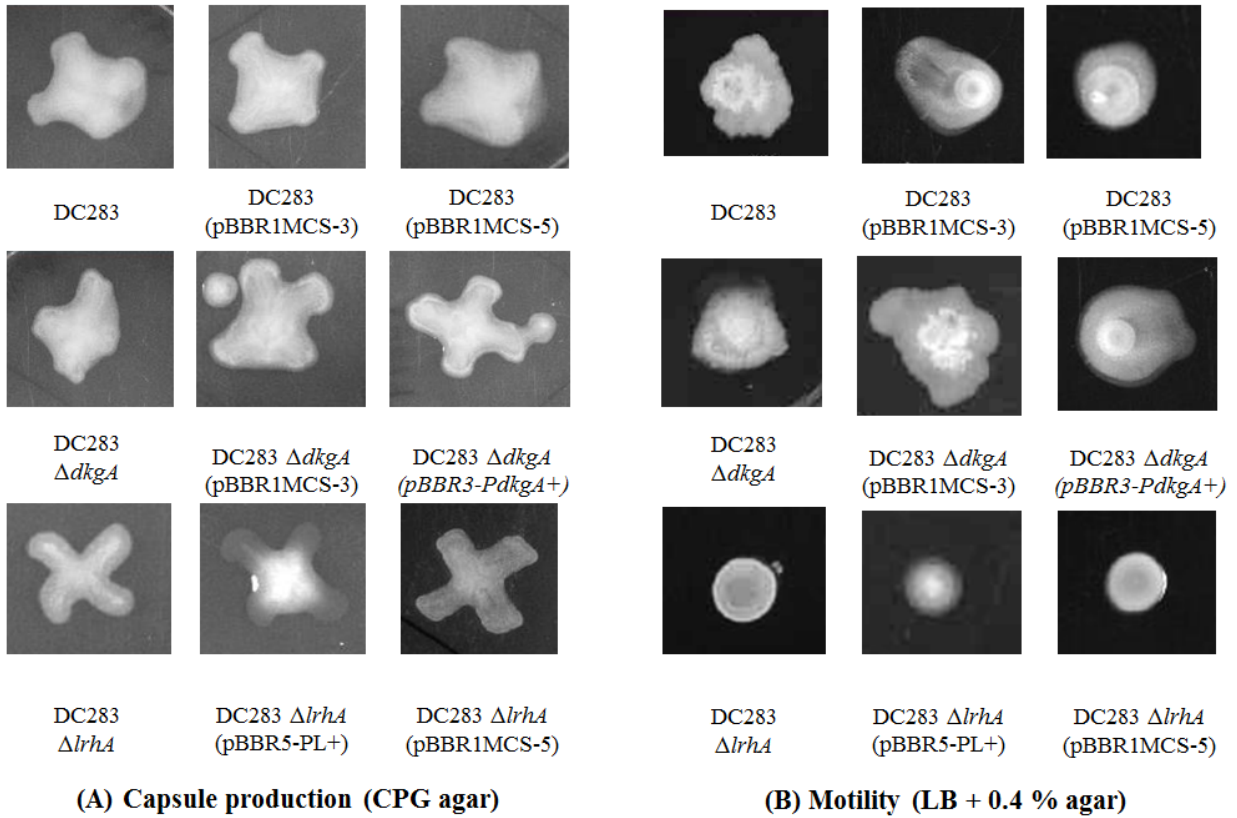


Figure 5.1: Phenotypic characterization of DC283 $\Delta dkgA$ and DC283 $\Delta lrhA$. (A) Capsule production by growth on CPG agar (B) motility assay by growth on 0.4% agar for *P. stewartii* strains indicated.

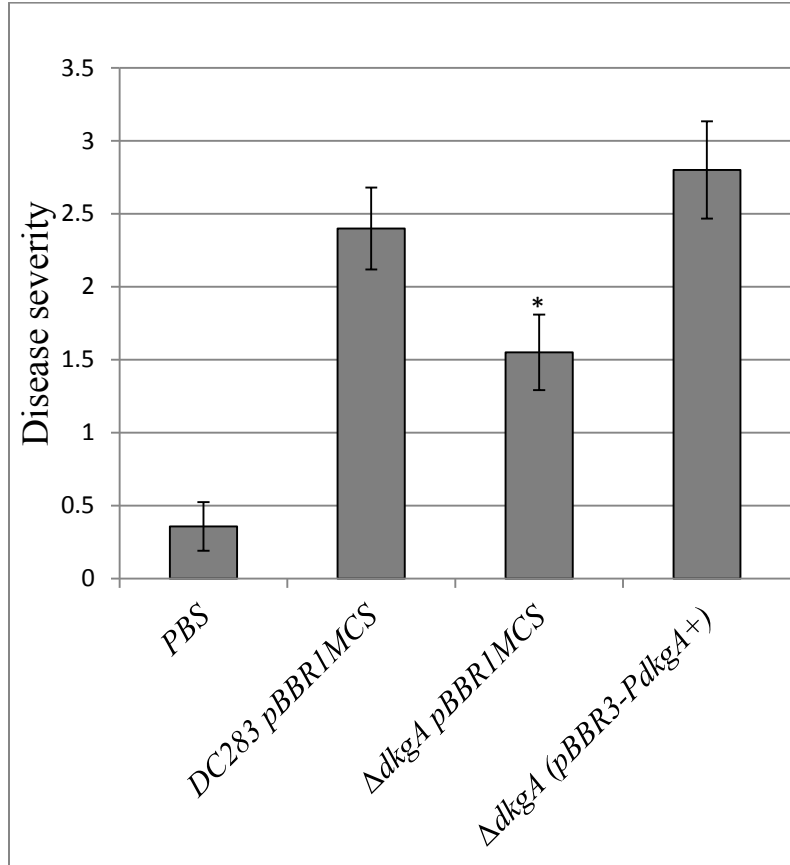


Figure 5.2: Plant virulence assays in sweet corn seedlings. Symptoms were blindly rated 10 days after inoculation on the following scale: 0 = no symptoms; 1 = few scattered lesions; 2 = scattered water soaking symptoms; 3 = numerous lesions and slight wilting; 4 = moderately severe wilt; 5 = death. The data presented is the mean of 10 replications. Asterisks denote statistically significant difference between DC283 and $\Delta dkgA$ (P-value <0.05).

Chapter Six
Overall Conclusions

Quorum sensing (QS) is a global regulatory system that allows bacteria to sense their surroundings and coordinate efforts across the population. Studies on QS aid in understanding the complex regulation via which bacteria respond to the environment and survive in a niche (1). Armed with this knowledge, strategies can be developed that interrupt or corrupt the bacterial communication to society's benefit. QS strategies can be utilized to prevent diseases, enhance desirable symbioses or increase production of bacterial valuables, such as organic acids (2). In order to implement these strategies, however, a complete understanding of how a bacterium utilizes QS is necessary.

Pantoea stewartii subsp. *stewartii* is a plant pathogenic proteobacterium that causes Stewart's wilt disease in corn plants (3). It is a xylem-associated pathogen that colonizes vascular tissue and causes blockage of water transport by producing a biofilm. It is transmitted to plants via an insect vector, the corn flea beetle *Chaetocnema pulicaria* (4). *P. stewartii* utilizes QS to regulate virulence by controlling the production of capsule, a key virulence factor (5). Two proteins form the core of the QS regulatory system in *P. stewartii*; the enzyme EsaI, which synthesizes the QS signal, an acylated homoserine lactone (AHL), and the master QS regulator EsaR, which alters gene expression depending on concentration of the AHL signal. EsaR is active at low cell densities in the absence of the AHL signal and either activates or represses transcription from select target promoters (6). This regulation is relieved at high cell densities upon binding of the AHL ligand by EsaR. At the molecular level, understanding how EsaR responds to AHL will help elucidate the mechanism of ligand interaction in the LuxR protein family, especially within the EsaR subfamily. In a broader sense, recognizing what EsaR regulates in *P. stewartii* allows for the identification of possible targets for disease intervention in plant pathogens with less

studied QS systems. Thus, *P. stewartii* is a model organism to study LuxR family structure/function as well as QS based regulation of crucial genes and their role in pathogenicity.

The mechanism of AHL binding in LuxR homologues and the resultant conformational changes it causes have been difficult to study due to the inability to purify ligand-free protein. Since EsaR is active in the absence of its ligand, the responsiveness of EsaR to AHL binding was examined using biochemical studies (7). A biologically active fusion protein of EsaR was purified and analyzed *in vitro* for changes in proteolytic cleavage patterns and multimeric state. Conformational changes occur upon AHL binding, but the oligomeric state of apo-EsaR and bound-EsaR remains unchanged. This raises the challenging question of how ligand binding causes drastic changes in activity, by modifying only the conformation of the dimeric EsaR protein. High-level structural information such as X-ray crystallography or Förster resonance energy transfer (FRET) based analysis of EsaR without and with AHL would aid in understanding the AHL responsiveness of this model LuxR-subfamily protein.

Prior to this thesis project, EsaR was known to repress its own expression and the expression of *rcaA* which encodes an activator of the capsular biosynthetic genes, and to activate the expression of a small RNA, EsaS, at low cell densities (6). At high cell densities, derepression or deactivation occurs allowing RcsA to activate expression of the capsule synthesis operon that leads to production of the capsular polysaccharide, stewartan (8). It is known that the temporal regulation of stewartan is crucial to the establishment of Stewart's wilt.

In order to identify additional genes temporally regulated by EsaR during QS, two approaches were used. First, strains of *P. stewartii* proficient and deficient in QS were analyzed for their proteomic profiles using two-dimensional SDS-PAGE gels (9). More than 30 proteins were identified to be differentially regulated in the two strains. Three promoters controlling expression of the respective genes were shown to be directly bound by EsaR and analyzed in-depth for their 20-bp EsaR binding sites. Next, a high-throughput whole transcriptome sequencing approach was undertaken. This RNA-Seq method allowed for visualization of gene expression in strains of *P. stewartii* proficient and deficient in QS. Eleven newly identified promoters were shown to be directly regulated by EsaR. Future work to define the precise EsaR binding sites on the identified promoters may lead to a more robust consensus sequence. The direct targets of EsaR can be broadly classified under three physiological responses: capsule production, motility & adhesion and stress response, that appear to be coordinately regulated.

These studies have added to the existing knowledge of the QS regulon in *P. stewartii* but have also opened up many interesting questions. The most pressing question is the role of the EsaR direct targets in plant pathogenesis and the mechanism by which these genes function. For two genes directly controlled by EsaR, *dkgA* and *lrhA*, gene deletions were carried out, and the mutant strains were analyzed phenotypically. The deletion of *dkgA*, encoding 2, 5 diketo-D-gluconate reductase, causes a loss of virulence in plant infection assays, possibly by affecting the ability of the bacterium to colonize and/or persist in the xylem of corn plants. The deletion of *lrhA*, encoding a repressor of chemotaxis, adhesion & motility, causes a loss of capsule production and motility. Preliminary experiments suggest that this affects the virulence of *P. stewartii* as well.

The set of genes known to be regulated by QS may be involved in plant pathogenesis and/or play a role in insect-vector colonization. While it is currently beyond the scope of this research to test the latter hypothesis, it is important to recognize the function of these genes in the natural environment of the plant pathogen. At the molecular level, the hierarchy of regulation between EsaR controlled genes, especially the regulatory proteins RcsA, LrhA and UspA, a stress response regulator, will prove informative. A coherent feed-forward model has been proposed for the regulation of these three proteins. Understanding the individual second-tier regulons controlled by each regulatory protein downstream of EsaR will elucidate the cascade of gene expression changes ensuing QS. It will be interesting to observe whether some QS regulated genes respond to lower concentrations of AHL and whether others require a higher threshold level of AHL. This would illuminate the temporal control of targets across the phases of growth. Additional deletion analysis of directly regulated targets of EsaR would allow for a better analysis of the pathogenesis process and proteins critical to virulence. Cumulatively, these findings will aid in understanding QS in this plant pathogen, a model organism for wilt disease, leading to the development of future plant disease intervention strategies.

REFERENCES:

1. **von Bodman SB, Willey JM, Diggle SP.** 2008. Cell-cell communication in bacteria: united we stand. *J. Bacteriol.* **190**:4377–4391.
2. **Ng W-L, Bassler BL.** 2009. Bacterial quorum-sensing network architectures. *Annu. Rev. Genet.* **43**:197–222.
3. **Roper MC.** 2011. *Pantoea stewartii* subsp. *stewartii*: lessons learned from a xylem-dwelling pathogen of sweet corn. *Mol. Plant Pathol.* **12**:628–37.
4. **Pataky J.** 2003. Stewart's wilt of corn. doi:10.1094/APSnetFeature-2003-0703.
5. **von Bodman SB, Farrand SK.** 1995. Capsular polysaccharide biosynthesis and pathogenicity in *Erwinia stewartii* require induction by an N-acylhomoserine lactone autoinducer. *J. Bacteriol.* **177**:5000–8.
6. **Schu DJ, Carlier AL, Jamison KP, von Bodman SB, Stevens AM.** 2009. Structure/function analysis of the *Pantoea stewartii* quorum-sensing regulator EsaR as an activator of transcription. *J. Bacteriol.* **191**:7402–9.
7. **Schu DJ, Ramachandran R, Geissinger JS, Stevens AM.** 2011. Probing the impact of ligand binding on the acyl-homoserine lactone-hindered transcription factor EsaR of *Pantoea stewartii* subsp. *stewartii*. *J. Bacteriol.* **193**:6315–22.
8. **Carlier AL, von Bodman SB.** 2006. The *rcaA* promoter of *Pantoea stewartii* subsp. *stewartii* features a low-level constitutive promoter and an EsaR quorum-sensing-regulated promoter. *J. Bacteriol.* **188**:4581–4.
9. **Ramachandran R, Stevens AM.** 2013. Proteomic analysis of the quorum-sensing regulon in *Pantoea stewartii* and identification of direct targets of EsaR. *Appl. Environ. Microbiol.* **79**:6244–52.

Appendix A

Chapter Three Supplemental Materials

Table A.1: Primers utilized in this study

Primer Name	Sequence (5' to 3')	Additional notes
Primers used to amplify promoters for EMSA assays		Used to amplify promoter of
p480-F	CTGACACGCAGGCCGGGGCACC	CKS-1750
p480-R	CTGTGCCGGACATCCGGCTG	
p711-F	CGTATGACGGTGTTCTGTCTGG	CKS-5296
p711-R	GCGCTATCTGTTGATTCTTGG	
PACCC-F	GGTCGTTAATCGCATCCCTGTG	<i>accC</i>
PACCC-R	GGCTTTTAGTCGGCTTCATCG	
PAHPF-F	GCAAAATCTAATTTCCGCATCGC	<i>ahpF</i>
PAHPF-R	GGTATCAAGCATAGTGAGTTCC	
PDEGP-F	GGCGGTGGAATAACCCGAG	<i>degP</i>
PDEGP-R	CTAAGCGCCAGGGCGCTTAAC	
PKGA-F	GCTGACACAGTAAGTCGTGG	<i>dkgA</i>
PKGA-R	CGCTGTGCTTAAGTCTAGC	
PESAR28F^a	TCTTGCCTGTACTATAGTGCAGGTTAAG	<i>esaR</i> (as positive control)
PESAR28R^a	CTTAACCTGCACTATAGTACAGGCAAGA	
PFABF-F	GGAAGAAGTGACCAACTCTGC	<i>fabF</i>
PFABF-R	CGCTTAGACACGTTTCGTC	
PFABI-F	GCGTGGCAACGCCAGCGTTG	<i>fabI</i>
PFABI-R	CCTTATGGTCATGGTAGTTGGC	
PFKPA-F	GTCAGCAGACCTCGGCAGAGC	<i>fkpA</i>
PFKPA-R	CGGACTGAGGGCCACAC	
FUSAF	GGCCTGGAAGCTTTTGAGGTTGC	<i>fusA</i>
FUSAR	GTA CGA GCC ATT TTA TTC CTC G	
PGALF-F	GAACCGTGGCTGTAAGTGTC	<i>galF, galE</i>
PGALF-R	GACATGCGTCAATTATGCCG	
PGALU-CDN	CTTACCCGCAAGACAGTGCCAGAAGTTAGC	<i>galU, CKS 2738</i>
PGALU-F	CGTCTGAGCAATAAACACCG	
PGLM-F	CGTTCTGGCCGATACCGCTATTCG	<i>glmU</i>
PGLM-R	CTGAGGAACGTTAAACGATTTAGC	

PGLPF-F	CCTGCAAGGCGTTGATGATGC	<i>glpF, glpK</i>
PGLPF-R	GTTGTTCCCTGAAGCGAGG	
PHTPG-F	TGACATCAGCAAAGCCGATCG	<i>htpG</i>
PHTPG-R	CTGCACGTAGAGTTTCAGACC	
PLRHA-F	CAGAGAGCATCTTTAGTACAGG	<i>lrhA</i>
PLRHA-R	GCGGGAAGCTGTGTAGTTGTC	
PMGLB-F	GCGATTCCGCGATGTAACCG	<i>mglB</i>
PMGLB-R	GCTGCGTCAAGCCGCGGAAG	
PNEMR-F	CTGTCGCTGTATTGCAGCC	<i>nemR</i>
PNEMR-R	CATCCTGGTAGACCAATCG	
PNHAR-F	CCGTCCATTGCGCACCACTG	<i>nhaR</i>
PNHAR-R	GACATGCGTCAATTATGCCGGATG	
POMPF-F	CGCCTATGTCACAGGCGTAC	<i>ompA, down-stream of ompF</i>
POMPF-R	CCAGAATGTTGCGCTTCATC	
POSMY-F	CGCGTTTTTCAGGGCCATTCTC	<i>osmY</i>
POSMY-R	CAACGCTACTGCGGCACAGG	
PPGM-F	CGTCTGGATACGGCCGCGTTTGC	<i>pgm</i>
PPGM-R	GGCCATTGGCGCTTCTCC	
PPHES-F	CATACTTTACGGGCAGGCATAGC	<i>pheT, downstream of pheS</i>
PPHES-R	GTTCTGCTAGTTGGGACATG	
PRPSB-F	GAGATTGCCATTAATTATTCCGC	<i>rpsB</i>
PRPSB-R	GTATCCCATACAACCGACCTC	
Primers for amplifying coding regions for qRT-PCR		Gene amplified
DKGA-CDNF	GGCAGCCTGAAAATTGTTAGC	<i>dkgA</i>
DKGA-CDNR	CGTATTAGCCGATAAACGTATCCG	
FABF-CDNF	GGAGGACGAACGTGTCTAAGC	<i>fabF</i>
FABF-CDNR	CGCCAGGTTTAGATTTTACGG	
RPSB-CDNF	GAGGTCGGTTGTATGGGATAC	<i>rpsB</i>
RPSB-CDNR	CAGAGCAAACCTTAATTAAGC	

LRHA-CDNF	CTTGTAATAACACCAGGATAGTAG	<i>lrhA</i>
LRHA-CDNR	GAAGACGGGATTTACTCTTCATCG	
GLPF-CDNF	CAACTATCATGAGTCAGACTACAACC	<i>glpF</i>
GLPF-CDNR	GAACTTACGCTTTACGTTTCATGC	
MGLB-CDNF	CTTACCCGATGTTCTTCCGC	<i>mglB</i>
MGLB-CDNR	CTGAGACAGGTTTTCTGATC	
27F	AGAGTTTGATCATGGCTCAG	<i>16S rRNA</i>
1429RLONG	ACCTTGTTACGACTTCACC	
qRT-PCR Primers		Target gene
DKGA-RTF	GCCCGGAGAAAGATCAGTACGTTG	<i>dkgA</i>
DKGA-RTR	GCTTTTGACCAGGCCTTGTTGC	
FABF-RTF	CGTCAATATGGTGGCGGGACATC	<i>fabF</i>
FABF-RTR	AGGCGGTCGCAATGGAAATGC	
RPSB-RTF	GCTCAAGGCTGGTGTTCCTTCG	<i>rpsB</i>
RPSB-RTR	ACGCGCACCGAAAATGAATGG	
LRHA-RTF	CGTCCGGTGGAGATGATGA	<i>lrhA</i>
LRHA-RTR	ATCCTTCTGCTGCACCCATT	
GLPF-RTF	TCTGGCCGGCATTTCCTC	<i>glpF</i>
GLPF-RTR	CCTGGCCCACGGAAATC	
MGLB-RTF	GATACGGCGATGTGGGATACCG	<i>mglB</i>
MGLB-RTR	GCGTTAGGGCCTGACAGC	
16S-RTF	GCCAGCAGCCGCGGTAAT	<i>16S rRNA</i>
16S-RTR	CGCTTTACGCCAGTAATTCC	
DNase I footprinting assays		Promoter amplified
FAM-PDKGA-R2	/6-FAM/-TTGGTCTGCCATATCCTGC	P_{dkgA}
PDKGAF	GCTGACACAGTAAGTCGTGG	
FAM-PLRHA-R2	/6-FAM/-TCTGTCATACACACACGCTG	P_{lrhA}
PLRHA-F2	GCCGTGCATTAATCGTTAATACGG	
PGLPF-FAMF	/6-FAM/-CCTGCAAGGCGTTGATGATGC	P_{glpF}
PGLPF-R	GTTGTTCTGAAGCGAGG	

^a Primer pair annealed to form EsaR binding site in P_{esaR}

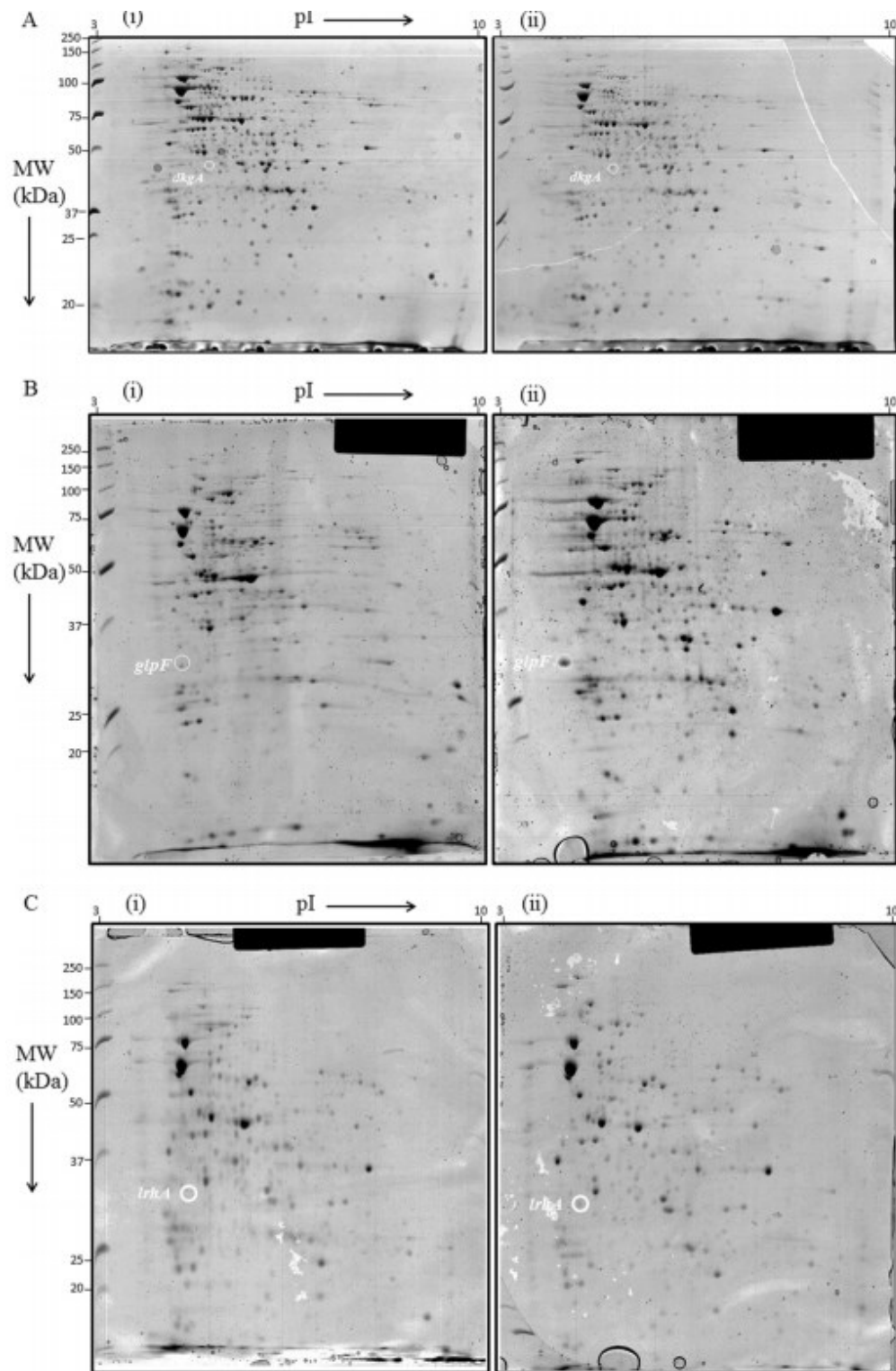


Figure A.1: Two-dimensional SDS PAGE experiments of *P. stewartii* DC283 strains. Panel A (i) ESN51 and (ii) ESN51 supplemented with 10 μ M AHL; panels B and C (i) E Δ IR

pBBR1MCS-3 (*esaR*-/*esaI*-) and (ii) ESΔIR pSVB60 (*esaR* complemented) depicting the three trials identifying differentially expressed protein spots. Locations of protein spots of DkgA, GlpF and LrhA are marked as examples in panel A, B and C, respectively. The positions of molecular weight standards are indicated on the left (in kDa) and the isoelectric pH (pI) gradient is indicated at the top from left to right.

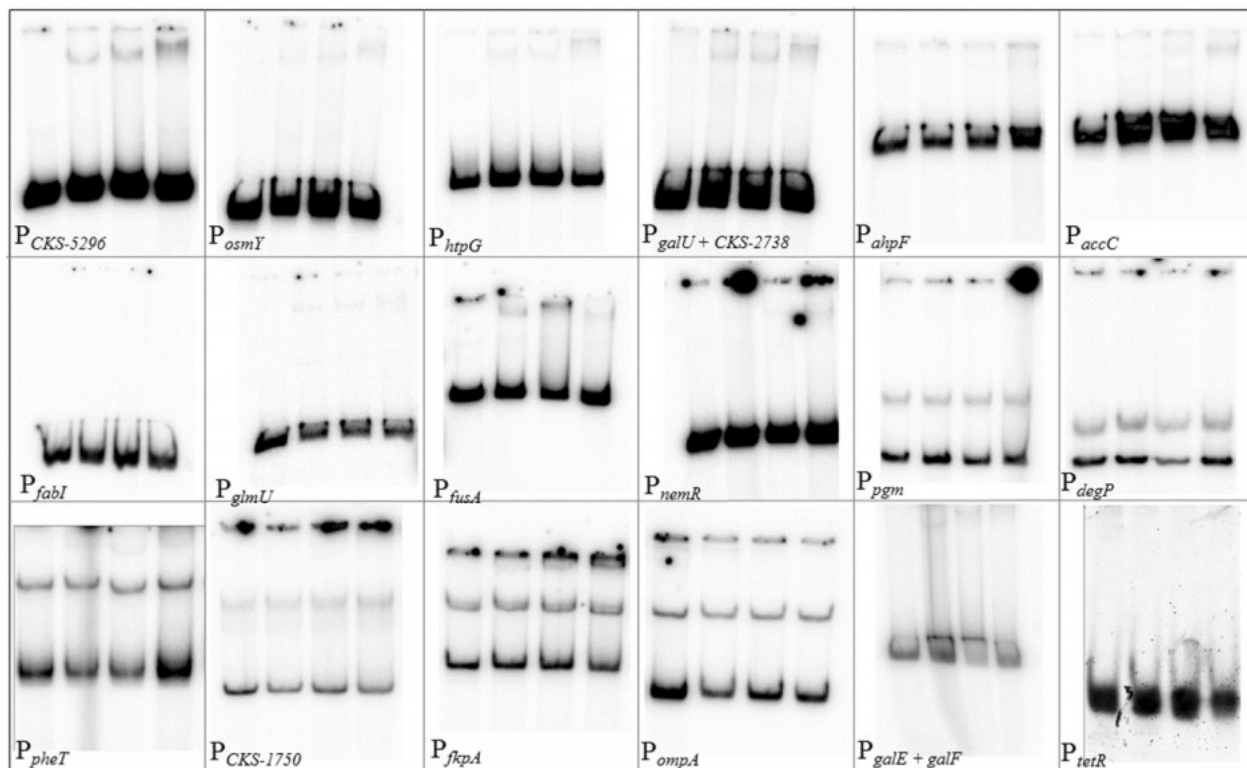


Figure A.2: Electrophoretic mobility shift assays on the promoters of genes in the QS

regulon. Concentration of DNA probe in all lanes is 1 nM. Lanes within each panel labeled with gene promoters consist of (left to right): DNA probe, DNA probe with 50 nM HMGE, DNA probe with 100 nM HMGE, and DNA probe with 100 nM HMGE plus 100 nM unlabeled DNA probe. The identity of the second band produced during PCR amplification of the gene promoters *P_{pgm}*, *P_{degP}*, *P_{pheT}*, *P_{CKS-1750}*, *P_{fkpA}*, and *P_{ompA}* is not known.

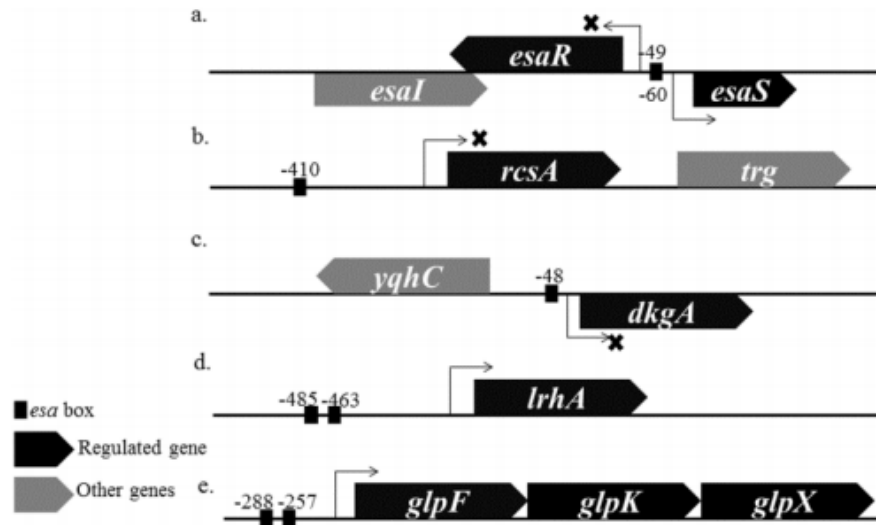


Figure A.3: Relative positions of *esa* box on the promoters of the direct targets of EsaR.

Numbers above or below the *esa* boxes denote base pairs from translational (ATG) start sites of the downstream open reading frames. The 'x' in front of the directional arrows indicates repression; absence of 'x' indicates activation. Model not drawn to scale.

Appendix B

Chapter Four Supplemental Materials

Table B.1: Primers utilized for amplifying EMSA probes and for qRT-PCR.

Primer name	Sequence (5' to 3')	Promoter amplified	Size of product (bp)
Primers used for amplification of DNA probes for EMSA			
PDKGA-F	GCTGACACAGTAAGTCGTGG	P_{dkgA} (1)	181
PDKGA-R	CGCTGTGCTTAAGTCTAGC		
PUC-TMP-F-FAM	/56-FAM/TACGGACGTCCAGCTGAG ATCTCCTAGGGGCC	pUC18- MCS	32
PUC-TMP-F	TACGGACGTCCAGCTGAGATCTCCTAGG GGCC		
PUC-CDN-R	GGCCCCTAGGAGATCTCAGCTGGACGTC CGTA		
PESAR28F	TCTGCCTGTACTATAGTGCAGGTTAAG	PesaR28 (2)	28
PESAR28R	CTAACCTGCACTATAGTACAGGCAAGA		
P9766-F-FAM	/56-FAM/AGGCGTTACCTCTCTGAACG	P_{spy}	318
P9766-R	AGTTTACGCATAACAGTGTCC		
P0526-F-FAM	/56-FAM/ACAGACAGGCAAAACAGTTCTG	$P_{CKS-0458,}$ <i>0459,0461</i>	313
P0526-R	GCTTGAATTTTCATAACCATTC		
YJBE-F	GGTATTTTGTGGCCCTATACTGG	P_{yjbE}	176
YJBE-R-FAM	FAM-AAGAGACGGCGACGAGTAAT		
P8505-F-FAM	/56-FAM/AGACCGTAACTGGCAAATTC	$P_{CKS-0881}$	173
P8505-R	CCTTCATTTGTCTACCCTCATTC		
CONI-F-FAM	/56-FAM/AATATCCCGCTCCGCTTGC58.	$P_{CKS-1103}$	254
CONI-R	TTTGAAATTACCGCCGCCGC		
P8895-F-FAM	/56-FAM/TGGACGGTAACCAGACATAAC	$P_{CKS-4689}$	212
P8895-R	GCAGGGAAAACCAGAACGGAA		
YCIF-F-FAM	/56-FAM/AGGTGAGGCGGAGCATTTA	P_{yciF}	219
YCIF-R	TTGACAGTCATAAAAGAGCCTC		
PWCEL-F-FAM	/56-FAM/ACGAAAAGCTAAGCGCTAAG	P_{wceL}	268
PWCEL-R	ATGGAGCCATGGTGTGATTC		
PLYSP-F-FAM	/56-FAM/CACGCTTTATCGCATCC	P_{lysP}	300
PLYSP-R	CGCAGGTTGTTGTGTTG		
POSMY-F	CGCGTTTTTCAGGGCCATTCTC	P_{osmY}	197
POSMY-R-FAM	/56-FAM/CAACGCTACTGCGGCACAGG		
PWCEG2-F-FAM	/56-FAM/CGTAAGCCCGGAGGATTAC	P_{wceG2}	396
PWCEG2-R	GTACTTGCCATAAAACCTGCTCTC		
ELAB-F-FAM	/56-FAM/TCAGGTGAAACAGCTGGTAAT	P_{elaB}	306
ELAB-R	GACTTCACCCCATTTGTTGC		
PUSPB-TMP-F-FAM	/56-FAM/TTCTGCACTGTTCTGCGGTGCC GGTAAGGAG	P_{uspB}	134
PUSPBR	GAACCACCAGCAGCGCACGCAACG		
PUSPA-F	GCAGAATTTGCCAACAACC	P_{uspA}	368

PUSPA-R-FAM	GTGGAAGGAGTTATATCATGGC		
NAM-F-FAM	/56-FAM/ATGCTCAGTTAATCCGTGCATTC	P _{CKS-5453}	163
NAM-R	GTGACTGACTCCATCCACCT		
PWCE-F-FAM	/56-FAM/TCAGAAACGCTTCAGGCTCAA	P _{wceG1}	108
PWCE-R	ATGCGCGATAACCATTTTACGT		
PYR-TMP-F-FAM	/56-FAM/AAAATGCCAGTATTGCC GGGCAGGGCGCCAT	P _{CKS-0678}	176
PPYRR-R	GGAGGCTGCCATACCGTCAGGATC		
ENDO-FAM-R	/56-FAM/TAACTCCGGTATAACAGACAA	P _{CKS-1289}	121
ENDO-F	ATTCGTGAGCCATACGTTAATG		
PHRPN-F-FAM	/56-FAM/ATTTTCAGACAGGAACCAGCACC	P _{hrpN}	139
PHRPN-R	CCAGCGGACTCGTATTCATACTC		

Primers utilized for template cloning and qRT-PCR

Primer name	Sequence (5' to 3')	Used for
9766CLONINGF	CAAGTAAAAAAGGACACTGTTATGCG	Cloning <i>spy</i> coding region
9766CLONINGR	CCGCTTTGTCATGCATCG	
9766RTF2	ATTATCGCCTCTGACAGCTTCGA	qRT-PCR, annealing at 62 °C
9766RTR2	GGCGTTGGCGGTCATTTT	
0526CLONINGF	TTTAATGTTATTTTTTCGAGGTTTTTGC	Cloning <i>CKS-0458</i> coding region
0526CLONINGR	AAACAGGTGACCGTCTTAC	
0526RTFWD3	CGGCACCAATTACGCGATCTAT	qRT-PCR, annealing at 62 °C
0526RTREV3	GCCGGGATCACCGGATT	
YJBECCLONING F	CCAATGTAGGTGTTGTTATGAAAAA CG	Cloning <i>yjbE</i> coding region
YJBECCLONINGR	GTTGTGGTCGTGGTAGTTG	
YJBERTF	GCATTACTCGTCGCCGTCTCT	qRT-PCR, annealing at 60 °C
YJBERTR	TGCTGCGCACCAAGCTT	
8505CLONINGF	GAATGAGGGTAGACAAATGAAGG	Cloning <i>CKS-0881</i> coding region
8505CLONINGR	AGGATGTGATCAGAGGTGAG	
8505RTF2	GTGCAGAAGATGAATCTGACCAAAA	qRT-PCR, annealing at 60 °C
8505RTR2	CATCCATTGGCGAAGTGGTTT	
CONIFWDCCLONING	GAGCATCGTGGTGATTCAGGTAAT	Cloning <i>CKS-1103</i> coding region
CONIREVCLONING	GCTGCTCTTTCCGCCTTTTTT	
CONIRTFWD	GCAGAGCATCGTGGTGATTCAG	qRT-PCR, annealing at 60 °C
CONIRTREV2	TGCTCTTTCCGCCTTTTTTACC	
8895 CLONING F	CAAATGGCAAATTAACCGTCCC	Cloning <i>CKS-4689</i> coding region
8895 CLONING R	TCAGAAGTTAAATCCGAGTTGC	
8895RTF2	CCCGGCGTTAATGACCAAAA	qRT-PCR, annealing at 64 °C
8895RTR2	CGCACTGGGAAAAATGATGCT	
FWDYCIFCLONING	ATGAGGCTCTTTTATGACTGTC	Cloning <i>yciF</i> coding region
REVCIFCLONING	TCATTTTCGCAACTCCTTCAG	

YCIFRTFWD	CCCTGGAAGGCCTGGTAGAA	qRT-PCR, annealing at 60 °C
YCIFRTREV	GCGTACTTCACCCTTTTCAACAGA	
WCELCLONINGF	GGAATCACACCATGGCTCC	Cloning <i>wceL</i> coding region
WCELCLONINGR	CAACCAAACTCCTGCGC	
WCELRTF	GGGTCGCTGGGTGAAAGG	qRT-PCR, annealing at 62 °C
WCELRTR	CTGCCATCCATTGCGTAGGA	
LYSPCLONINGF	TCGCGCCTTATTTTACCCAG	Cloning <i>lysP</i> coding region
LYSPCLONINGR	GCAGGCCAATATAGGTCGC	
LYSPRTF	GCCGTTTGCCGGAGGTT	qRT-PCR, annealing at 64 °C
LYSPRTR	CCTGGAAGAAAAGCCGACAA	
OSMYCLONINGF	GATGATATCGATGCACACAATAAGC	Cloning <i>osmY</i> coding region
OSMYCLONINGR	TTAACACTTTTTACGCCTTCGATAGC	
OSMYRTFWD	CGAAAATCGACAGCTCAATGAAGA	qRT-PCR, annealing at 60 °C
OSMYRTREV	CCACCAGCGCCGCTTT	
WCEG2CLONINGF	CATTAAAGAGAGCAGGTTTTATGGC	Cloning <i>wceG2</i> coding region
WCEG2CLONINGR	GGCAATATCCGTCCACAGC	
WCEG2RTF	GCGCGTCGCGAATGG	qRT-PCR, annealing at 60 °C
WCEG2RTR	CCCCGATGCGGGTAAT	
ELABCLONINGF	ATGTCAGGAAAATTGAAGATGCCG	Cloning <i>elaB</i> coding region
ELABCLONINGR	TTACTTACGACCGAGCAGGAAG	
ELABRTF	CCCGCCGCTACACCAATC	qRT-PCR, annealing at 62 °C
ELABRTR	CAAACGGGTTAGACTGCATCTGAT	
USPA-CDNF-ECOR	GAATTCACCGCTGCCATTCTG	Cloning <i>uspA</i> coding region
USPA-CDNR-SMA	CCCGGGCTATTATTCGTCATCCT	
USPA-RTF	AACCCATCTGGCGCTGAAAA	qRT-PCR, annealing at 60 °C
USPA-RTR	CGTCAATCAGGCCGGTGTA	
27F	AGAGTTTGATCATGGCTCAG	Cloning <i>16S rRNA</i> coding region
1429RLONG	ACCTTGTTACGACTTCACC	
16S-RTF	GCCAGCAGCCGCGGTAAT	qRT-PCR, annealing at 60 °C
16S-RTR	CGCTTTACGCCAGTAATCC	

Table B.2: List of genes differentially expressed 2-fold or higher in the RNA-Seq data.

<i>P. stewartii</i> v5b accession number	Locus Tag	Gene name	Protein product	Fold regulation ^a
ACV-0290526	CKS0458		Sigma-fimbriae uncharacterized paralogous subunit	11.5 (R)
ACV-0288878	CKS4672	<i>yjbE</i>	Yjbe secreted protein	7.7 (R)
ACV-0290502	CKS0482	<i>dkgA</i>	Methylglyoxal reductase, acetol producing / 2,5-diketo-D-gluconate reductase A	6.8 (R)
ACV-0287180	CKS1103		Conidiation-specific protein 10	6.7 (R)
ACV-0290434	CKS0551		Carbonic anhydrase	6.4 (R)
ACV-0290065	CKS3595		L-sorbose dehydrogenase	6.2 (R)
ACV-0285957	CKS2570	<i>rcaA</i>	Colanic acid capsular biosynthesis activation accessory protein rcaA	5.8 (R)
ACV-0290380	CKS0606	<i>yciF</i>	Protein yciF	5.8 (R)
ACV-0288895	CKS4689		Conjugative transfer protein	5.8 (R)
ACV-0288505	CKS0881		Protein of unknown function DUF1471	5.7 (R)
ACV-0290433	CKS0552		Sulfate permease	5.6 (R)
ACV-0290433	CKS3219		Cellulose synthase (UDP-forming)	5.3 (R)
ACV-0290523	CKS0461		Sigma-fimbriae usher protein	5.1 (R)
ACV-0289538	CKS2247		Exopolysaccharide biosynthesis protein	4.7 (R)
ACV-0290525	CKS0459		Sigma-fimbriae uncharacterized paralogous subunit	4.4 (R)
ACV-0289613	CKS2172	<i>lysP</i>	Lysine-specific permease	4.4 (R)
ACV-0287610	CKS5070	<i>osmY</i>	Osmotically inducible protein osmY	4.3 (R)
ACV-0286879	CKS2708		Undecaprenyl-phosphate galactose phosphotransferase	4.2 (R)
ACV-0291148	CKS1361	<i>lysA</i>	Diaminopimelate decarboxylase	4.2 (R)
ACV-0287973	CKS1762		Permease of the drug/metabolite transporter (DMT) superfamily	4.1 (R)
ACV-0287347	CKS2413	<i>elaB</i>	Protein of unknown function DUF883	4.0 (R)
ACV-0289537	CKS2248		Glycosyl transferase, family 2	3.9 (R)
ACV-0287576	CKS5036		Inositol-1-monophosphatase	3.9 (R)
ACV-0288877	CKS4671		Predicted outer membrane lipoprotein	3.8 (R)
ACV-0291056	CKS1267	<i>mltB</i>	Membrane-bound lytic murein transglycosylase B precursor	3.6 (R)
ACV-0290321	CKS0665	<i>yqiD</i>	Uncharacterized membrane protein yqiD	3.6 (R)
ACV-0285999	CKS2612		Phage holin	3.6 (R)
ACV-0286176	CKS4567		Secretion system regulator of degu/uvry/bvga type	3.5 (R)

ACV-0286473	CKS3213		Sensory box histidine kinase/response regulator	3.5 (R)
ACV-0289540	CKS2245	<i>etp</i>	Low molecular weight protein-tyrosine-phosphatase Wzb	3.4 (R)
ACV-0290611	CKS0373		PTS system, cellobiose-specific IIB component	3.4 (R)
ACV-0286146	CKS4537		Pathogenicity 1 island effector protein	3.4 (R)
ACV-0290322	CKS0664	<i>yqjC</i>	Periplasmic protein yqjc	3.4 (R)
ACV-0289544	CKS2241		Undecaprenol-phosphate galactosephosphotransferase/O-antigen transferase	3.4 (R)
ACV-0290342	CKS0644		Diaminobutyrate-pyruvate transaminase & L-2,4-diaminobutyrate decarboxylase	3.3 (R)
ACV-0287057	CKS1226	<i>rbsD</i>	Ribose ABC transport system, high affinity permease rbsd	3.3 (R)
ACV-0285656	CKS1834		Glycerol dehydrogenase	3.3 (R)
ACV-0289276	CKS3527		Conidiation-specific protein 10	3.3 (R)
ACV-0286016	CKS2629		Phage tail sheath protein FI	3.2 (R)
ACV-0286242	CKS4633		Haemolysin expression modulating protein	3.2 (R)
ACV-0286848	CKS2740	<i>hns</i>	DNA-binding protein H-NS	3.2 (R)
ACV-0288977	CKS4771		Acyltransferase 3	3.1 (R)
ACV-0289287	CKS3516		Oligogalacturonide transporter	3.1 (R)
ACV-0286703	CKS2983		Phytochelatin synthase, bacterial type	3.1 (R)
ACV-0289663	CKS2121		Sugar (Glycoside-Pentoside-Hexuronide) transporter	3.1 (R)
ACV-0288875	CKS4669	<i>yjbH</i>	Yjbh outer membrane lipoprotein	3.1 (R)
ACV-0286463	CKS3223		Response regulator	3.1 (R)
ACV-0290379	CKS0607	<i>yciE</i>	Protein ycie	3.0 (R)
ACV-0288793	CKS1592		Bacterioferritin-associated ferredoxin	3.0 (R)
ACV-0290781	CKS0202	<i>ybaY</i>	Glycoprotein-polysaccharide metabolism	2.9 (R)
ACV-0289712	CKS3319	<i>yehH</i>	Probable membrane protein YPO2012	2.9 (R)
ACV-0287846	CKS2944	<i>malt</i>	Transcriptional activator of maltose regulon	2.9 (R)
ACV-0287445	CKS3703		L-fucose operon activator	2.9 (R)
ACV-0289531	CKS2254	<i>wzxC</i>	Lipopolysaccharide biosynthesis protein	2.9 (R)
ACV-0289985	CKS0827		DNA topoisomerase III	2.8 (R)
ACV-0286735	CKS5564		Cro repressor	2.8 (R)
ACV-0289539	CKS2246		Tyrosine-protein kinase Wzc	2.8 (R)
ACV-0289331	CKS3472	<i>katE</i>	Catalase	2.8 (R)
ACV-0286491	CKS3195	<i>fliD</i>	Flagellar hook-associated protein	2.8 (R)

ACV-0289060	CKS4855	<i>blc</i>	Outer membrane lipoprotein Blc	2.8 (R)
ACV-0288017	CKS1718		ABC transporter, permease protein	2.8 (R)
ACV-0285912	CKS2092	<i>elaB</i>	Elab protein	2.8 (R)
ACV-0287316	CKS2444		Bicupin, oxalate decarboxylase family	2.7 (R)
ACV-0288949	CKS4743		Ferrous iron transport protein A	2.7 (R)
ACV-0287980	CKS1755		ISEhe3 ORFB family protein	2.6 (R)
ACV-0286081	CKS5373		Mobilization protein	2.6 (R)
ACV-0290522	CKS0462		Sigma-fimbriae usher protein	2.6 (R)
ACV-0286178	CKS4569		Secreted effector protein	2.6 (R)
ACV-0285958	CKS2571	<i>fliR</i>	Flagellar biosynthesis protein flir	2.6 (R)
ACV-0290524	CKS0460		Sigma-fimbriae chaperone protein	2.6 (R)
ACV-0287392	CKS2368		Protein gp55 precursor	2.5 (R)
ACV-0288299	CKS4132		Phage-related protein	2.5 (R)
ACV-0290571	CKS0413		Protein gp47	2.5 (R)
ACV-0285931	CKS2111		Putative protein secretion efflux system (hemolysin-type secretion transmembrane protein)	2.5 (R)
ACV-0291295	CKS3815		Probable secreted protein	2.5 (R)
ACV-0287381	CKS2379		NUDIX hydrolase	2.5 (R)
ACV-0288416	CKS0970	<i>uspB</i>	Universal stress protein B	2.5 (R)
ACV-0286147	CKS4538		Type III secretion apparatus	2.4 (R)
ACV-0285724	CKS1903		Gifsy-1 prophage ci	2.4 (R)
ACV-0289580	CKS2205		DEAD/DEAH box helicase domain protein	2.4 (R)
ACV-0286474	CKS3212		Beta-galactosidase/beta-glucuronidase	2.4 (R)
ACV-0287848	CKS2942		GCN5-related N-acetyltransferase	2.4 (R)
ACV-0288740	CKS1539		Extracellular metalloprotease	2.4 (R)
ACV-0285615	CKS1793	<i>mdtJ</i>	Spermidine export protein mdtj	2.4 (R)
ACV-0290819	CKS0164		Major tail tube protein	2.4 (R)
ACV-0285925	CKS2105		Large repetitive protein	2.4 (R)
ACV-0289726	CKS3333	<i>chaB</i>	Cation transport regulator chab	2.4 (R)
ACV-0291048	CKS1259		Carbon storage regulator	2.4 (R)
ACV-0286541	CKS3145		Na ⁺ /solute symporter	2.4 (R)
ACV-0290836	CKS0147		Phage major capsid protein #Fam0066	2.4 (R)
ACV-0290231	CKS2766	<i>ompW</i>	Outer membrane protein W precursor	2.3 (R)
ACV-0288415	CKS0971	<i>uspA</i>	Universal stress protein A	2.3 (R)
ACV-0289541	CKS2244		Polysaccharide export protein	2.3 (R)
ACV-0286159	CKS4550	<i>fliC</i>	Flagellar biosynthesis protein flic	2.3 (R)
ACV-0290049	CKS3579		Hypothetical transporter yido, benzoate like (bene), MFS superfamily	2.3 (R)

ACV-0285616	CKS1794	<i>mdtI</i>	Spermidine export protein mdti	2.3 (R)
ACV-0288310	CKS4143	<i>cycA</i>	D-serine/D-alanine/glycine transporter	2.3 (R)
ACV-0288792	CKS1591		Bacterioferritin	2.3 (R)
ACV-0285956	CKS2569	<i>trg</i>	Methyl-accepting chemotaxis protein iii (ribose and galactose chemoreceptor)	2.3 (R)
ACV-0288137	CKS3968	<i>cspD</i>	Cold shock protein cspd	2.3 (R)
ACV-0289123	CKS4920	<i>yhbO</i>	Thij/pfpi family protein	2.3 (R)
ACV-0286131	CKS4522	<i>yopD</i>	Type III secretion chaperone protein for yopd (sycd)	2.2 (R)
ACV-0287802	CKS5262		1-deoxy-d-xylulose 5-phosphate reductoisomerase	2.2 (R)
ACV-0286754	CKS5584		Membrane glycoprotein	2.2 (R)
ACV-0287487	CKS3898		Resolvase	2.2 (R)
ACV-0287296	CKS2464		Formate dehydrogenase related protein	2.2 (R)
ACV-0286133	CKS4524		Type III secretion inner membrane protein	2.2 (R)
ACV-0290639	CKS0345		Filamentous haemagglutinin family outer membrane protein	2.2 (R)
ACV-0290490	CKS0494		Probable PTS system regulatory protein	2.2 (R)
ACV-0289733	CKS3340	<i>impM</i>	Protein phosphatase impm	2.2 (R)
ACV-0288759	CKS1558	<i>mscL</i>	Large-conductance mechanosensitive channel	2.1 (R)
ACV-0286947	CKS4182	<i>msyB</i>	Acidic protein	2.1 (R)
ACV-0290319	CKS0667	<i>yqjK</i>	Inner membrane protein	2.1 (R)
ACV-0289713	CKS3320		GGDEF domain protein	2.1 (R)
ACV-0288317	CKS4150	<i>uvrY</i>	Bara-associated response regulator uvry	2.1 (R)
ACV-0290634	CKS0350		Filamentous haemagglutinin family outer membrane protein	2.1 (R)
ACV-0287438	CKS3710		Citrate carrier protein	2.1 (R)
ACV-0289200	CKS5001		Fimbrial protein precursor	2.1 (R)
ACV-0287318	CKS2442	<i>aldB</i>	Aldehyde dehydrogenase	2.1 (R)
ACV-0289333	CKS3470		Malto-oligosyltrehalose synthase	2.1 (R)
ACV-0290092	CKS2905		Predicted sugar transporter	2.1 (R)
ACV-0289765	CKS3372	<i>astE</i>	Succinylglutamate desuccinylase	2.1 (R)
ACV-0290158	CKS2839	<i>ydbJ</i>	Probable lipoprotein YPO2331	2.1 (R)
ACV-0290320	CKS0666	<i>yqjE</i>	Inner membrane protein yqje	2.1 (R)
ACV-0286141	CKS4532		Type III secretion system apparatus protein	2.1 (R)
ACV-0289817	CKS3427		Cyclopropane-fatty-acyl-phospholipid synthase	2.1 (R)
ACV-0291055	CKS1266	<i>phnA</i>	Alkylphosphonate utilization operon protein phna	2.1 (R)

ACV-0289262	CKS3541		Oxidoreductase domain protein	2.1 (R)
ACV-0289305	CKS3498	<i>yaiL</i>	Nucleoprotein/polynucleotide-associated enzyme	2.1
ACV-0288910	CKS4704		Glutathione S-transferase	2.1 (R)
ACV-0286079	CKS5371		DNA topoisomerase III	2.0 (R)
ACV-0289533	CKS2252	<i>wcaK</i>	Colanic acid biosynthesis protein weak	2.0 (R)
ACV-0287480	CKS3905		IS911 orfa	2.0 (R)
ACV-0290648	CKS0336		Glycerol metabolism operon regulatory protein	2.0 (R)
ACV-0286153	CKS4544		Lytic transglycosylase, catalytic	2.0 (R)
ACV-0286540	CKS3146		Dihydrodipicolinate synthase	2.0 (R)
ACV-0289525	CKS2260		Undecaprenyl-phosphate N-acetylglucosaminyl 1-phosphate transferase	2.0 (R)
ACV-0286180	CKS4571		Virulence protein	2.0 (R)
ACV-0288001	CKS1734		Predicted P-loop atpase fused to an acetyltransferase COG1444	2.0 (R)
ACV-0287490	CKS3895		Insertion element iso-IS1n protein insb	2.0 (R)
ACV-0287730	CKS5190	<i>ampD</i>	N-acetylmuramoyl-L-alanine amidase ampd	2.0 (R)
ACV-0290480	CKS0504		Modulator of drug activity B	2.0 (R)
ACV-0291279	CKS3797	<i>ybgC</i>	4-hydroxybenzoyl-coa thioesterase family active site	2.0 (A)
ACV-0291071	CKS1282	<i>cysN</i>	Sulfate adenylyltransferase subunit 1	2.0 (A)
ACV-0286673	CKS3013		L-2,4-diaminobutyrate decarboxylase	2.0 (A)
ACV-0286288	CKS4321		2-ketogluconate utilization repressor ptxs	2.0 (A)
ACV-0288879	CKS4673	<i>pgi</i>	Glucose-6-phosphate isomerase	2.0 (A)
ACV-0286633	CKS3053		Homoserine/homoserine lactone efflux protein	2.0 (A)
ACV-0286664	CKS3022		Anion transporter	2.0 (A)
ACV-0286674	CKS3012		Diaminobutyrate--2-oxoglutarate aminotransferase	2.0 (A)
ACV-0290487	CKS0497		PTS system, fructose-specific IIA component	2.0 (A)
ACV-0290953	CKS0001	<i>purH</i>	IMP cyclohydrolase / Phosphoribosylaminoimidazolecarboxamide formyltransferase	2.0 (A)
ACV-0289042	CKS4836		Aldo-keto reductase	2.0 (A)
ACV-0286416	CKS3270	<i>hrpF</i>	HrpF protein (hrp cluster)	2.0 (A)
ACV-0285631	CKS1809		Protease II	2.0 (A)
ACV-0290302	CKS0684	<i>diaA</i>	Phosphoheptose isomerase	2.0 (A)
ACV-0290872	CKS0110		SOS-response repressor and protease	2.1 (A)

			lexa	
ACV-0289133	CKS4930		Cell division protein ftsi [Peptidoglycan synthetase]	2.1 (A)
ACV-0289168	CKS4965		Extracellular solute-binding protein, family 5	2.1 (A)
ACV-0287497	CKS3888		Ardr protein	2.1 (A)
ACV-0287177	CKS1106	<i>cpxR</i>	Copper-sensing two-component system response regulator cpxr	2.1 (A)
ACV-0287013	CKS4248	<i>ndh</i>	Nadh dehydrogenase	2.1 (A)
ACV-0288326	CKS1771		Formate efflux transporter	2.1 (A)
ACV-0286411	CKS3275		Elicitor of the hypersensitivity reaction hrpn (hrp cluster)	2.1 (A)
ACV-0291078	CKS1289		Endoribonuclease L-PSP	2.2 (A)
ACV-0287426	CKS3722	<i>tatE</i>	Twin-arginine translocation protein tate	2.2 (A)
ACV-0289322	CKS3481	<i>tppB</i>	Di/tripeptide permease dtpa	2.2 (A)
ACV-0287320	CKS2440		Glutamine amidotransferase	2.2 (A)
ACV-0286882	CKS2705		D-amino acid dehydrogenase small subunit	2.2 (A)
ACV-0286239	CKS4630		Cellulase	2.2 (A)
ACV-0286270	CKS4303		D-tyrosyl-trna(tyr) deacylase	2.2 (A)
ACV-0285737	CKS1916		Endodeoxyribonuclease rusa	2.2 (A)
ACV-0291281	CKS3799	<i>tolR</i>	Tol biopolymer transport system, tolR protein	2.2 (A)
ACV-0286568	CKS3118		Hypothetical transmembrane protein coupled to NADH-ubiquinone oxidoreductase chain 5 homolog	2.3 (A)
ACV-0289622	CKS2163	<i>fruB</i>	Fructose-specific phosphocarrier protein hpr/PTS system, fructose-specific IIA component	2.3 (A)
ACV-0287580	CKS5040		Methionine synthase, vitamin-B12 independent	2.3 (A)
ACV-0286034	CKS2647		Ospg	2.3 (A)
ACV-0291280	CKS3798	<i>tolQ</i>	Mota/tolq/exbb proton channel family protein	2.3 (A)
ACV-0289470	CKS2315	<i>dacD</i>	D-alanyl-D-alanine carboxypeptidase	2.3 (A)
ACV-0288517	CKS0869	<i>yrfF</i>	Iga: a membrane protein that prevents overactivation of the Rcs regulatory system	2.4 (A)
ACV-0289327	CKS3476		Membrane-bound lysozyme inhibitor of c-type lysozyme	2.4 (A)
ACV-0288393	CKS0993		Inositol-1-monophosphatase	2.4 (A)
ACV-0288957	CKS4751		Endo-1,4-beta-xylanase	2.5 (A)
ACV-0288510	CKS0876	<i>ompR</i>	Two-component system response	2.5 (A)

			regulator ompR	
ACV-0288385	CKS1001		Possible ABC transporter, periplasmic substrate X binding protein precursor	2.5 (A)
ACV-0289585	CKS2200	<i>ahpF</i>	Alkyl hydroperoxide reductase protein F	2.6 (A)
ACV-0291275	CKS3793		Cytochrome d ubiquinol oxidase subunit I	2.6 (A)
ACV-0290308	CKS0678		Pyridoxal-5'-phosphate-dependent enzyme, beta subunit	2.6 (A)
ACV-0287924	CKS3653		Conserved hypothetical protein from phage origin	2.6 (A)
ACV-0291072	CKS1283	<i>cysD</i>	Sulfate adenylyltransferase subunit 2	2.6 (A)
ACV-0287591	CKS5051	<i>yaiE</i>	Cytoplasmic protein yaiE	2.7 (A)
ACV-0286569	CKS3117		NADH dehydrogenase, subunit 5	2.7 (A)
ACV-0286289	CKS4322		Periplasmic binding protein/laci transcriptional regulator	2.7 (A)
ACV-0287790	CKS5250	<i>degP</i>	Htra protease/chaperone protein	2.8 (A)
ACV-0286426	CKS3260		Nitrate/nitrite sensor protein	2.9 (A)
ACV-0288744	CKS1543		Lipase	2.9 (A)
ACV-0290791	CKS0192		COG0803: ABC-type metal ion transport system, periplasmic component/surface adhesin	3.0 (A)
ACV-0287183	CKS1100	<i>sbp</i>	Sulfate-binding protein sbp	3.0 (A)
ACV-0285895	CKS2075	<i>lrhA</i>	LysR family transcriptional regulator lrhA	3.2 (A)
ACV-0287319	CKS2441		Methyltransferase	3.2 (A)
ACV-0289810	CKS3417	<i>sufE</i>	Sulfur acceptor protein sufe for iron-sulfur cluster assembly	3.2 (A)
ACV-0289269	CKS3534		Membrane-fusion protein	3.3 (A)
ACV-0285804	CKS1984		Phage-related protein	3.5 (A)
ACV-0289993	CKS0835		ATPase involved in chromosome partitioning	4.7 (A)
ACV-0290094	CKS2903	<i>esaR</i>	Quorum-sensing transcriptional activator esaR	5.4 (A)
ACV-0290093	CKS2904	<i>esaI</i>	N-3-oxooctanoyl-L-homoserine lactone synthase	7.3 (A)
ACV-0290388	CKS0598		Methyl-accepting chemotaxis sensory transducer	7.5 (A)
ACV-0289766	CKS3373	<i>spy</i>	Periplasmic protein related to spheroplast formation	9.5 (A)

^a (A) denotes fold activation, (R) denotes fold repression by EsaR as seen in the RNA-Seq data.

REFERENCES:

1. **Ramachandran R, Stevens AM.** 2013. Proteomic analysis of the quorum-sensing regulon in *Pantoea stewartii* and identification of direct targets of EsaR. *Appl. Environ. Microbiol.* **79**:6244–52.
2. **Minogue TD, Wehland-von Trebra M, Bernhard F, von Bodman SB.** 2002. The autoregulatory role of EsaR, a quorum-sensing regulator in *Pantoea stewartii* ssp. *stewartii*: evidence for a repressor function. *Mol. Microbiol.* **44**:1625–35.

Appendix C

Analysis of EsaR Binding Sites Within the Promoter of *uspA* Using DNase I Footprinting Assays

Analysis of EsaR binding sites within the promoter of *uspA* using DNase I footprinting

assays. The promoter of *uspA* is directly regulated by EsaR, the master quorum-sensing regulator EsaR in *P. stewartii* (Chapter Four). P_{uspA} was analyzed for the presence of EsaR binding sites using DNase I footprinting assays that were carried out as discussed in Chapter Three, using FAM-labeled primer PuspA-R-FAM (/5'FAM/CCATGATATAACTCCTTCCAC) and non-labeled primer PuspA-F (GCAGAATTTGCCAACAACC).

```
>uspA + 400-bp upstream
GAACAGTGCAGAACGCGCACCGTGCTGAACAGTCCCTGCAGAATTTGCCAACAACCCCGTTAAGCGATTTGTAGT
TTTTATTTTTGAATCATCAGAAAAGTAACAGCCATGTGATCAAGGCTGCTTTTTTTAGTTTAGGAGAAATGTTCAATTTTT
ACCAGCGAGGATTTTCGTTTTATACGAGTAAAAATCGTTCATCATTGATCTTATTCACAAGCCAGACGGCTTCAGAAGCAT
TTGTTAACACACAGGGCTATACTTTCAGGTATAACAAAAGCATTGCCTGTATTGCAGGTTACCCATTTTG
GTGGCGCTCATCGCCCGTTCGCGCAATGGATTTTCGAGCTGTGACGCGTCTGGAAACCGCTGCCATTCTGAATCTCGTGG
AAGGAGTTATATCATGGCTTATAAACATATCCTGATTGCAGTCGATCTTTCGCCAGAAAGTCAGTTATTAGTGGAT
AAAGCTGTCTCGCT

>UspA1 :   ACAGGGCTATACTTTCAGGT           8/20
>EsaR:    GCCTGTACTATAGTGCAGGT
>UspA2 :   GCATTGCCTGTATTGCAGGT           14/20
```

Figure C.1: The promoter region of *uspA*. Sequence of a portion of the *uspA* gene (red letters) and 400-bp upstream region showing the location of three primer sequences (underlined) and the two predicted EsaR binding sites, UspA1 (in green letters) and UspA2 (in yellow letters). Alignment of each predicted EsaR binding site in comparison to the 20-bp *esa* box (EsaR) shows that UspA1 and UspA2 are conserved in 8 and 14 of the 20 bases, respectively.

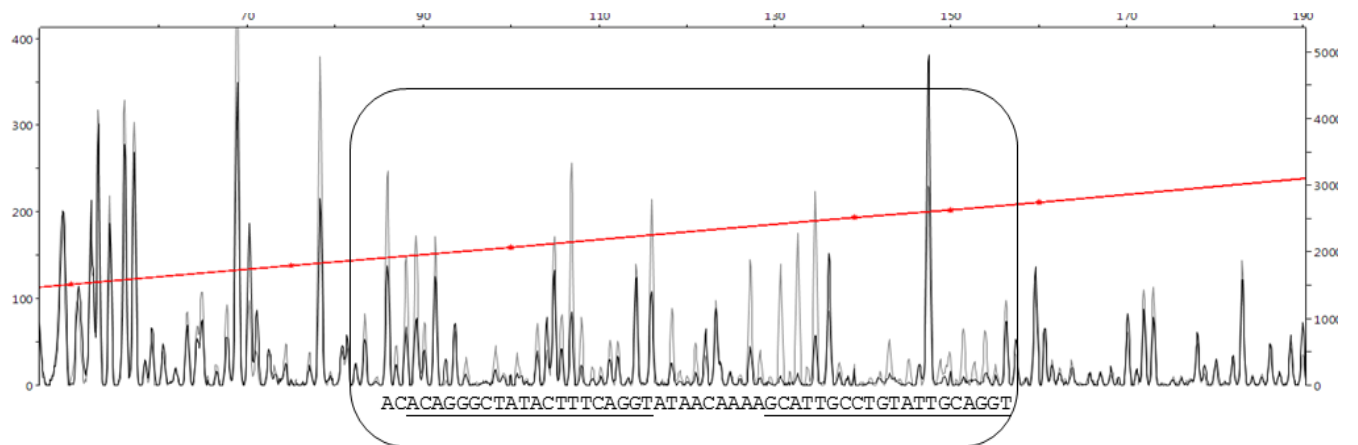


Figure C.2: DNase I footprinting assay of EsaR binding sites in the non-coding strand of P_{uspA} . Capillary electrophoresis of 6-FAM-labeled DNA fragments of P_{uspA} from DNase I protection assays in the presence (black) and absence (grey) of HMGE, the EsaR fusion protein demonstrates that HMGE binds to specific sequences in the promoter region of P_{uspA} and protects against DNase I digestion. The rounded rectangle highlights the binding region. The protected sequences are shown at the bottom of the rounded rectangles and those bases believed to be the 20-bp EsaR binding site determined through similarity to the *esa* box are indicated by underlining. The red line indicates the size-calibration plot generated by the size standards. The x-axis denotes size in base pairs and the y-axis denotes relative fluorescence units.